Outcome and toxicity modelling after stereotactic radiotherapy of central lung tumors

Marloes Duijm

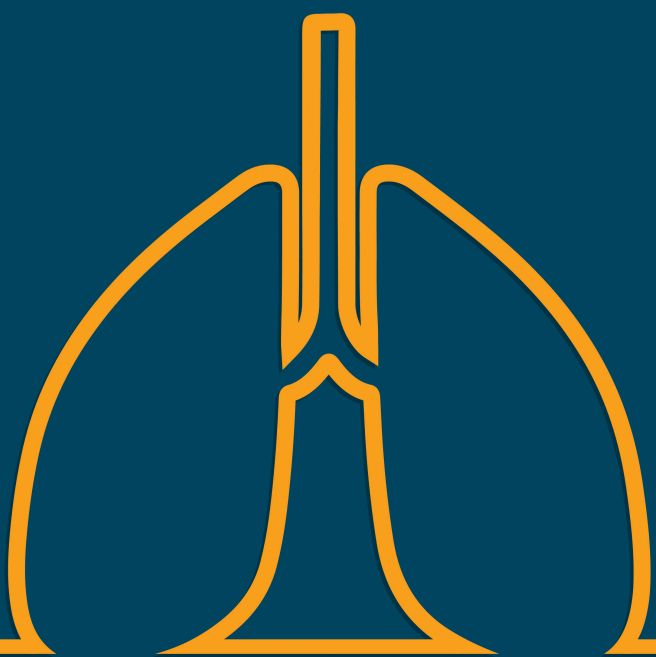

Outcome and toxicity modelling after stereotactic radiotherapy of central lung tumors

Marloes Duijm

Printed by: Ridderprint | www.ridderprint.nl

ISBN: 978-94-6416-327-8

Outcome and Toxicity Modelling after Stereotactic Radiotherapy of Central Lung Tumors

Uitkomsten en toxiciteit modellering na stereotactische radiotherapie van centrale longtumoren

Proefschrift

ter verkrijging van de graad van doctor aan de
Erasmus Universiteit Rotterdam
op gezag van de rector magnificus

Prof. dr. F.A. van der Duijn Schouten

en volgens het besluit van het College voor Promoties.

De openbare verdediging zal plaatsvinden op
dinsdag 19 januari 2021 om 13:30 uur

door

Marloes Duijm
geboren te Leiden

Erasmus University Rotterdam

Erasmus

Promotiecommissie

Promotor:	prof. dr. M.S. Hoogeman
Overige leden:	prof. dr. N.A. Nout prof. dr. J.G.J.V. Aerts prof. dr. D. de Ruysscher
Copromotor:	dr. J.J.M.E. Nuyttens

Voor opa de Carpentier

Content

CHAPTER 1

General introduction and outline of the thesis

1.1 Epidemiology and treatment

Lung cancer is the most commonly diagnosed malignancy and the leading cause of cancer-related death worldwide (1). In the Netherlands, over 13.000 people were diagnosed with lung cancer in 2017, representing 12% of the national cancer diagnoses (2). Based on pathology, lung cancer can be divided in two groups: small cell lung cancer (SCLC) and non-small cell lung cancer (NSCLC), where the latter accounts for 80 – 85% of all lung cancers diagnoses. Five years after the diagnosis of NSCLC only 25% of the patients is still alive (3). Based on the size of the primary tumor and whether the disease has spread to lymph nodes or distant organs, NSCLC can be divided in different stages according to the TNM classification for lung cancer (*Appendix 1A – B*). When using this classification, every stage reflects an overall survival prognosis (4, 5) *(Figure 1)*.

Figure 1 – Overall survival by clinical stage according to the TNM classification*

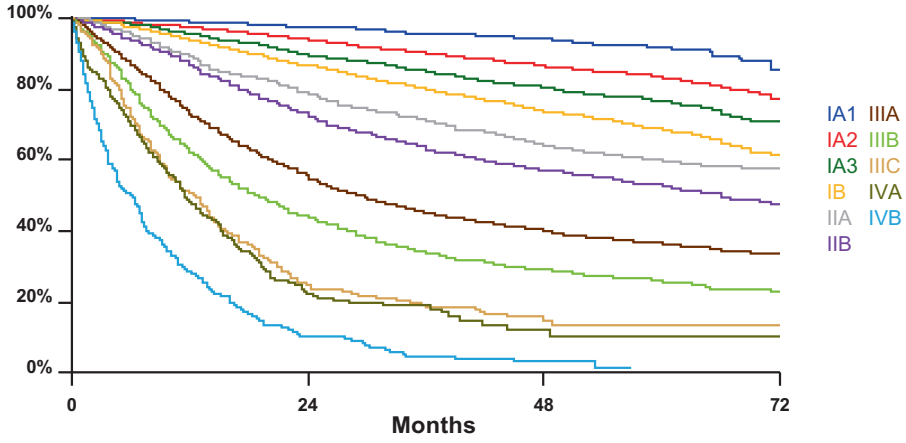

** eight edition (ref: Goldstraw 2015)*
The different stages are explained in Appendix 1A – B.

Early stage NSCLC are tumors which in principle can be treated locally with surgery or radiotherapy, with surgery as the preferred treatment according to the EMSO and the Dutch national guidelines (5, 6). If a patient is unfit for surgery due to comorbidities, or is unfit for lobectomy and a segment resection or wedge resection are the alternatives, stereotactic radiotherapy can be considered as the non-surgical treatment (6).

1.2 Stereotactic radiotherapy for lung tumors

For nearly 20 years, stereotactic body radiation therapy (SBRT) has been the radiation treatment modality for early stage NSCLC. The first prospective cohorts described patients

treated with 60 Gy in 10 fractions and with 48 Gy in 4 fractions. The results were promising having a low local recurrence rate and a 3 years overall survival of 56 – 83%, without any grade 3 toxicity or higher reported (7, 8). In the following years, multiple studies analyzed SBRT in early stage NSCLC and all found comparable outcomes. Higher local control and overall survival were demonstrated when prescribing a biologically equivalent dose (BED_{10}, using an α/β ratio of 10 Gy) of 100 Gy and higher (9).

Nowadays, SBRT is widely accepted as standard treatment for inoperable early stage NSCLC patients and for those refusing surgery (10-12). However, there is a subgroup of patients that carries unique and significant toxicity risks and therefore requires more specific attention, i.e. the centrally located tumors (10, 11).

1.3 Central lung tumors

A publication of a prospective trial did result in the distinction between peripherally and centrally located lung tumors treated with SBRT (13). This phase II trial, published in 2006, treated patients with medically inoperable early-stage NSCLC with SBRT in 3 fractions of 20 – 22 Gy without having an enrollment restriction based on tumor localization. Although the survival and disease outcomes were promising, an 11-fold higher risk of high-grade toxicity for patients having a tumor located within 2 cm of the proximal bronchial tree was reported (13).

Since this publication, risk-adapted fractionation schedules associated with lower BED_{10} are used for patients having a centrally located tumor. When using these adapted schedules, overall survival rates are comparable to peripherally located tumors, but the local control rates are slightly lower (14) highlighting the need of a dose of ≥ 100 Gy BED_{10} (15). Additionally, dose-constraints are used for the organs at risk (OAR) to prevent high-grade toxicity and nowadays, people are aware of excluding the OAR from the high-dose region to decrease toxicity risks (9).

Stereotactic body radiation therapy for central lung tumors is currently practiced by multiple institutions, however without proper evidence-based guidelines. In the last years the first results of prospective multicenter studies are gradually published (16, 17), but most of the treatment consensus is based on retrospective experience of institutes shared in literature. Some studies have suggested to not treat tumors within 1 cm of the bronchial tree because of high toxicity probabilities, while other studies have reported high local control with acceptable toxicity rates (16-18).

Despite all publications, the use of OAR dose-constraints and the first reports of prospective trials, high-grade toxicity after SBRT is still reported. This is keeping the discussion about the treatment of central lung tumors ongoing and is highlighting the need for more evidence-based guidelines.

If SBRT for a central lung tumor is declined, alternatives are a lower stereotactic dose, conventional radiotherapy, chemotherapy or no treatment. For a well-balanced treatment decision individualized toxicity risks and treatment outcomes, such as overall survival and disease control, should be taken into to account. The aim of this thesis is to improve decision making in SBRT of centrally located lung tumors by modelling the outcome in terms of overall survival, local control and toxicity probabilities of the esophagus and bronchial structures.

1.4 This thesis

A well-balanced treatment decision should start with the patient's life expectancy. When patients are older or the performance status is lower, survival probabilities decline. If the survival probability of a patient is low, should any risk on life threatening toxicity be taken? **Chapter 2** will discuss the overall survival probabilities for patients with centrally located NSCLC considered for SBRT using a nomogram, which is a feasible tool to describe the individual prognosis of a clinical event. This survival nomogram offers individualized predictions using multiple prognostic characteristics. Each of these characteristics can be scored for an individual patient such that the total sum of points will be linked to the 6 months, 1, 2 and 3 years overall survival probability.

When the survival probability of the patient is promising, the chances on local disease control have to be estimated. Next to the known cut-off of 100 Gy BED_{10}, studies have searched for predictive dosimetric and clinical factors to minimize the local recurrence probability (19, 20). In case of a central tumor, fulfilling the dose-constraints of the OAR can result in less coverage of the planning target volume (PTV) with the prescribed dose. Whether a compromised dose on the PTV has consequences in terms of disease control is unknown. The impact of the underdosage of the PTV is discussed in **Chapter 3** as well as other possible clinical and treatment characteristics predictive for disease control in central lung tumors treated with SBRT.

The expected toxicity after treatment of a central lung tumor is depending on the organs close to the tumor. When the tumor is close to the bronchial structures, it is inevitable to prescribe some dose to the bronchi. Dose to the bronchi can result in stenosis, occlusion or fistula formation, and in some cases even death. **Chapter 4** is describing the radiological changes of the bronchi after SBRT and its relation to the prescribed dose. Whether these radiographic changes will result in clinical toxicity is discussed in **Chapter 5**. Within this chapter, clinical pulmonary and radiographic bronchial toxicity is evaluated and after identifying the predictors for clinical toxicity, normal tissue complication probability (NTCP) models were derived.

Another important organ to consider within the treatment of central lung tumors is the esophagus. Toxicity of the esophagus can be seen as radiation esophagitis. **Chapter 6** is describing the incidence of low-grade radiation esophagitis and its relation to the prescribed dose. Late effects in the esophagus can consist of strictures, perforation and fistulation, which can be life-threatening for patients. To evaluate late toxicity of the esophagus, another cohort of patients was analyzed in which late high-grade esophageal toxicity was found. **Chapter 7** is describing these cases and their relation with SBRT. In both chapters, NTCP models were derived and evaluated against currently used esophagus dose-constraints in order to improve decision making in the treatment of central lung tumors with SBRT.

The previous chapters and further perspectives are discussed in **Chapter 8**.

2

CHAPTER 2

The development and external validation of an overall survival nomogram in medically inoperable centrally located early stage non-small cell lung carcinoma

M. Duijm [1], E. Oomen-de Hoop [1], N.C. van Voort van der Zyp [2], P. van de Vaart [2], H. Tekatli [3], M.S. Hoogeman [1], S. Senan [3], J.J. Nuyttens [1]

[1] Department of Radiation Oncology, Erasmus MC Cancer Institute, Rotterdam, The Netherlands
[2] Department of Radiation Oncology, Haaglanden MC, The Hague, The Netherlands
[3] Department of Radiation Oncology, Cancer Center Amsterdam, VU University Medical Center, Amsterdam, The Netherlands

Submitted to Radiotherapy & Oncology, May 2020

Abstract

Introduction

Current nomograms predicting survival prognosis after stereotactic body radiation therapy (SBRT) in non-small cell lung cancer (NSCLC) are based on peripherally located tumors. However, patients with a central lung tumor tend to be older, the tumor is often bigger and fraction-schedules are risk-adapted. Therefore, we developed and externally validated a nomogram to predict overall survival (OS) in patients having centrally located early-stage NSCLC treated with SBRT.

Methods

Patients who underwent SBRT for centrally located NSCLC were identified and baseline characteristics were obtained. With a Cox proportional hazards model a nomogram to predict 6 month, 1-, 2- and 3- year OS was built. Bootstrap sampling was used to validate the model building procedure. To determine generalizability, external validation was performed on a cohort of central lung tumor patients treated with SBRT from another center. Discriminatory ability was measured with the concordance index (C-index) and calibration plots were used to compare Kaplan-Meier-estimated and nomogram-predicted OS.

Results

The nomogram was built on data of 220 patients and consisted of the following variables: PTV, age, WHO performance status, tumor lobe location and mean dose to the PTV. The C-index of the nomogram (corrected for optimism) was moderate at 0.61. Calibration plots showed favorable predictive accuracy. The external validation showed acceptable validity with a C-index of 0.60.

Conclusions

We developed and externally validated the first nomogram to estimate the OS probability in patients with centrally located NSCLC treated with SBRT. This nomogram could help to identify patients with low survival prognosis and support clinicians in decision making.

2.1 Introduction

Stereotactic body radiation therapy (SBRT) is the standard of care for patients with early-stage non-small cell lung cancer (ES-NSCLC) not suitable for surgery (10, 11). Although the overall outcome of this treatment is promising, the treatment of centrally located lung tumors is challenging and cases of high-grade toxicity are reported by recent prospective trials (17, 21). Within this subgroup of central tumors, predicting the individual survival probability could prevent physicians from exposing patients who have a short life expectancy to high toxicity risks.

The individual survival probability can be quantified with a nomogram, a tool that incorporates prognostic characteristics to calculate the survival prognosis. Nomograms were more reliable in predicting survival of patients with resectable NSCLC compared to predictions using the TNM staging system (22, 23). Current nomograms predicting overall survival (OS) in lung cancer after SBRT focus on peripheral ES-NSCLC or oligometastatic lung disease (24-26). However, compared to patients with a peripheral tumor, patients with a central tumor are older (27), their tumors are bigger (27, 28), and radiation schedules are more fractionated (10, 11). Therefore, our aim was to develop and externally validate a OS nomogram in patients having centrally located ES-NSCLC treated with SBRT.

2.2 Material and Methods

The nomogram was constructed based on 220 patients who underwent SBRT for centrally located ES-NSCLC between 2006 – 2016 in the Erasmus Medical Center (EMC) or Haaglanden Medical Center (HMC). Baseline patient, tumor and treatment characteristics were obtained. A central tumor was defined as a tumor located within 2 cm of the esophagus and/or the bronchial structures (trachea, main bronchus, bronchus intermedius or upper, middle or lower lobe bronchi). Patients were excluded because of previous irradiation with overlapping fields, synchronous pulmonary lesions, concurrent chemotherapy during SBRT or no follow-up data available. Treatment planning and delivery of both centers have been described previously (29, 30). In summary, HMC initially used a stereotactic linear accelerator (Novalis, Brainlab AG, Munich Germany). From 2016 onwards an accelerator with cone-beam CT-guidance was used (Elekta AB, Stockholm, Sweden). Treatment consisted of either 8 fractions of 7.5 Gy (3 times a week) or 12 fractions of 5 Gy (4 times a week) if the planning target volume (PTV) was overlapping or too close to the organs at risk (OAR). Until 2014, the gross tumor volume (GTV) was contoured on 6 scans randomly taken during the breathing cycle. Thereafter, the tumor was contoured in 10 respiratory phases of the 4D-CT scan. To account for respiratory-induced motion an internal target volume (ITV) was used, which was expanded with 5 mm (6 mm in craniocaudal direction) for the Novalis and with 6 mm for the Elekta to create the PTV. Treatment

planning aimed to prescribe 100% and 90% of the dose to ≥ 95% and ≥ 99% of the PTV, respectively. At the EMC, SBRT was delivered using the Cyberknife Robotic Radiosurgery System (Accuray Inc, Sunnyvale, AC). When the PTV was close to the bronchial structures, 5 fractions of 9 – 12 Gy were prescribed and when the PTV was close to the esophagus 6 – 7 fractions of 7 – 8 Gy were prescribed. The PTV consisted of the GTV plus 5 mm. The dose was prescribed to the 100% isodose line covering ≥ 95% of the PTV and the maximum dose was < 160%. To meet the constraint of the OAR, both institutions allowed underdosage of the PTV.

To examine the generalizability of the model, an independent cohort of 92 patients with centrally located NSCLC treated with SBRT at the VU Medical Center between 2008 – 2015 was used for external validation. Treatment was delivered using coplanar Volumetric Modulated Arc Therapy RapidArc™ (Varian Medical Systems, Palo Alto, USA) and online cone-beam CT based setup to the target. Treatment consisted of 12 fractions of 5 Gy when the PTV was overlapping the trachea or main bronchi and for all other localizations 8 fractions of 7.5 Gy were used. The ITV was expanded with 5 mm to create the PTV. Similarly to the HMC, ≥ 95% and ≥ 99% of the PTV had to receive 100% and 90% of the prescribed dose, respectively.

Doses were recalculated to a biologically equivalent dose using an α/β-ratio of 10 Gy (BED_{10}), using the following formula $BED = D \times (1 + \frac{d}{\alpha/\beta})$ with D = total dose and d = dose per fraction. The primary endpoint was OS, calculated from the first day of SBRT until death, or the last moment of contact for patients who were still alive. A Cox regression analysis was done to determine the association of the following parameters with OS: age, gender, charlson comorbidity index (CCI; 0 – 3 versus ≥ 4), WHO performance status (0 versus 1 – 4), previous (lung)malignancies, availability of pathology, forced expiratory volume in 1 second (FEV_1), tumor lobe location (tumor located in the upper/middle lobe or mediastinum versus tumor located in the lower lobe), tumor diameter, PTV, disease stage, maximum and minimum point dose to the PTV (D_{max}, D_{min}), PTV mean dose (D_{mean}, analyzed continuous and categorical: < 100 Gy BED_{10} versus ≥ 100 Gy BED_{10}) and dose to 2 / 50 / 98 percent of the PTV ($D_{2\%}$ / $D_{50\%}$ / $D_{98\%}$).

Model building

The nomogram was based on a Cox proportional hazards model, using the following step-wise model building procedure. First, the FEV_1 was disregarded because of > 10% missing values. Complete case analysis was used for variables with < 5% missing values. All categorical variables were considered for the initial model, while continuous variables were only considered if they had a *p*-value ≤ 0.20 in univariate Cox regression. Since disease stage,

tumor diameter and PTV were highly correlated, only PTV was considered for the model. Hence, an initial model was built using the prognostic factors gender, age, PTV, tumor lobe location, WHO performance status, CCI, availability of pathology, previous (lung) malignancies and PTV D_{mean}. As the data provided no evidence for interaction between these variables, no interaction terms were considered in the model.

The model building steps were formulated as strict programmable decision rules aimed at arriving at the most parsimonious model with maximum predictive ability, so that the model building procedure could be internally validated. Initially, the prognostic factors were modeled flexibly, e.g. allowing highly non-linear relationships. Subsequently, following a predefined grid, less flexible functions were applied. The simplification was stopped once it compromised the fit of the model compared to the most flexible model. Depending on the distribution of the prognostic factor, suitable measures of fit were used. Age and PTV were modelled flexibly using restricted cubic splines (RCS) with 5 degrees of freedom (d.f.). First, the effect of age and PTV were modelled simultaneously and evaluated using Akaike's information criteria (AIC) as the compared models were not nested (31). The range of RCS up to 5 d.f. and the linear effect were evaluated. The model with the smallest AIC was selected. The remaining variables were assessed independently using the likelihood ratio test where *p*-value < 0.10 was used for inclusion in the model.

Internal validation

The model building procedure was validated by applying it to 1000 bootstrap samples and predicting the original sample based on the resulting model. Discriminative ability of the model was measured with the concordance index (C-index). The C-index can range from 0.5 (random chance) to 1.0 (perfect prediction). Internal validation was also used to assess the degree of overfitting to the sample at hand (calibration slope), and the resulting optimism in C-index. The estimated optimism-corrected calibration slope was used to shrink model predictions and thus increase their external validity (31), which resulted in the final model. Calibration plots in 1000 bootstrap samples were used to compare Kaplan-Meier-estimated and nomogram-predicted 6-month, 1-year, 2-year and 3-year OS.

External validation

The final model was used to predict 6-month, 1-year, 2-year, and 3-year OS in the external validation cohort. The model's discriminative ability was measured using the C-index. For the construction of the calibration plots, the predicted survival probabilities were grouped in 4 equally sized groups.

Statistical analyses were performed using IBM SPSS statistics version 24.0 (SPSS Inc., Chicago, IL, USA) and R software, version 3.4.1 (open source; www.r-project.org). This study was approved by the Medical Ethics Committee in all 3 hospitals.

2.3 Results

Two hundred and twenty patients diagnosed with ES-NSCLC and treated with ≤ 12 fractions of SBRT were included for model building. The majority of the patients were diagnosed with stage II NSCLC (52%) and were treated with 5 fractions of 9 – 12 Gy (37%) or 8 fractions of 7.5 Gy (31%). Histology was available in 58% of the patients, with squamous cell carcinoma as most frequent (68 of 129 patients). Patient and tumor characteristics are listed in *Table 1*. Of the 220 patients, 145 had died (66%) at the time of analysis. The median OS was 28 months, 95% confidence interval (95% CI) 23 – 35 months. The OS was 92% at 6 months, 76% at 1 year, 55% at 2 years and 41% at 3 years (*Figure 1*).

Table 1 – Patient and tumor characteristics

	Primary cohort (n = 220)		**External cohort (n = 92)**	
	n (%) / median (IQR, range)		n (%) / median (IQR, range)	
Age (years)	76	(68 – 82, 51 – 94)	74	(68 – 81, 49 – 94)
Gender				
Female	89	(40%)	27	(29%)
Male	131	(60%)	65	(71%)
COPD				
No COPD	39	(18%)	25	(27%)
GOLD I – II	113	(51%)	35	(38%)
GOLD III – IV	61	(28%)	24	(26%)
Unknown	7	(3%)	8	(9%)
Charlson comorbidity index				
0 – 2	128	(58%)	38	(41%)
3 – 5	83	(38%)	46	(50%)
6 – 9	9	(4%)	8	(9%)
WHO performance status				
0	74	(34%)	12	(13%)
1	117	(53%)	50	(55%)
2	14	(6%)	27	(29%)
3 – 4	6	(3%)	3	(3%)
unknown	9	(4%)	0	(0%)
Tumor histology				
No pathology available	91	(42%)	37	(40%)
Squamous cell carcinoma	68	(31%)	29	(32%)
Adenocarcinoma	40	(18%)	12	(13%)
Large cell carcinoma	18	(8%)	11	(12%)
Different	3	(1%)	3	(3%)
Tumor lobe location				
Tumor in lower lobe	64	(29%)	24	(26%)
Tumor not in lower lobe	156	(71%)	68	(74%)

Table 1 – Patient and tumor characteristics (continued)

	Primary cohort (n = 220)		External cohort (n = 92)	
	n (%) / median (IQR, range)		n (%) / median (IQR, range)	
Disease stage TNM 8th				
IA / IB	83	(38%)	53	(58%)
IIA / IIB	115	(52%)	27	(29%)
IIIA	22	(10%)	7	(8%)
recurrence	0	(0%)	5	(5%)
Dose fractionation schemes				
3 fractions of 20 Gy	2	(1%)	0	(0%)
5 fractions of 9/10/11/12 Gy	82	(37%)	0	(0%)
6 fractions of 7/8 Gy	17	(8%)	0	(0%)
7 fractions of 7 Gy	18	(8%)	0	(0%)
8 fractions of 7.5 Gy	69	(31%)	66	(72%)
12 fractions of 5 Gy	32	(15%)	26	(28%)
PTV (cc)	81	(44 – 140, 8 – 927)	75	(50 – 134, 9 – 509)
PTV D_{mean} (Gy BED_{10})				
< 100	48	(22%)	0	(0%)
≥ 100	172	(78%)	92	(100%)

Abbreviations: BED_{10} = biologically effective dose using α/β-ratio of 10 Gy, COPD = chronic obstructive pulmonary disease, D_{mean} = mean dose, Gy = Gray, IQR = interquartile range, PTV = planning target volume, WHO = world health organization

Factors associated with worse OS in the univariate analysis were higher age (continuous variable per 5 years; HR 1.12, 95% CI 1.02 – 1.24), localization of the tumor in lower lobe (versus other locations; HR 1.66, 95% CI 1.17 – 2.34), higher disease stage (II versus I; HR 1.74, 95% CI 1.20 – 2.52 and III versus I; HR 3.75, 95% CI 2.15 – 6.51), bigger PTV (continuous variable per 100 cc; HR 1.24, 95% CI 1.10 – 1.38) and PTV D_{mean} BED_{10} lower than 100 Gy (versus ≥ 100 Gy; HR 1.52, 95% CI 1.05 – 2.20; *Appendix 2A*).

Nomogram

Nine patients with missing WHO performance status were omitted from the building procedure. PTV and age were both modeled using 3 d.f.. During the model building the categorical parameters gender, availability of pathology, previous (lung)malignancies and CCI were excluded. The building procedure based on 211 patients resulted in the final model (*Figure 2*) including the variables: age, WHO performance status, PTV, tumor lobe location and PTV D_{mean}. Each subcategory of an included variable resembles a score on the point scale. After adding up these points, the total amount of points correlates to the OS-probability at 6 months, 1 year, 2 years and 3 years. *Figure* 3 shows the parameter estimates of the final model.

Figure 1 – Overall survival for the primary and external validation cohort

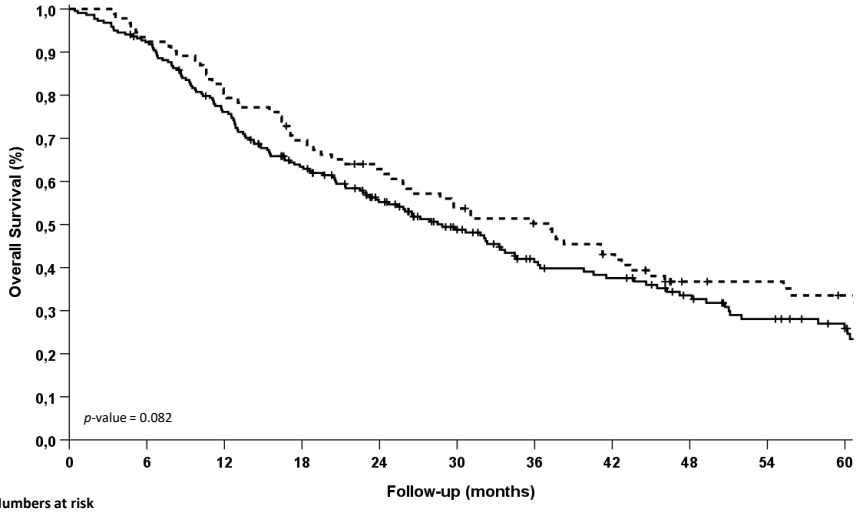

solid line = primary cohort, dashed line = external cohort

Figure 2 – Final model of the nomogram for prediction of 6 month, 1 year, 2 year and 3 year overall survival

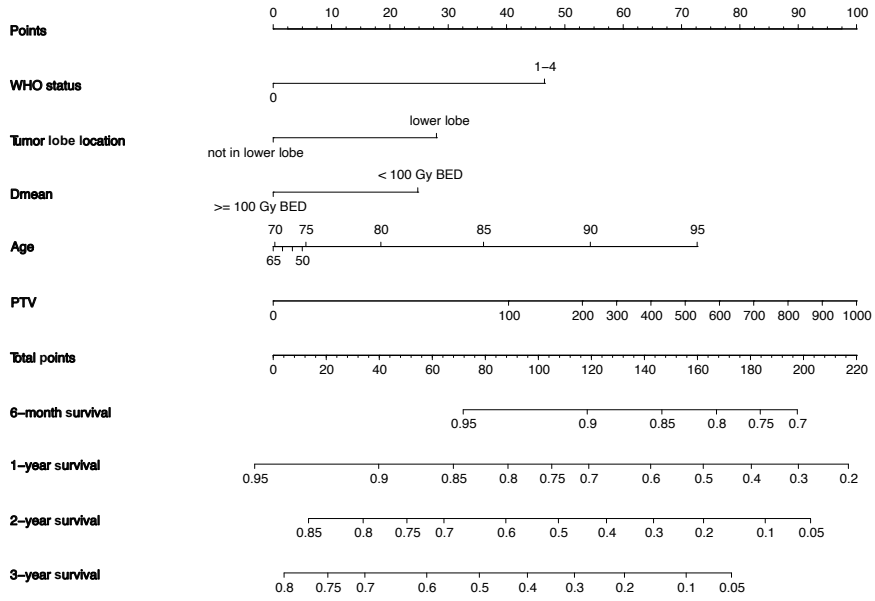

Abbreviations: BED = biologically effective dose, D_{mean} = mean dose, Gy = Gray, PTV = planning target volume, WHO status = world health organization performance status

Figure 3 – Parameter estimates of the final model used to generate the nomogram

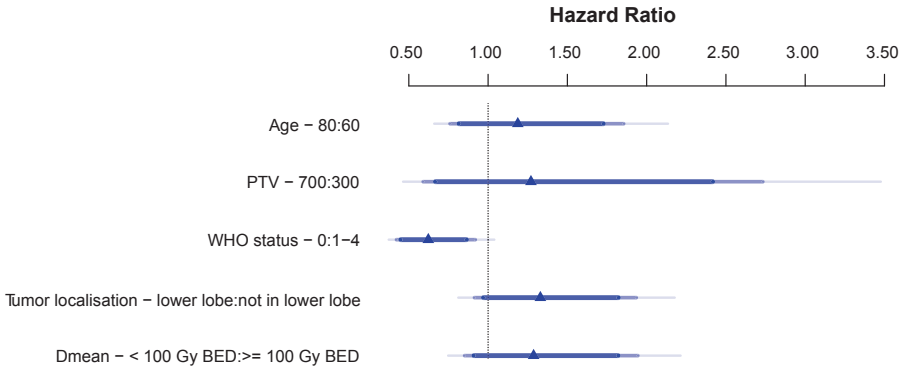

The triangle indicates the hazard ratio surrounded by the 90%, 95% and 99% confidence interval.
Abbreviations: BED = biologically effective dose, D_{mean} = mean dose, Gy = gray, PTV = planning target volume, WHO status = world health organization performance status

Internal validation

The frequencies of prognostic factor selection was 99% in 1000 bootstrap samples for age and PTV. In 94% WHO performance status was selected, while this was 62% for tumor lobe location and 61% for PTV D_{mean}. The C-index was 0.66 in the original sample and was corrected for optimism through bootstrap sampling to 0.61 (*Appendix 2B*). The optimism-corrected calibration slope was estimated at 0.62. *Figure 4* shows the calibration plots modeled per time frame, demonstrating the correlation between the observed and predicted probabilities at 6-month, 1-year, 2-year and 3-year OS.

External validation

Within the external cohort 58% of patients were diagnosed with stage I NSCLC and most patients were treated with 8 fractions of 7.5 Gy (72%). Histology was obtained in 60% of patients, and > 50% of these histology samples were squamous cell carcinoma (*Table 1*). Sixty-six patients had died at the time of analysis (67%) and the median OS was 31 months (95% CI 20 – 42 months). The corresponding survival curve is shown in *Figure 1*. The C-index was 0.60, which is equal to the results of the sample used to build the model. The dashed lines in *Figure 4* show the calibration plots of the external validation.

Figure 4 - Calibration plots of Kaplan-Meier-estimated versus nomogram-predicted overall survival (OS) for the primary cohort (black solid line) and the external validation cohort (dashed grey line) for A) 6 months B) 1 year C) 2 years and D) 3 years.

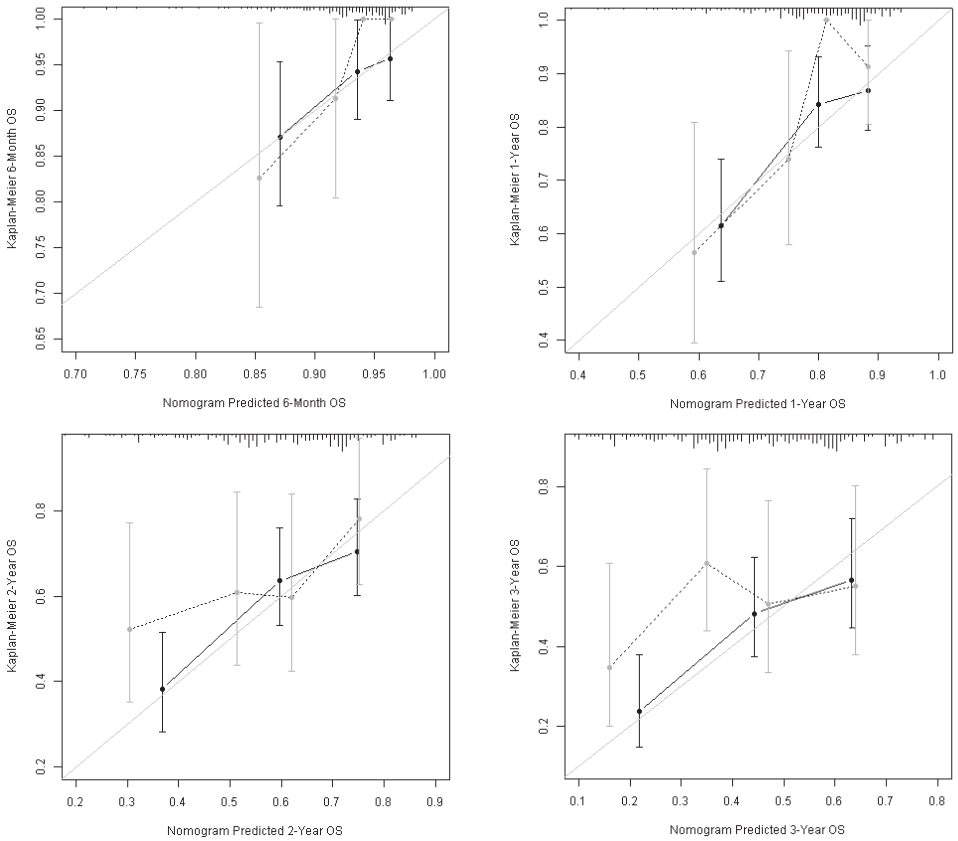

The error bars indicate the 95% confidence intervals. A plot along the 45-degree line would indicate perfect agreement between estimated and predicted overall survival. The vertical lines at the upper border of the graphs are representing the distribution of the predicted probabilities

2.4 Discussion

This is the first survival nomogram based exclusively on central lung tumors treated with SBRT. The nomogram includes patient-, tumor- and treatment-specific parameters and is based on the parameters: age, WHO performance status, PTV, tumor lobe location and PTV D_{mean}. The nomogram showed moderate discriminatory ability (C-index corrected for optimism of 0.61) and favorable predictive accuracy based on the calibration plots of the primary cohort. Moreover, this nomogram was validated by using an external cohort, showing acceptable external validity having a C-index of 0.60 which is comparable with the

training dataset. The nomogram illustrated PTV and age as having the largest contribution to prognosis, as the most points are allocated to these variables. For example, switching age from 70 to 85 years is reflecting to more points as having a tumor in the lower lobe. Additionally, the survival prognoses were better for a patient having a PTV of 100 cc treated with PTV D_{mean} < 100 Gy BED_{10}, as compared to a PTV of 500 cc treated with a PTV D_{mean} ≥ 100 Gy BED_{10}.

Other nomograms predicting overall survival in patients with early-stage NSCLC treated with SBRT are based on combined (peripherally and centrally located tumors) patient groups and only predict overall survival at 4 and 5 years (24, 26). Although these nomograms have a higher C-index (0.66 and 0.73 respectively), none of them performed an external validation. A nomogram for surgery developed by Liang et al. predicted overall survival at 1, 2 and 3 years for patients with resected NSCLC. This nomogram was based on more than 5000 patients resulting in a higher C-index (0.71) compared to the TNM staging system and included external validation (23).

Many but not all of the factors included in our nomogram were included in nomograms for ES-NSCLC treated with SBRT or surgery. Our study identified age as an important factor for OS, which is supported by the nomograms of Kang et al. and Louie et al. (24, 26). These nomograms are mainly based on patients with peripherally located ES-NSCLC treated with SBRT. Next to age, these studies also included tumor size and performance status. Although we included the PTV, this is inevitably correlated to tumor size. In contrast to other nomograms, we showed that a tumor located in the lower lobe predicts for worse OS. To our knowledge, this was not included in previously published nomograms for ES-NSCLC treated with SBRT or surgery. However, previous publications have found that tumor location in the lower lobe is predictive for inferior survival in the treatment of ES-NSCLC with SBRT and surgery (32, 33). An explanation can be the higher rates of unsuspected nodal involvement for tumors located in the lower lobe resulting in upstaging (34). Another variable which was predictive in our cohort but not included in other SBRT nomograms, is the dosimetric parameter PTV D_{mean} (BED_{10}). However, there are several studies confirming the relation between OS and dose (7, 35, 36). Moreover, the role of dose, particularly ≥ 100 Gy BED_{10}, is well known for its relation with local control (7, 19, 35, 37). The relation between OS and age, tumor size/PTV and performance status have also been described multiple times in studies focusing on central tumors (38, 39) or ES-NSCLC treated with SBRT in general (35-37, 40-43).

Although the primary and external cohort both involve centrally located lung tumors treated with SBRT, there are some differences between both groups. This is reflected in the OS curves (*Figure 1*), showing a trend to a slightly better OS in the external cohort. The 2-year OS rate was 55% in the primary cohort and 63% in the external cohort. This difference could be explained by the variation in disease stage: 58% stage I NSCLC in the external cohort versus 38% in the primary cohort (*Table 1*). Despite this difference in disease stage distribution between groups, the nomogram performed well in the external cohort and can therefore be used to predict OS in a general patient population with centrally located ES-NSLSC scheduled for SBRT. Additionally, the inclusion of patients from 3 different institutes has minimized the risk of bias by local institutional practice patterns.

Limitations of this study are those inherent in its retrospective nature. Additionally, central lung tumors treated with SBRT are less frequent compared to the peripheral tumors or patients treated with surgery. This is reflected in a smaller group for our model building, which makes it harder to create a good fitting model. However, the total patient group of > 300 patients with central lung tumors represents the largest reported series in literature so far.

Whether a nomogram is acceptable to use in clinical practice, is depending on several conditions. First, the performance of competing prediction tools available for this patient group should be weighed with the performance of the new nomogram. Secondary, prior to clinical application a nomogram should be tested in an external cohort (44). Regarding our nomogram, no other OS nomograms are available in this specific patient group and therefore a comparison is not possible. In addition, no other studies have demonstrated > 2 independently predictive factors for OS after SBRT in central lung tumors. Our nomogram was tested in an external cohort, which showed equal outcomes. Broad applicability of this tool within different institutes was shown and therefore we believe this model could be used to support clinical decision making.

In conclusion, to facilitate informed treatment decisions, we developed and externally validated a model that can predict the OS-probabilities for an patient having a centrally located NSCLC which will be treated with SBRT. The prognosis is made based on 5 factors of which the relation with OS in NSCLC was already known in literature, but are now combined within a nomogram specific for centrally located NSCLC treated with SBRT. The factors age, PTV, performance status, tumor lobe location and PTV D_{mean} will give a clear prediction for 6-month, 1-year, 2-year and 3-year OS.

3

CHAPTER 3

Prognostic factors of local control and disease free survival in centrally located non-small cell lung cancer treated with stereotactic body radiation therapy

M. Duijm [1], N.C. van der Voort van Zyp [2], P.V. Granton [1], P. van de Vaart [2], M.E. Mast [2], E. Oomen-de Hoop [1], M.S. Hoogeman [1], J.J. Nuyttens [1]

[1] Department of Radiation Oncology, Erasmus MC Cancer Institute, Rotterdam, The Netherlands
2 Department of Radiation Oncology, Haaglanden MC, The Hague, The Netherlands

Acta Oncologica, Vol. 59, No. 7, pp. 809 – 817, 2020

Abstract

Background

Stereotactic body radiation therapy (SBRT) results in high local control (LC) rates in patients with non-small cell lung cancer (NSCLC). For central lung tumors, risk-adapted fractionation schedules are used and underdosage to the planning target volume (PTV) is often accepted to respect the dose constraints of the organs at risk in order to avoid high rates of toxicity. The purpose of this study was to analyze the effect of PTV underdosage and other possible prognostic factors on local- and disease control after SBRT in patients with central lung tumors.

Material and Methods

Patients with centrally located NSCLC treated with SBRT were included. The doses were converted into biologically equivalent dose using α/β-value of 10 Gy (BED_{10}). Underdosage to the PTV was defined as the (percentage of) PTV receiving less than 100 Gy BED_{10}; (%)PTV < 100 BED_{10}. Potential prognostic factors for LC and Disease Free Survival (DFS) were evaluated using Cox regression analysis.

Results

Two hundred and twenty patients received ≤ 12 fractions of SBRT. LC-rates were 88% at 2 years and 81% at 3 years. Twenty-seven patients developed a local recurrence. Both the PTV < 100 BED_{10} and %PTV < 100 BED_{10} were not prognostic for LC. Tumor size and forced expiratory volume in 1 second (FEV_1) were independently prognostic for LC. Disease progression was reported in 75 patients with DFS-rates of 66% at 2 years and 56% at 3 years. Disease recurrence was independent significantly associated with larger tumor diameter, lower lobe tumor location and decreased FEV_1. Grade 4-5 toxicity was reported in 10 patients (8 with ultra-central tumors) and was fatal in at least 3 patients.

Conclusion

Decrease in tumor coverage was not correlated with the local recurrence probability. The LC and DFS were promising after SBRT of centrally located NSCLC with tumor size, FEV_1 and tumor location (for DFS only) as prognostic factors.

3.1 Introduction

Stereotactic body radiation therapy (SBRT) is the golden standard in patients having early stage non-small cell lung cancer (NSCLC) not suitable for surgery (10, 11). Over more than 15 years ago, reports of high-grade toxicity after stereotactic radiotherapy resulted in the definition of a 'central lung tumor' together with the proposal of risk-adapted fractionation schedules (13, 45) and accompanying dose constraints for organs at risk (OAR) (46). Despite these risk-adapted schedules and dose constraints, high-grade toxicity has been reported in recent prospective studies (16, 17, 39). This resulted in a higher awareness for toxicity in the treatment of central tumors, wherein prioritizing dose constraints of the OAR over tumor coverage is recommended.

Additionally, a clear fractionation consensus for centrally located lung tumors is missing. As such, risk-adapted schedules vary between institutes. These different risk-adapted schedules are not all resulting in the same biologically equivalent dose (using an α/β-ratio of 10 Gy; BED_{10}). Multiple studies report high local control (LC) rates when prescribing a minimum of 100 Gy BED_{10} (35, 47-49). However, a fractionation schedule with a minimum dose of 100 Gy BED_{10} covering more than 95% of the planning target volume (PTV), can still result in a wide variety of dose distributions to the PTV. This variety of dose in combination with the heterogeneity of stereotactic treatment plans, asks for additional PTV parameters to define the optimal treatment plan that gives adequate local tumor control (50). Therefore, additional PTV parameters, such as D_{mean} (19, 50) and $D_{95\%}$ (19), have been proposed by various studies in the stereotactic treatment of NSCLC. Additionally, the ICRU 91 suggests the use of the median dose to the PTV ($D_{50\%}$) as a representative absorbed-dose value for the PTV (51).

Taking the increased priority of the OAR dose constraints and the previous mentioned studies in mind, the question can be raised whether only a prescribed dose of more than 100 Gy BED_{10} is enough for adequate tumor control. Moreover, prioritizing the OAR constraints can result in a reduced PTV coverage and the effect of this underdosage on the LC probability is unknown. The purpose of this research is to determine the effect of reduced tumor coverage and other possible prognostic factors on local and disease control in patients with centrally located NSCLC treated with SBRT.

3.2 Material and Methods

We identified patients having $T_{1\text{-}4}N_0M_0$ NSCLC treated between 2006 and 2016 with risk-adaptive stereotactic radiotherapy in 2 Dutch centers: Erasmus Medical Center (EMC) and Haaglanden Medical Center (HMC). Tumors were considered central when the tumor was located within 2 cm of the esophagus and/or the bronchial structures (trachea, main bronchus, bronchus intermedius or upper-, middle-, or lower- lobe bronchi). Patients were excluded if they had: a second lung nodule, previous radiation with overlapping fields,

chemotherapy during SBRT and if they did not have any follow-up. Diagnostic work-up consisted of a PET scan. An MRI scan of the brain was not performed in these patients without nodal disease.

Treatment planning and delivery of both centers have been previously described (29, 52). Briefly, the treatment in the HMC was initially delivered with a stereotactic linear accelerator (Novalis, Brainlab AG, Munich Germany), that was replaced by a linear accelerator with cone-beam CT-guidance (Elekta AB, Stockholm, Sweden) in 2013. Patients were treated with 60 Gy in 8 fractions 3 times a week or, 60 Gy in 12 fractions 4 times a week if the PTV overlapped with or was too close to the OAR. The PTV consisted of an internal target volume (ITV) that was expanded with 5 mm (6 mm in craniocaudal direction) for the Novalis linear accelerator and 6 mm in all directions for the Elekta linear accelerator. Until 2014, the ITV was created by expanding the gross tumor volume (GTV) based on 6 scans taken randomly during the breathing cycle. Thereafter, the ITV was created by contouring the tumor in 10 respiratory phases of the 4D CT scan. The treatment dose was prescribed to the 100% isodose line and the maximum dose was not allowed to exceed 140%. At least 95% of the PTV had to receive 100% of the prescribed dose and 99% of the PTV had to receive 90% of the prescribed dose. In EMC, patients were treated with the Cyberknife Robotic Radiosurgery System (Accuray Inc, Sunnyvale, AC) with 5 fractions of 9 – 12 Gy or, when the tumor was close to the esophagus, 6 – 7 fractions of 7 – 8 Gy, except in 2 patients who received 3 fractions of 20 Gy. The PTV consisted of the GTV plus 5 mm. The dose to the PTV was prescribed to the 70 – 90% isodose line covering at least 95% of the PTV. At both institutions, underdosage was allowed in order to meet the dose constraints of the OAR (*Appendix 3A*) or an acceptable dose to the OAR at the discretion of the treating physician.

Follow-up was generally performed 3 weeks, 3, 6, 12, 18 and 24 months following SBRT and annually thereafter. Patient records from hospitals and general practitioners were screened for disease control, survival status and toxicity. A local recurrence was defined as a recurrence within or adjacent to the PTV. Disease progression was defined as a tumor recurrence in any part of the body. In the absence of a biopsy, (local) tumor recurrence was defined as a 20% increase in tumor size on the CT scan compared with the previous CT scan according to the Response Evaluation Criteria In Solid Tumors (RECIST, version 1.0). In addition, a corresponding avid lesion on the PET scan was required. In order to visualize the location of all the local recurrences, we contoured the center of the treated tumor as a small 3D circle (diameter 7 mm) on one CT scan. Local control was calculated from the start of SBRT until the moment of diagnosis of the local recurrence. For patients without an event, the last date of a follow-up visit in the hospital was used. Overall survival and disease free survival (DFS) were calculated using the first date of SBRT and the date of death or disease progression, respectively. For patients without an event, the last date of follow-up visit or

the last date of contact was used. As the last date of follow-up contact was used, death was not a competing risk for disease recurrence. Underdosage of the tumor is described as absolute and relative volume of the PTV receiving less than 100 Gy BED_{10}. All cases with grade 3 or higher toxicity according to the definition of the Common Terminology Criteria for Adverse Events (version 4.03) were scored. Toxicity was considered acute if it occurred within 3 months from the start of the SBRT and late if it occurred thereafter.

Because of variations in the treatment schedules, all doses were converted into a BED_{10} using the following formula: $BED = D \times (1 + \frac{d}{\alpha/\beta})$ with D = total dose, d = dose per fractions and α/β-value is 10 Gy. Dosimetric PTV parameters were derived from the dose volume histogram (DVH) of each patient: maximum and minimum point dose (D_{max}, D_{min}), mean dose (D_{mean}), dose to 2 / 50 / 98 percent of the PTV ($D_{2\%}$ / $D_{50\%}$ / $D_{98\%}$) and volume of the PTV receiving less than 100 Gy BED_{10} (PTV < 100 BED_{10}).

Cox regression was used to determine LC and DFS and to test possible prognostic factors for (local) disease control. The following factors were entered into the univariate analyses: age, gender, previous (lung)malignancies, WHO status (0 versus ≥ 1), charlson comorbidity score (CCS; 0 – 2 versus ≥ 3), chronic obstructive pulmonary disease (COPD; GOLD 0 – 1 versus 2 – 4), forced expiratory volume in 1 second (FEV_1), endobronchial tumor location, availability of pathology, localization of the tumor in the upper/middle lobe or mediastinum versus the lower lobe, disease stage (TNM 8^{th}; IA – IIA versus IIB – IIIA), tumor size, PTV volume, prescribed dose (< 100 Gy BED_{10} versus ≥ 100 Gy BED_{10}), D_{max} BED_{10}, D_{min} BED_{10}, D_{mean} BED_{10}, $D_{2\%}$ BED_{10}, $D_{50\%}$ BED_{10} (as a continuous variable and dichotomized to < 100 Gy BED_{10} versus ≥ 100 Gy BED_{10}), $D_{98\%}$ BED_{10}, PTV < 100 BED_{10} and percentage of the PTV receiving less than 100 Gy BED_{10} (%PTV < 100 BED_{10}). The univariate analyses was followed by a multivariate analyses (MVA) with backward selection for all factors having a *p*-value < 0.20. When multiple correlating variables were significant in univariate analyses, only the factor with the highest clinical relevance was entered in the MVA. The proportional hazards assumption, assuming that the hazard between the groups is constant over time, was checked for each variable that was entered into the Cox regression. Kaplan-Meier estimates were calculated for all clinical outcomes and curves were compared using log-rank tests. Tumor size was not only analyzed as a continuous variable, but also dichotomized with a cutoff of 5 cm, such that we could examine the relevance of this cutoff criteria used by the RTOG 0813 study for inclusion (in which tumors had to be ≤ 5 cm) (16). In all analyses a *p*-value ≤ 0.05 was considered statistically significant. Analyses were performed using IBM SPSS statistics version 25.0.0.1 software package (SPSS Inc., Chicago, IL). This retrospective study received approval from the medical ethical committees of both centers.

3.3 Results

For this analysis 220 patients were eligible. Patient- and treatment characteristics are shown in *Table 1*. The diagnosis was confirmed by pathology in 58% of patients. All but one patient had a diagnostic PET-CT scan. In this patient pathology was available. The majority of the patients was diagnosed with stage I (38%) or stage II lung cancer (52%). The most commonly used fractionation schedules were 5 fractions (37%), 8 fractions (31%) and 12 fractions (15%).

Local control rates were 92% at 1 year, 88% at 2 years and 81% at 3 years. Twenty-seven patients (12%) were diagnosed with a local recurrence. No clear pattern of local relapse could be visualized when delineating all recurrences on one CT scan (*Figure 1*). Relative and absolute PTV underdosage were both not prognostic for a local recurrence (PTV < 100 BED_{10} *p*-value = 0.593 and %PTV < 100 BED_{10} *p*-value = 0.127). The median PTV receiving less than 100 Gy BED_{10} was 4.2 cc in patients with a recurrence compared to 1.2 cc in patients without a recurrence. The median percentage of the PTV receiving less than 100 Gy BED_{10} was the same in patients with and without a local recurrence (both 2%, *Table 2*).

Figure 1 – Pattern of recurrence: a) anterior view and b) lateral view

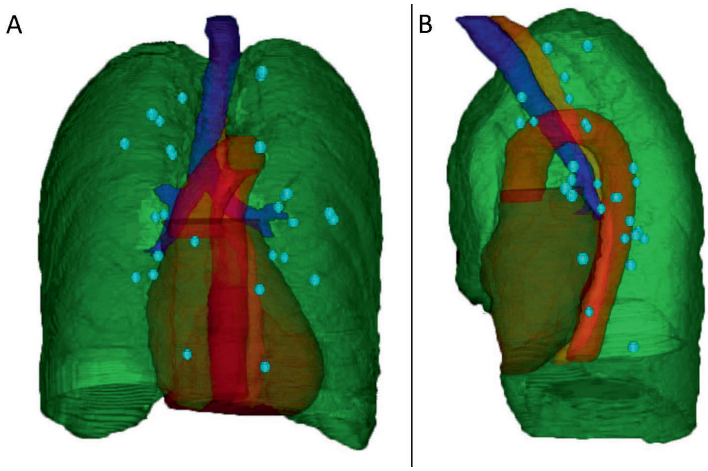

Small light blue circles represent the center of mass of each tumor reporting local recurrence. Color legend organs at risk: orange = esophagus, dark blue = bronchial tree (trachea, main bronchus, bronchus intermedius or upper-, middle- or lower- lobe bronchi), light red = aorta, dark red = heart.

Factors prognostic for the development of a local recurrence using univariate analysis were a larger tumor diameter (continuous variable), higher disease stage, a tumor localized in the lower lobe and a prescribed dose of < 100 Gy BED_{10} (*Table 2*). The 1 year LC rate was significantly higher for tumors < 5 cm compared to tumors ≥ 5 cm (96% versus 84%, *p*-value < 0.001, *Figure 2a*). When the prescribed dose was lower than 100 Gy BED_{10}, patients were twice as likely to develop a local recurrence: Hazard Ratio (HR) 2.24, 95% Confidence Interval (CI) 1.02 – 4.95, *p*-value = 0.045. A PTV $D_{50\%}$ of < 100 Gy BED_{10} was not prognostic

for local recurrence (LC at 1 year 85% for $D_{50\%}$ of < 100 Gy BED_{10} versus 93% for $D_{50\%}$ of ≥ 100 Gy BED_{10}, *p*-value = 0.139, *Figure 2b*).

Table 1 – Patient- and tumor-characteristics (n = 220)

	n (%) / median (IQR, range)	
Age (years)	76	(68 – 82, 51 – 94)
Gender		
Female	89	(40%)
Male	131	(60%)
COPD		
No COPD	39	(18%)
GOLD I – II	113	(51%)
GOLD III – IV	61	(28%)
Unknown	7	(3%)
Charlson Comorbidity Index		
0 – 2	128	(58%)
3 – 5	83	(38%)
6 – 9	9	(4%)
WHO performance Scale		
0	74	(34%)
1	117	(53%)
2	14	(6%)
3 – 4	6	(3%)
Unknown	9	(4%)
Tumor histology		
No pathology available	91	(42%)
Squamous cell carcinoma	68	(31%)
Adenocarcinoma	40	(18%)
Large cell carcinoma	18	(8%)
Different	3	(1%)
Disease stage TNM 8th		
IA / IB	83	(38%)
IIA / IIB	115	(52%)
IIIA	22	(10%)
Prescribed amount of fractions		
3 fractions of 20 Gy	2	(1%)
5 fractions of 9/10/11/12 Gy	82	(37%)
6 fractions of 7/8 Gy	17	(8%)
7 fractions of 7 Gy	18	(8%)
8 fractions of 7.5 Gy	69	(31%)
12 fractions of 5 Gy	32	(15%)
Tumor diameter (mm)	44	(33 – 58, 9 – 105)

Abbreviations: COPD = chronic obstructive pulmonary disease, Gy = gray, IQR = interquartile range, PTV = planning target volume

Table 2 – Results of the Cox regression analyses focusing on patient- and dosimetric factors prognostic for local recurrence for patients with $T_{1\text{-}4}N_0M_0$ NSCLC treated with SBRT

Characteristic		Local control		Local progression		Univariate analysis	
		median (IQR) / n (%)		median (IQR) / n (%)		Hazard Ratio (95%CI)	*p*-value
Age		76	(68 – 81)	71	(62 – 77)	0.97 (0.93 – 1.01)	0.091
FEV_1 [a]		64	(50 – 80)	60	(48 – 72)	0.98 (0.96 – 1.01)	0.119
Gender	Male	117	(89%)	14	(11%)	1	
	Female	76	(85%)	13	(15%)	1.18 (0.55 – 2.51)	0.672
Localisation of tumor	UMM	140	(90%)	16	(10%)	1	
	Lower	53	(83%)	11	(17%)	2.26 (1.05 – 4.88)	*0.038*
WHO status [b]	0	64	(86%)	10	(14%)	1	
	1 – 4	120	(88%)	17	(12%)	1.12 (0.51 – 2.45)	0.775
COPD [c]	0 – 1	63	(91%)	6	(9%)	1	
	2 – 4	125	(87%)	19	(13%)	1.30 (0.52 – 3.25)	0.580
Pathology available	No	83	(91%)	8	(9%)	1	
	Yes	110	(85%)	19	(15%)	1.97 (0.86 – 4.51)	0.107
CCS	0 – 2	113	(88%)	15	(12%)	1	
	≥ 3	80	(87%)	12	(13%)	1.14 (0.53 – 2.44)	0.741
Previous malignancies [d]	No	115	(86%)	18	(14%)	1	
	Yes	78	(90%)	9	(10%)	0.84 (0.38 – 1.87)	0.666
Previous lung carcinoma [d]	No	175	(89%)	22	(11%)	1	
	Yes	18	(78%)	5	(22%)	1.51 (0.57 – 4.02)	0.404
Endobronchial tumor	No	154	(87%)	23	(13%)	1	
	Yes	39	(91%)	4	(9%)	1.05 (0.36 – 3.08)	0.923
Disease stage	IA – IIA	122	(93%)	9	(7%)	1	
	IIB – IIIA	71	(80%)	18	(20%)	4.43 (1.97 – 9.94)	*< 0.001*
Tumordiameter (mm)		42	(32 – 54)	54	(38 – 62)	1.04 (1.02 – 1.06)	*0.001*
PTV volume (cc)		75	(42 – 135)	118	(50 – 157)	1.00 (1.00 – 1.01)	0.054
PTV < 100 BED_{10} (cc)		1.2	(0.2 – 27.4)	4.2	(0.4 – 75.4)	1.00 (1.00 – 1.00)	0.593
%PTV < 100 BED_{10}		2%	(0% – 38%)	2%	(1% – 55%)	2.26 (0.79 – 6.43)	0.127
Prescribed dose BED_{10}	< 100	56	(84%)	11	(16%)	1	
	≥ 100	137	(90%)	16	(10%)	0.45 (0.20 – 0.98)	*0.045*
PTV D_{max} BED_{10}		144	(127 – 175)	139	(122 – 157)	0.99 (0.98 – 1.01)	0.193
PTV $D_{2\%}$ BED_{10}		139	(121 – 163)	134	(115 – 152)	0.99 (0.98 – 1.01)	0.203
PTV D_{mean} BED_{10}		122	(102 – 136)	115	(97 – 132)	0.99 (0.97 – 1.01)	0.278
PTV $D_{50\%}$ BED_{10}		123	(103 – 137)	117	(98 – 132)	0.99 (0.97 – 1.01)	0.279
PTV $D_{98\%}$ BED_{10}		100	(84 – 105)	92	(77 – 104)	0.99 (0.97 – 1.01)	0.383
PTV D_{min} BED_{10}		75	(64 – 90)	72	(56 – 85)	0.99 (0.97 – 1.01)	0.186
PTV $D_{50\%}$ BED_{10}	< 100	39	(85%)	7	(15%)	1	
	≥ 100	154	(89%)	20	(11%)	0.49 (0.21 – 1.12)	0.092

[a] 24 cases missing; [b] 9 cases missing; [c] 7 cases missing; [d] proportional hazard assumption is violated

Abbreviations: BED_{10} = biologically effective dose using α/β-ratio of 10 Gy, CCS = charlson comorbidity score, COPD = chronic obstructive pulmonary disease, D_{max} = maximum point dose, D_{mean} = mean dose, D_{min} = minimum point dose, D..% = dose to .. percent of the PTV, FEV_1 = forced expiratory volume in 1 second, NSCLC = non-small cell lung cancer, PTV = planning target volume, PTV < 100 Gy BED_{10} = volume of the PTV which is receiving less than 100 Gy BED_{10}, SBRT = stereotactic body radiation therapy, UMM = upper/middle lobe or mediastinum, %PTV < 100 Gy BED_{10} = percentage of the volume of the PTV which is receiving less than 100 Gy BED_{10}.

Table 3 – Results of the Cox regression analyses focusing on patient- and dosimetric factors prognostic for disease free survival for patients with $T_{1\text{-}4}N_0M_0$ NSCLC treated with SBRT

						Univariate analysis	
Characteristic median (IQR) / n (%)		**Disease control**		**Disease progression**		**Hazard Ratio** (95%CI)	***p*-value**
Age		77	(70 – 81)	72	(64 – 79)	0.98 (0.95 – 1.00)	0.066
FEV_1 [a]		65	(50 – 84)	60	(49 – 72)	0.99 (0.97 – 1.00)	*0.047*
Gender	Male	83	(63%)	48	(37%)	1	
	Female	62	(70%)	27	(30%)	0.77 (0.48 – 1.24)	0.281
Localisation of tumor	UMM	112	(72%)	44	(28%)	1	
	Lower	33	(52%)	31	(48%)	2.36 (1.49 – 3.74)	*< 0.001*
WHO [b]	0	50	(68%)	24	(32%)	1	
	1 – 4	91	(66%)	46	(34%)	1.26 (0.77 – 2.07)	0.354
COPD [c]	0 – 1	52	(75%)	17	(25%)	1	
	2 – 4	88	(61%)	56	(39%)	1.41 (0.82 – 2.42)	0.220
PA available	No	61	(67%)	30	(33%)	1	
	Yes	84	(65%)	45	(35%)	1.22 (0.77 – 1.94)	0.393
CCS	0 – 2	84	(66%)	44	(34%)	1	
	≥ 3	61	(66%)	31	(34%)	0.96 (0.61 – 1.53)	0.877
Previous malignancies	No	85	(64%)	48	(36%)	1	
	Yes	60	(69%)	27	(31%)	0.86 (0.54 – 1.38)	0.527
Previous lung carcinoma [d]	No	131	(66%)	66	(34%)	1	
	Yes	14	(61%)	9	(39%)	0.92 (0.46 – 1.86)	0.821
Endobronchial tumor	No	114	(64%)	63	(36%)	1	
	Yes	31	(72%)	12	(28%)	1.04 (0.56 – 1.94)	0.895
Disease stage	IA – IIA	101	(77%)	30	(23%)	1	
	IIB – IIIA	44	(49%)	45	(51%)	3.23 (2.03 – 5.13)	*< 0.001*
Tumordiameter (mm)		38	(30 – 51)	51	(39 – 61)	1.03 (1.02 – 1.04)	*< 0.001*
PTV volume (cc)		64	(39 – 129)	102	(67 – 154)	1.00 (1.00 – 1.00)	*0.003*
Prescribed dose BED_{10}	< 100	41	(61%)	26	(39%)	1	
	≥ 100	104	(68%)	49	(32%)	0.70 (0.43 – 1.13)	0.144
PTV D_{max} BED_{10}		144	(130 – 173)	140	(122 – 176)	1.00 (0.99 – 1.00)	0.314
PTV $D_{2\%}$ BED_{10}		140	(122 – 164)	136	(115 – 163)	1.00 (0.99 – 1.00)	0.258
PTV D_{mean} BED_{10}		122	(102 – 136)	120	(100 – 135)	0.99 (0.98 – 1.01)	0.253
PTV $D_{50\%}$ BED_{10}		123	(103 – 136)	120	(101 – 136)	0.99 (0.98 – 1.01)	0.252
PTV $D_{98\%}$ BED_{10} [#]		101	(85 – 106)	92	(82 – 105)	0.99 (0.98 – 1.01)	0.244
PTV D_{min} BED_{10}		77	(64 – 89)	73	(62 – 89)	0.99 (0.98 – 1.01)	0.307
PTV $D_{50\%}$ BED_{10}	< 100	28	(19%)	18	(24%)	1	
	≥ 100	117	(81%)	57	(76%)	0.60 (0.35 – 1.01)	0.056

[a] 24 cases missing; [b] 9 cases missing; [c] 7 cases missing; [d] proportional hazard assumption is violated

Abbreviations: BED_{10} = biologically effective dose, CCS = charlson comorbidity score, COPD = chronic obstructive pulmonary disease, D_{max} = maximum point dose, D_{mean} = mean dose, D_{min} = minimum point dose, D..p = dose to .. percent of the PTV, FEV_1 = forced expiratory volume in 1 second, NSCLC = non-small cell lung cancer, PTV = planning target volume, SBRT = stereotactic body radiation therapy, UMM = upper/middle lobe or mediastinum.

The MVA included age, localization of the tumor (upper/middle lobe or mediastinum versus lower lobe), FEV_1, availability of pathology (no versus yes), tumor diameter, %PTV < 100 BED_{10}, PTV D_{min} BED_{10}, prescribed dose in BED_{10} (< 100 Gy versus ≥ 100 Gy) and PTV $D_{50\%}$ BED_{10} (< 100 Gy versus ≥ 100 Gy). Factors independently prognostic for local tumor recurrence in MVA were larger tumor size and lower FEV_1: HR tumor diameter 1.04, 95% CI 1.02 – 1.06, *p*-value = 0.001 and HR FEV_1 0.97, 95% CI 0.95 – 1.00, *p*-value = 0.031.

Disease progression was reported in 75 patients (34%). The DFS was 73% at 1 year, 66% at 2 years and 56% at 3 years. Disease free survival was significantly better for patients with tumors smaller than 5 cm (*p*-value < 0.001, *Figure 2c*). There was a trend for increased DFS in patients who received PTV $D_{50\%}$ of ≥ 100 Gy BED_{10} (*p*-value = 0.053, *Figure 2d*). Factors prognostic for progressive disease using univariate analyses were lower FEV_1, larger tumor size (continuous), larger PTV volume, tumors located in the lower lobe and disease stage IIB – IIIA (*Table 3*). Factors prognostic for progressive disease using multivariate analyses were larger tumor diameter (HR 1.03, 95% CI 1.02 – 1.04, *p*-value < 0.001), lower FEV_1 (HR 0.98, 95% CI 0.97 – 0.99, *p*-value = 0.004) and localization of the tumor in the lower lobe (HR 1.87, 95% CI 1.12 – 3.11, *p*-value = 0.017).

Thirty-eight percent of the patients had a tumor overlapping or adjacent to the proximal bronchial tree (PBT) and/or the esophagus; 67 patients to the PBT, 8 to the esophagus and 9 patients to both. The incidence of the local recurrences of these ultracentral tumors was only slightly higher compared to the central tumors: 14% versus 11%. The LC at 1 year was 91% for ultracentral tumors and 92% for central tumors (*p*-value = 0.095). Although these comparable LC rates, almost all cases (8 of 10) of grade 4-5 toxicity occurred in the group of ultracentral tumors. These 8 patients all had an ultracentral tumor due to proximity to the PTB. Details of the grade 4-5 toxicity cases are outlined below. In the group of 10 patients reporting grade 4-5 toxicity greater concession was done to the %PTV < 100 BED_{10}. The median %PTV < 100 BED_{10} was 26% in patients with grade 4-5 toxicity versus 2% in the rest of the patients. Three of the 10 patients received < 100 Gy BED_{10} in more than 90% of the volume of the PTV and in 3 patients less than 2.5% of the PTV received < 100 Gy BED_{10}.

One patient had grade 4 toxicity and 9 patients had grade 5 toxicity. Grade 4 was scored because of a necrotic post obstruction pneumonia. The PET scan showed a fibrotic mass most likely caused by the radiation. Of the 9 patients with grade 5 toxicity, 3 deaths were likely due to SBRT, while 6 deaths were possibly related to SBRT. The 3 patients with a death likely related to SBRT had hemoptoe 4.5, 9 and 22 months after treatment. The tumor was adjacent to the intermediate bronchus or main bronchus, and there was no evidence of disease recurrence in these patients. Three other patients, having their death possibly related to SBRT, died due to fatal hemoptoe in the presence of disease recurrence. In this group, 2 patients did not have an ultracentral tumor. In the last 3 patients, respiratory failure was the cause of death which was also possibly related to the SBRT. One patient died

due to a COPD exacerbation and 2 patients died of atelectasis in the lung in combination with disease progression. SBRT could not be excluded as a cause of death in these last 3 patients. Grade 3 or higher toxicity was scored in 12% (n = 27) of the patients. The overall survival was 55% at 2 years, 42% at 3 years and 26% at 5 years.

Figure 2 – Kaplan-Meier curves for local control (A, B) and disease free survival (C, D)

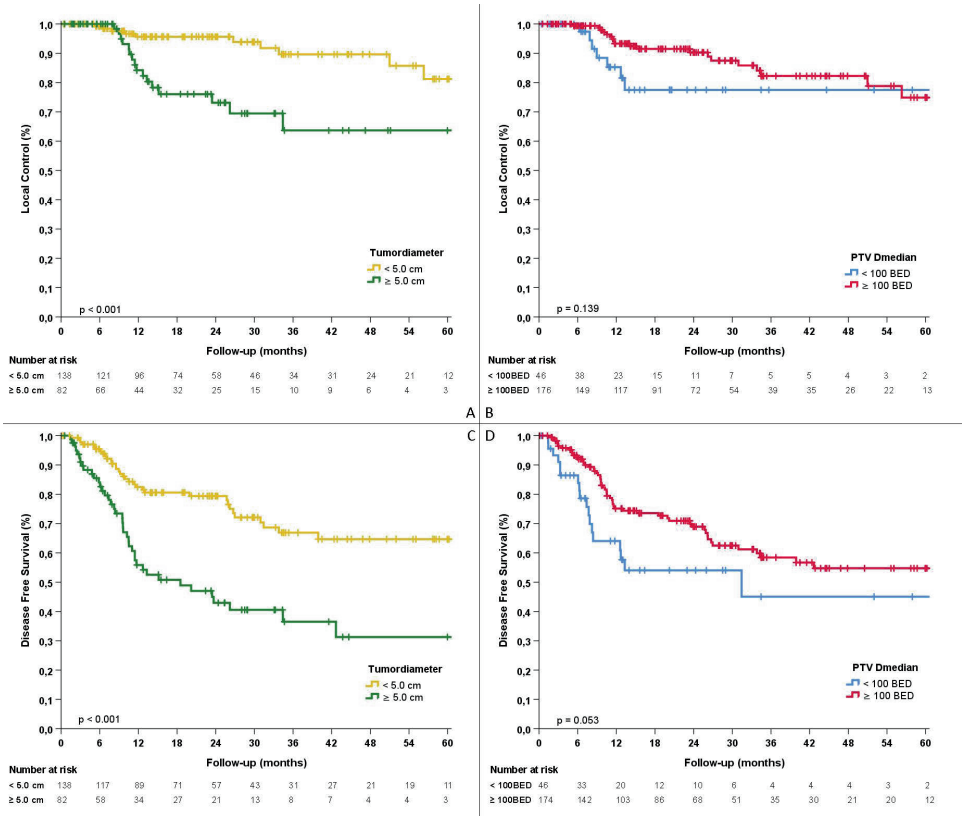

3.4 Discussion

Stereotactic treatment of central lung tumors frequently comes with underdosage of the PTV due to nearby OARs, however as far as we know the consequences of this underdosage were still unknown. Within our cohort, neither the absolute nor the relative amount of PTV underdosage was prognostic for a local recurrence. We did find the following factors to be independent significantly prognostic: larger tumor size and a lower FEV_1 for local and disease recurrence and additionally a tumor location in the lower lobe for disease recurrence.

Our reported LC rates were comparable to other studies (*Table 4*) (19, 27, 28, 35, 37, 39, 43, 47, 53-56). The univariate analysis showed a significant correlation between a prescribed dose of ≥ 100 Gy BED_{10} and local tumor control. Previous studies confirmed the importance of a higher (prescribed) radiation dose on LC within the stereotactic treatment of centrally located NSCLC (19, 47). Tumor size has been frequently analyzed as a prognostic factor for local recurrence in patients with NSCLC treated with SBRT, but data is conflicting (20). Concerning studies only including central lung tumors, tumor size has been analyzed within one small study without finding a correlation (39). The authors stated that the study was underpowered due to the small number of events. For the same reason other central lung tumor studies were unable to define any prognostic factors (38, 57). However, within multiple combined (including both central and peripheral tumors) studies, larger tumor size was prognostic for local recurrence in SBRT treatment as in our analysis (19, 35, 43, 54, 56). Only 2 studies analyzed FEV_1 as a prognostic factor, but without describing the same correlation we found (28, 43). However, a poor FEV_1 is commonly caused by smoking and it is known that people who smoked had worse outcomes (58). Within our analysis, the incidence of local recurrences was almost similar between the ultracentral and central tumors and the LC rates were not significantly different. Other studies comparing LC for patients with an ultracentral versus a central lung tumor after SBRT confirmed these equal LC rates (59-61).

Prognostic factors for DFS after SBRT in NSCLC have rarely been published. Several studies have only reported local-, regional- and distant control as separate analyses while others have reported only the DFS rates without possible prognostic factors. Three studies have confirmed our outcome that a larger tumor is correlated with disease recurrence, 2 analyzing DFS (39, 56) and one analyzing distant control (43). FEV_1 has been analyzed in one study focusing on DFS and one on distant control, but was not prognostic in either study (28, 43). Chang et al. investigated COPD for potential association with DFS, but did not find a relation (38). In our cohort, patients with tumors located in the lower lobe were at higher risk for disease recurrence, this was confirmed by another study (33). An explanation can be the more frequent upstaging due to unsuspected nodal involvement in lower lobe tumors that is seen after surgery. This can also be the case in tumors treated with SBRT (34). With regards to tumor location, other analyses have an inferior local and distant control for central tumors compared with peripheral tumors (55, 56). There was no significant correlation between dose and disease control in our study, which is comparable to other studies analyzing dosimetry as prognostic factor for DFS or distant control (28, 38, 41, 43).

Although some characteristics had missing values, we did enter all characteristics having a *p*-value of < 0.20 into the MVA. This resulted in an analysis based on 196 patients with an adequate number of events (23 local failure events and 66 disease progression events) to run a reliable MVA. However, next to the prognostic patient characteristics, we did not find a relation between local recurrence and dose to the PTV or PTV underdosage. The number of events may be too small for an elaborate MVA and it may not be able to identify a potentially weaker association between dosimetric factors and disease control. In the MVA for both LC and DFS, we only included tumor size and not PTV volume and disease stage as these factors were highly correlated. Of the 3 factors tumor size was chosen as it is the most clinical relevant characteristic. A limitation of this study is its retrospective nature. Additionally, as mentioned in the tables, some characteristics did not fulfill the proportional hazard assumption in the Cox regression. Hence, the parameter being estimated by the Cox procedure may not be a meaningful measure of the between group difference and should be further examined in future research.

Table 4 – Literature analyzing local control after stereotactic treatment of lung tumors

				Potential Prognostic Characteristics										Local control rates	
	Number of patients		Number of local failures	Age	Gen-der	Histo-logy	KPI	FEV_1	Loca-tion	Tumor size	GTV	Tumor stage	Dose	1 year	2 year
Central tumors															
This manuscript	220		27	–	–		– [d]	++	+ [e]	++		+	+ (100 BED_{10}) [f]	92%	88%
Modh et al.[a] (18)	125		19	–	–		–				++		–	86%	79%
Roach et al. (6)	51		4			–				–					85%
Rowe et al. (10)	47 [b]		2										+ (100 BED_{10}) [3)]		94%
Schanne et al. (19)	90		?	–	–	–	–	–				–	+ (D_{max} > 70 Gy)	76%	
Lung tumors	*% central*														
Bral et al. (20)	40	*43%*	3							+ (4cm)		+		97%	84%
Horner et al. (21)	126	*33%*	12	–	–	++	+	–		++			++ (150 Gy) [g]	99%	90%
Olsen et al. (9)	130	*12%*	8	–	–				–	+				75-100%	50-100%
Park et al. (22)	251	*44%*	21						– (C/P)	–			–		88-89%
Samson et al. (23)	245	*52%*	13	–	–	–	–		++ (C/P) – (lobe)	–		–	–		91%
Stephans et al.(24)	603	*26%*	?	–	–		–			–					87%
Ye et al. [c] (25)	127	*40%*	22	+	+				+ (C/P)	++			–		81%
Zhao et al. (14)	1092	*10%*	40	–	–	–			–	+ (2.5cm)	+ ($8.3cm^3$)		+ [h]		97%

Age, tumor size, GTV volume and dose were analyzed as continues variables, unless specified otherwise.

– tested in univariate analysis but not significant, + significant in univariate analysis, ++ significant in multivariate analysis

[a] patients with BED_{10} < 80 (n = 17) were excluded from the local failure analysis; [b] amount of lesions irradiated; [c] local-regional failure as endpoint; [d] WHO status, [e] lower lobe versus other locations, [f] prescribed dose; [g] total dose in EQD_2 at PTV isodose center; [h] significant for various cut-offs: prescribed dose 100 Gy BED_{10}, PTV_{mean} 130 Gy BED_{10}, PTV_{max} 140 Gy BED_{10}, PTV_{min} 73 Gy BED_{10}, PTV D_{95} 87 Gy BED_{10}, PTV D_{99} 76 Gy BED_{10}.

Abbreviations: BED_{10} = biologically equivalent dose using an α/β-ratio of 10 Gy, C/P = central versus peripheral location, EQD_2 = equivalent dose in 2 Gy fractions using α/β – ratio of 10 Gy, FEV_1 = forced expiratory volume in 1 second, GTV = gross tumor volume, KPI = karnofsky performance index, PTV = planning target volume

4

CHAPTER 4

Dose and volume of the irradiated main bronchi and related side effects in the treatment of central lung tumors with stereotactic radiotherapy

M. Duijm [1], W. Schillemans [1], J.G. Aerts [2], B. Heijmen [1], J.J. Nuyttens [1]

[1] Department of Radiation Oncology, Erasmus MC Cancer Institute, Rotterdam, The Netherlands
[2] Department of Pulmonology, Erasmus MC Cancer Institute, Rotterdam, The Netherlands

Seminars in Radiation Oncology, Vol. 26, No. 2, pp. 140 – 148, 2016

Abstract

High radiation dose to the main bronchi can result in stenosis, occlusion or fistulation, and death. Only 8 articles have reported side effects to the main bronchi from stereotactic body radiation therapy (SBRT), mostly with only one symptomatic complication per article. Therefore, we calculated the dose to the bronchial structures, such as trachea; mainstem bronchi; intermediate bronchus; upper-, middle- and lower-lobe bronchus; and the segmental bronchi in 134 patients with central tumors and calculated the normal tissue complication probability (NTCP) for each of these structures, with toxicity determination based upon computed tomography imaging. No side effects were found in the trachea, and only stenosis occurred in the main bronchus and bronchus intermedius. Higher grades of side effects, such as occlusion and atelectasis, were only seen in the upper-, middle-, and lower bronchi and the segmental bronchi. When 0.5 cc of a segmental bronchi was irradiated to 50 Gy in five fractions, it was about 50% likely to be occluded radiographically. For grade 1 radiographically evident side effects, the 50% risk level for a 5-fraction D_{max} was 55 Gy for mid-bronchi and 65 Gy for mainstem bronchi. To assure the relationship between clinical toxicity and side effects to the bronchi, further investigation is needed.

4.1 Introduction

For several years, stereotactic body radiotherapy (SBRT) has been used for the treatment of stage I inoperable non-small cell lung cancer (NSCLC) and solitary lung metastases. This resulted in promising results for the survival and local control (35, 47, 48). However, when treating central lung tumors (13, 46, 54), these results are sometimes combined with high toxicity. Central lung tumors are defined as those tumors being located less than 2 cm from the trachea, mainstem bronchus, main bronchi or esophagus; less than 6mm from the heart or tumors located in the mediastinum (Figure 1). High radiation dose to the main bronchi can result in stenosis, occlusion or fistula formation, and death (45, 54, 62). Not only SBRT causes radiation-induced side effects of the lung and bronchus, but also by other modalities. Gollins et al. (63) reported 38% and 58% bronchial stenosis after intraluminal brachytherapy (ILT) with a single dose of 15 and 20 Gy at 1 cm, respectively. Fibrotic reactions were seen 10 – 13 months post ILT (64).

Figure 1 – Bronchial structures

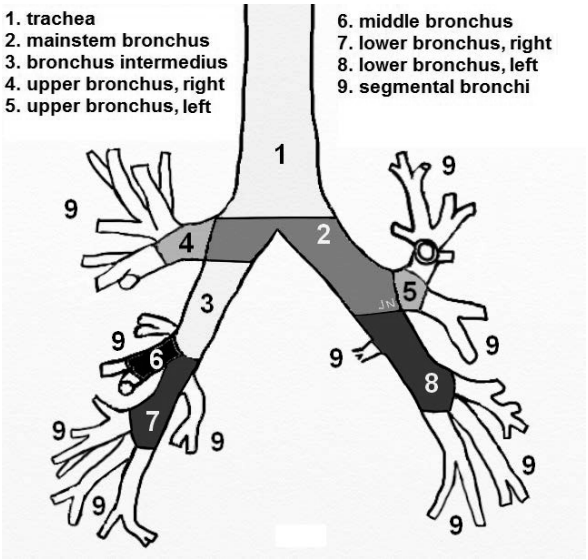

Bronchial stenosis has also been reported after high-dose external beam radiotherapy. Miller et al. (65) used computed tomography (CT) scans to assess the incidence of bronchial stenosis after radiation treatment twice daily with high external beam radiotherapy. They reported a 1-year and 4-year actuarial rate of stenosis of 7% and 38%, respectively, with a median overall survival of 2.5 years. A suggestion for a dose-response effect was also found: 4% and 25% at a dose of approximately 74 Gy and 86 Gy, respectively. Kelsey et al.(66) analyzed the bronchial stenosis of the mainstem bronchus in 18 patients with CT-scans and

found in 17 of the 18 patients a decrease in the airway caliber ranging from 6% – 57%. The stenosis appeared to be dose dependent (p = 0.08), progressed with increasing time after radiotherapy (p = 0.04) and was worse in patients who also received chemotherapy (p = 0.04). Although 17 of the 18 patients were diagnosed with stenosis, only 2 were known to have symptomatic bronchial stenosis.

Despite those records, there is still no clear consensus about the dose-related side effects of the bronchial structures in SBRT. Therefore, the aim of this study was to calculate the dose to the bronchial structures, such as trachea; mainstem bronchi; intermediate bronchus; upper-, middle- and lower-lobe bronchus and the segmental bronchi, to determine the time for the onset of side effects and to calculate the normal tissue complication probability (NTCP) of the side effects as seen on a CT scan for each of these structures.

4.2 Methods

Patients

From July 2006 – December 2012, 134 patients with 143 central tumors were treated with SBRT on a robotic Cyberknife (Accuray Inc, Sunnyvale, CA) treatment unit (67). The planning target volume (PTV) was constructed by adding a 5 mm margin to the gross tumor volume (GTV). The PTV dose was prescribed at the 70% – 95% isodose line, which covered at least 80% of the PTV. It was allowed to underdose the GTV or PTV or both to respect the constraints of the organs at risk (OAR). For the first 102 patients, dose calculations were performed using the ray-tracing algorithm implemented in the MultiPlan treatment planning system. For the other patients, a novel Monte Carlo (MC) dose-calculation algorithm was used in MultiPlan.

According to the tumor location, various dose-prescription schedules were used. Tumors located near the esophagus (less than 2 cm) were in the first part of the study treated with 6 fractions of 8 Gy (n = 26), later with 7 fractions of 8 Gy (n = 8), and when the MC calculation algorithm was available with 7 fractions of 7 Gy (n = 9). All other central tumors (close to the mainstem bronchus, but not the esophagus) were initially treated with 5 fractions of 9 Gy (n = 5). This dose was subsequently escalated to 5 fractions of 10 Gy (n = 18) and later to 5 fractions of 12 Gy (n = 23). When the MC calculation algorithm was available, these tumors were treated with 5 fractions of 11 Gy (n = 19). A patient was treated with 3 fractions of 20 Gy. Over time, the constraints to the OAR changed, because no severe toxicity was seen and the prescription changed due to the use of the MC calculation algorithm. The current dose constraints for the bronchial structures and OAR are shown in Table 1.

Table 1 – Currently used dose constraints

		Dose Constraints for	
		55 Gy (5 fractions)	49 Gy (7 fractions)
Organ	Volume	Total dose (Gy)	Total dose (Gy)
Spinal Cord	Any point	27.5	32.9
Esophagus	Any point	35	42
Trachea	Any point	45	49
Main bronchus	Any point	55	49
Brachial plexus	Any point	30	35
Lung	30 %	16	18

Dose (re)-calculation for the study

For the purpose of the study, dose distributions for the first 102 patients, planned with the ray-tracing algorithm, were re-calculated with the more advanced MC dose-calculation algorithm. To compare doses in the OAR across the various fractionation schemes, all doses were converted into an equivalent dose of 2 Gy (EQD_2) and a Biologically Equivalent Dose (BED). The BED and EQD_2 were calculated using the following formulas: $BED = D * (1 + (d/(\alpha/\beta))$ and $EQD_2 = D * (d + \alpha/\beta)/(2.0 + \alpha/\beta)$ where D = total dose and d = dose per fraction. For the tumors and normal tissues, we assumed α/β ratios of 10 and 3 (late side effects), respectively. The D_{max} was the maximum dose of a structure in a point calculated by the planning system. Apart from D_{max}, the volumes receiving an EQD_2 of 65, 80, 90, 100, and 130 Gy, and the volume receiving a BED of 100 Gy were calculated. Patients whose bronchial structures received an EQD_2 lower than 65 Gy were excluded in the analyses.

Assessment of side effects of the bronchi and survival

In total, 690 bronchial structures were delineated in the planning CT-scan together with the PTV and GTV, and the structures 397 that had V_{65} Gy ≥ 0 cc were included in the analysis. The bronchial structures were divided into 4 groups based on diameter: (T) trachea; (MI) mainstem bronchus and intermediate bronchus; (UML) upper-, middle-, and lower lobe bronchi; and (SB) segmental bronchi (branches of the upper-, middle-, and lower bronchi). This difference was made because of the anatomical difference between those structures. To evaluate the late side effects in the bronchial structures, CT scans were compared with the planning CT scan and 3 side effects were scored: (1) stenosis, (2) occlusion without atelectasis in the same segment and (3) occlusion with atelectasis in the same segment. For each patient, all available CT scans after the SBRT were scored based on side effects of the irradiated bronchi. A bronchus was not scored if the bronchus was a branch of an already occluded bronchus with atelectasis. By scoring all the available CT scans, we wanted to measure the different time points of the development of the side effects. All available CT

scans were independent scored by 2 researchers (M. Duijm and J. Nuyttens) and at different time periods.

The first moment of the occurrence of a side effect for all structures was calculated using a Kaplan-Meier curve, with the follow-up until the moment of side effects, or when no side effects were reported until death or last follow-up CT scan. For the UML and SB, the moment of atelectasis was calculated in the same manner as described earlier, with the moment of atelectasis vs no side effect or, stenosis or occlusion. The log-rank test was used for the statistical significance of differences between the curves.

Overall survival was calculated, using Kaplan-Meier curves, from the first day of treatment until the patient died. Patients lost in follow-up or patients who were still alive were censored on the last day of contact. The group was split into patients with and without measured side effects on the CT scan to determine the effect of side effects on the survival. We evaluated the cause of death of each patient, to ensure radiation was not (a part of) the cause of death.

4.3 Results

After (re-)calculation with the MC dose-calculation algorithm, 109 of the 134 patients had one or more bronchial structure(s) that received at least a total EQD_2 of 65 Gy_3. Of the 109 patients, side effects of the bronchial structures could be evaluated in 104 patients with 109 tumors. The CT scans of the remaining 5 patients were missing, because 2 patients died within 2 months after radiotherapy and no imaging was made. Only a chest X-ray was done in the other 3 patients, 2 of them died in less than 7 months after radiotherapy, and despite the 60-months survival of the last patient, no CT scan was done because of high comorbidity.

The patient characteristics are shown in *Table 2*. The median D_{max} in EQD_2 of the 4 groups, (T) trachea; (MI) mainstem bronchus and intermediate bronchus; (UML) upper-, middle-, and lower-lobe bronchi; and (SB) segmental bronchi, are 93 Gy_3, 103 Gy_3, 124 Gy_3 and 121 Gy_3, respectively. The details of the D_{max} and the median volume of the structures irradiated to the different EQD_2 levels are shown in *Table 3*.

In total 207 CT scans were scored, with a mean of 14.2 months after radiotherapy (minimum 0.77 months – maximum 68.1 months). Side effects were found in 59 patients (56.7%). No side effects were found in group T. In this group, the median V_{65} EQD_2 was 0.365 cm^3 and the median V100 EQD_2 was 0.077 cm^3.

Table 2 – Patient and tumor characteristics

Patient characteristics		
Median age, y (range)	73	(34 – 88)
Male / female	59 / 45	
Charlson comorbidity score		
> 4	14	(14%)
3 – 4	17	(16%)
1 – 2	51	(49%)
0	22	(21%)
Cumulative illness score		
> 6	14	(14%)
5 – 6	19	(18%)
0 – 4	71	(68%)
Tumor characteristics		
Histology		
Large-cell carcinoma	15	(13.5%)
Squamous-cell carcinoma	27	(25%)
Adenocarcinoma	15	(13.5%)
Undifferentiated carcinoma	3	(3%)
Others	3	(2%)
No biopsy or inconclusive biopsy	47	(43%)
Primary / metastatic lung cancer	63 / 46	
Median gross tumor volume, cm^3 (range)	31	(1 – 367)
Median planned tumor volume, cm^3 (range)	67	(5 – 523)
Median tumor diameter, cm (range)	46	(10-105)

Table 3 – Median observed D_{max} and the dose and volume in cm_3 per structure group

	Trachea	**Main and intermediate bronchus**	**Upper, middle, and lower bronchi**	**Segmental bronchi**
D_{max} (EQD_2)	93	103	124	121
range	66 – 137	65 – 173	67 – 233	39 – 245
D_{max} (BED)	155	172	206	202
range	111 – 228	109 – 288	112 – 388	80 – 408
Median V_{65}	0.365	0.820	0.633	0.307
range	0.003 – 4.602	0.002 – 8.457	0.001 – 5.791	0.001 – 1.890
number of structures V_{65} > 0	25	67	130	201
Median V_{80}	0.236	0.615	0.502	0.294
range	0.001 – 2.253	0.001 – 7.775	0.001 – 5.131	0.001 – 1.890
number of structures V_{80} > 0	18	55	113	175
Median V_{90}	0.063	0.408	0.518	0.294
range	0.004 – 1.213	0.004 – 6.122	0.001 – 4.607	0.002 – 1.890
number of structures V_{90} > 0	15	49	100	161
Median V_{100}	0.077	0.280	0.453	0.274
range	0.002 – 0.731	0.003 – 3.626	0.002 – 4.145	0.001 – 1.890
number of structures V_{100} > 0	8	36	92	142
Median V_{130}	0.010	0.041	0.075	0.186
range	0.010 – 0.010	0.003 – 1.743	0.001 – 2.878	0.001 – 1.184
number of structures V_{130} > 0	2	14	51	84

In all structures except group T some side effects were found, but only the group of UML and SB reported occlusion and atelectasis. Side effect were found after 1 year in 31% of the structures and after 2 years in 42.7% of the structures side effects were found. *Figure 2* shows the first moment of side effects for the different structure groups. After 1 year, side effects occurred for the MI, UML, and SB in 14.6%, 29.1% and 41.4% of the structures, respectively, and in 29.5%, 49.8%, and 47.5% of the structures after 2 years (p = 0.021). The median time for the first occurrence of a side effect was 26 and 25 months for the UML and SB, respectively.

Figure 2 – a) First moment of side effects per structure group; b) Moment until the occurrence of atelectasis

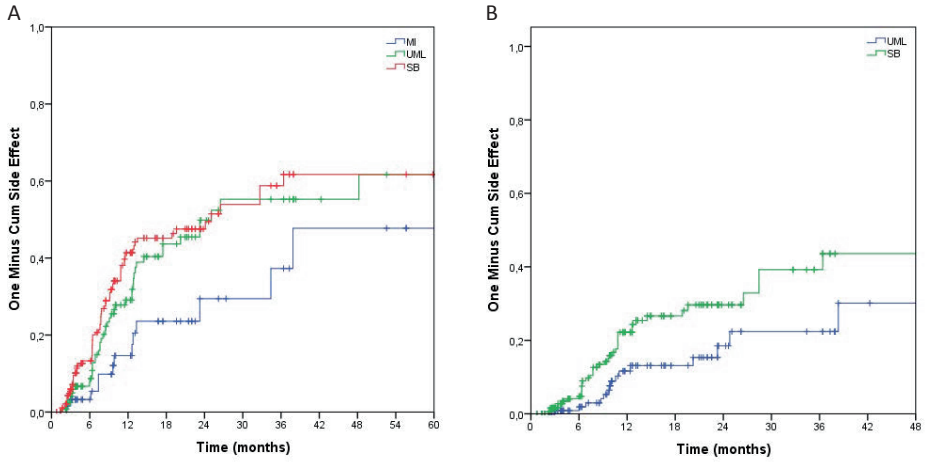

Abbreviations: MI = mainstem bronchus and intermediate bronchus; UML = upper, middle and lower lobe bronchi; SB = segmental bronchi

The median volume for the MI was 0.820 cm^3 at the V_{65} EQD_2, 0.280 cm^3 at the V_{100} EQD_2 and 0.041cm^3 at the V_{130} EQD_2. Stenosis was found in 13 of the 67 MI structures. Of the 130 structures in the UML group, 22 showed stenosis, 6 showed occlusion, and 15 showed atelectasis at the end of the follow-up. The median volume was 0.633 cm^3 at the V_{65} EQD_2, 0.453 cm^3 at the V_{100} EQD_2 and 0.057 cm^3 at the V_{130} EQD_2.

The SB groups contained 200 structures, of which 10 showed stenosis at the end of the follow-up, 22 showed occlusion and 42 showed atelectasis. The median V_{65} EQD_2 was 0.307 cm^3, the median V_{100} EQD_2 was 0.274 cm^3 and the median V_{130} EQD_2 was 0.186 cm^3.

Figure 2 shows the time to atelectasis for the UML and SB. In the UML, atelectasis was found after 1 year in 11.6% of the structures and in 18.5% after 2 years. In the SB, atelectasis was found after 1 year in 24.3% of the structures and in 29.7% after 2 years. The 2 groups had a significant different incidence of side effects (p = 0.018).

We compared the patients with side effects and without side effects and found several significant differences for different structures. The details are shown in *Table 4*. The D_{max} and irradiated volumes at different dose levels were significantly different in the UML group and SB group when comparing structures with toxicity and without toxicity. A 25% probability of complication (stenosis) was found at a D_{max} for the MI group of 136 Gy. For the UML group (mid-bronchi), a 25% probability of complication (any) was found at a D_{max} of 110 Gy, and for the SB group, a 25% probability of complication (any) was found at a D_{max} of 55 Gy. The details of the NTCPs are shown in *Figures 3 – 5*.

Table 4 – Volumes and dose of irradiated bronchi related to side effects

	D_{max} EQD_2	D_{max} BED	V_{65} EQD_2	V_{80} EQD_2	V_{100} EQD_2	V_{100} BED
Trachea						
Mean without side effects	93	155	1.063	0.545	0.166	1.422
Mean with side effects	n.a.	n.a.	n.a.	n.a.	n.a.	n.a.
Percentage of structures with side effects	0	0	0	0	0	0
Main bronchus or bronchus intermedius						
Mean without side effects	105	175	1.3	0.967	0.573	1.5
Mean with side effects	116	194	2.1	1.315	1.247	2.3
Percentage of structures with side effects	20	20	20	22	22	20
p-value	0.100	0.100	0.130	0.170	0.100	0.120
Upper-, middle-, and lower- bronchi						
Mean without side effects	113	189	0.7	0.649	0.5	0.766
Mean with side effects	143	239	1.15	1.055	0.891	1.2
Percentage of structures with side effects	33	33	33	36	40	33
p-value	> 0.0001	> 0.0001	0.007	0.015	0.014	0.010
Segmental bronchi						
Mean without side effects	121	202	0.326	0.302	0.287	0.365
Mean with side effects	135	225	0.438	0.442	0.409	0.456
Percentage of structures with side effects	37	37	37	38	43	37
p-value	0.011	0.011	0.008	0.002	0.011	0.036

The overall survival for the 104 patients was 74% at 1 year and 51% at 2 years. Looking at the patients with measured occlusion or atelectasis or both on their upper-, middle-, lower bronchi or segmental bronchi compared with the other patients, there was no difference in overall survival ($p = 0.964$). Also, 74 of the 104 patients died – 36 of them as a consequence of malignancy, 15 died of progression of the primary tumor, 16 died of metastasis, and 5 patients died due to a secondary malignancy. A total of 5 patients died due to a pneumonia and 1 patient died due to hemoptysis. A total of 32 patients died due to others causes (cardiac, stomach bleeding, sepsis, liver failure, etc.). The cause of death in 8 patients was unknown.

Figure 3 – The NTCP of the main bronchi according to D_{max}, V_{65}, V_{80}, V_{100} for the end point adverse event (AE) of radiographically evident stenosis.

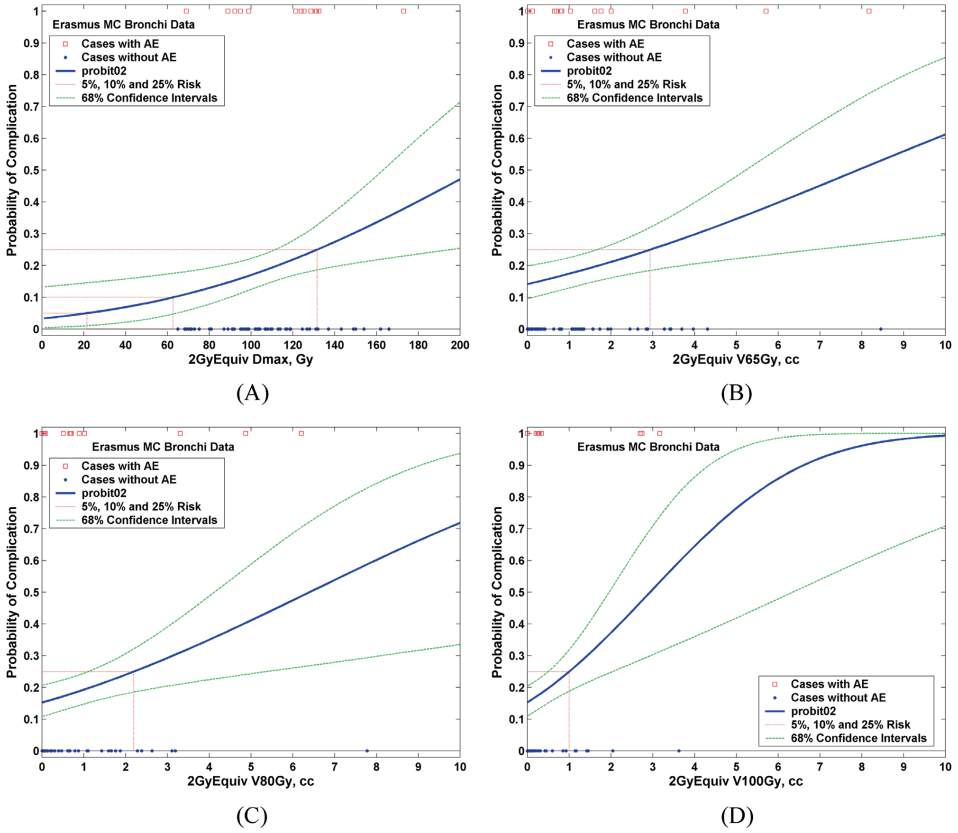

Figure 4 – The NTCP of the mid-bronchi according to the D_{max}, V_{65}, V_{80}, V_{100} for the end point adverse event (AE) of radiographically event stenosis, occlusion and atelectasis

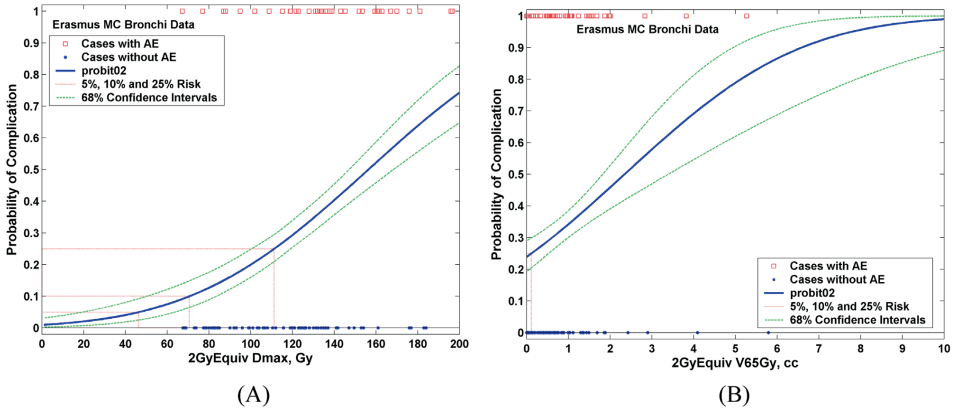

Figure 4 – The NTCP of the mid-bronchi according to the D_{max}, V_{65}, V_{80}, V_{100} for the end point adverse event (AE) of radiographically event stenosis, occlusion and atelectasis (continued)

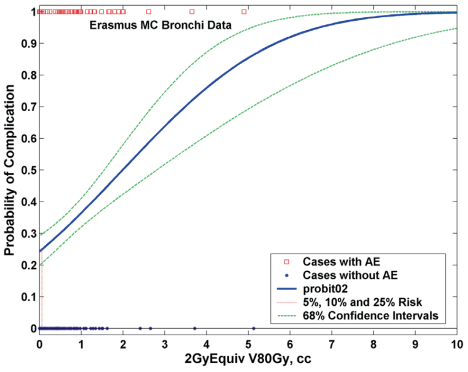

(C)

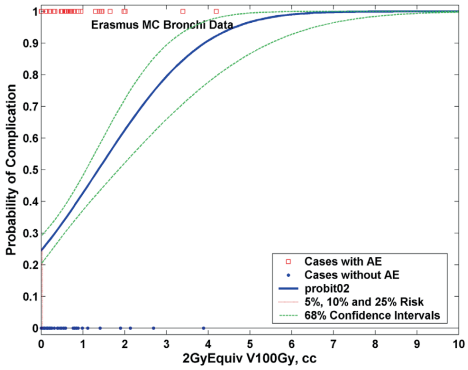

(D)

Figure 5 – The NTCP of the segmental bronchi according to the D_{max}, V_{65}, V_{80}, V_{100} for the end point adverse event (AE) of radiographically event stenosis, occlusion and atelectasis.

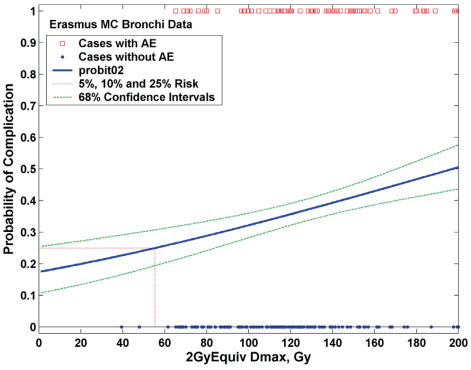

(A)

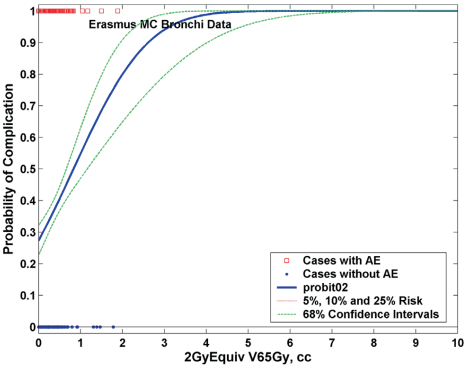

(B)

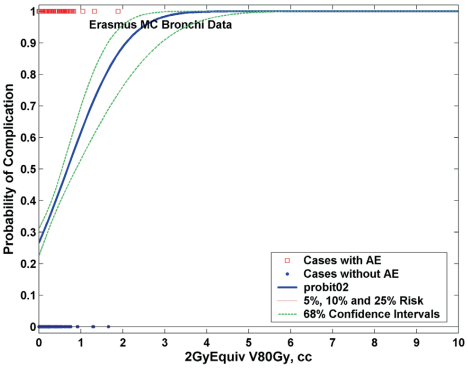

(C)

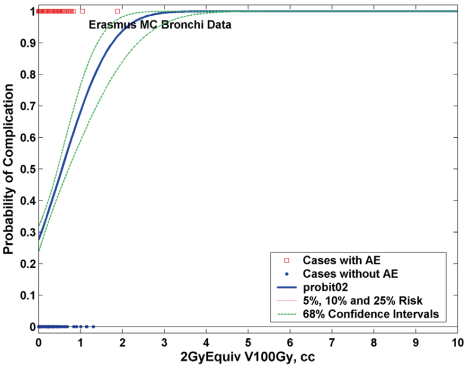

(D)

4.4 Discussion

Multiple studies have described bronchial strictures after radiotherapy, but in most cases the fractionation scheme and D_{max} were the only available parameters. In a study on conventional external beam radiotherapy, bronchial stenosis was found in 8 patients. In the group treated with 74 Gy, 3 patients (4%) were reported with bronchial stenosis, 1 patient (5%) in the group of 80 Gy and 4 patients (25%) in the group of 86 Gy (65). After stereotactic treatment, 3 studies reported the death of 3 patients due to a bronchial stricture. In those patients, the dose in EQD_2 differed from 67 – 84 Gy_3 (35, 64, 68). In another study, several cases of atelectasis were reported. The tumors of these patients were located next to the main bronchi and were treated with 50 – 100 Gy_3 (68). An overview of the side effects to the main bronchi is described in Table 5. Looking at these different studies, no significant cut-off point in the D_{max} can be found.

Table 5 – An overview of the side effects to the main bronchi in SBRT for central lung tumors

Reference	Number of patients with side effects	Description of the side effects	Treatment schedule	Dose in EQD_2
Joyner et al. (69)	1	Stenosis of right lower-lobe bronchus	3 x 12 Gy	108 Gy_3
Song et al. (45)	6	Died due to complete stricture (n = 1)	4 x 12 Gy	144 Gy_3
		Complete (n = 2) and partial (n = 3) stricture	3 x 20 Gy / 4 x 10-12 Gy	104 – 276 Gy_3
Bral et al. (54)	1	Died due to bronchial stenosis	4 x 15 Gy	216 Gy_3
Oshiro et al. (70)	1	Grade 3 stenosis	10 x 6 Gy	108 Gy_3
Unger et al. (62)	1	Fistula mainstem bronchus	4 x 12 Gy	144 Gy_3
Haasbeek et al. (71)	1	Bronchial stenosis with atelectasis	3 x 10-12 Gy	78-108 Gy_3
Lee et al. (41)	1	Died due to bronchus obstruction	5 x 10 Gy	130 Gy_3
	5	Partial stenosis	5 x 10 Gy / 7 x 8 Gy	123-130 Gy_3
Baumann et al. (68)	10	Atelectasis	Unknown	50-100 Gy_3

In this study, not only the D_{max} was an important parameter, but also the volume of the bronchial structure. In the group of the mainstem bronchus and intermedius bronchus, no significantly different numbers were found when comparing the group with side effects and the group without side effects. In the UML and SB group, all the dose levels were significantly different. Figure 3 shows that for mainstem bronchus, the D_{max} EQD_2 = 208.2 Gy corresponded to 50% risk of radiographically evident stenosis; this equates to 65 Gy in 5 fractions. The UML mid-bronchi had lower tolerance to grade 1 side effects, as Figure 4 shows that 50% risk occurs at a lower D_{max} dose of EQD_2 = 156.4 Gy, which would be 55 Gy in 5 fractions. Segmental bronchi were more susceptible to occlusion than the other segments of bronchus. The large percentage volume $D_{50\%}$ had a steeper slope than D_{max}, revealing volume dependence. When 0.5 cc of a segmental bronchi was irradiated to 50 Gy

in five fractions, it was 50% likely to become occluded radiographically, but because of the diversity of bronchi in the anatomy, the occlusion of a few segmental bronchi did not frequently lead to symptomatic side effects. In the segmental bronchi, occlusion with atelectasis was approximately twice as likely as occlusion without atelectasis. The volume-response models were all steeper than the dose-response models, so the volume of bronchi irradiated has an important role for each segment of bronchi that was studied. For some of the side effects, 1 cc of a segment of bronchi irradiated to a particular dose had about 1.33 times the risk as compared with 0.5 cc of the same segment irradiated to the same dose. In other words, doubling the irradiated volume could increase the risk by approximately 33%. When sufficient data with grade 3 or higher complications becomes available, it will be very important to study the volume effects more in detail. Mid-bronchus had visible occlusion in 21 of the 130 contoured structures, and in this segment, occlusion was 2.5 times more likely to occur with atelectasis than without.

A patient died due to hemoptysis. This patient had tumor abutting the pulmonary vein over several centimeters and this patient died suddenly 3 months after the treatment. Fatal hemoptysis (FH) is often reported after ILT and ranges from 7% – 22% (72). After ILT, prognostic factors strongly correlated with FH and were the total BED (p = 0.001), the treatment intent (p < 0.001) and the number of fractions applied (p = 0.001). The median total BED value was 102 Gy in patients with FH whereas it was 66 Gy in patients with no FH (73). Whether our patient died due to a direct complication of the SBRT itself or due to tumor invasion in the blood vessel is a matter of debate, because either the high dose to the blood vessel or tumor invasion into the blood vessel could have been the cause of the death.

A total of 5 patients died due to a pneumonia, an exacerbation of chronic obstructive pulmonary disease (COPD) or shortness of breath related to tumor progression. It is not clear whether late side effects of the radiation contributed to pneumonia and so to death.

The stereotactic treatment with real-time tumor tracking uses small margins because of to the use of in-room interfraction and intrafraction tumor motion compensation by the respiratory tracking system. This system allows treatment with an accuracy of 2 mm or less while patients breath normally and therefore less healthy tissue is irradiated, and so the risk for side effects is lower.

Speiser and Spratling (64) reported that the mean time for fibrotic reactions was 10 – 13 months after ILT. The mean time to develop side effects was 14 months for the MI group, 15 months for the UML group, and 11 months for the SB group.

We did not correlate clinical lung toxicity such as dyspnea and cough as this was not the purpose of this research. Dyspnea and cough can be caused by other causes such as COPD, cardiac disease, and radiation pneumonitis. As at least 30% of our population had a high Charlson comorbidity score or cumulative illness score, the high comorbidity would

influence the toxicity such as dyspnea or cough. A patient with COPD Gold IV (the most advanced stage of COPD) will probably have more toxicity from an occlusion of an upper bronchus compared to a patient with the same side effect but without COPD. For this reason, we did not correlate the clinical toxicity with our results.

4.5 Conclusion

No side effects were found in the trachea and only stenosis in the main bronchus and bronchus intermedius, so the doses we prescribed are associated with low NTCP risks. Higher grades of side effects, such as occlusion and atelectasis, were only seen in the upper-, middle-, and lower bronchi and the segmental bronchi. Most of the side effects occurred in the first 24 months after treatment with the largest amount in the first 12 months. When 0.5 cc of a segmental bronchus was irradiated to 50 Gy in 5 fractions, it was about 50% likely to be occluded radiographically, but symptomatic toxicity could still be avoided as long as some segmental bronchi in each branch of lung were outside the high-dose region. For grade 1 radiographically evident side effects, the 50% risk level for a 5-fraction D_{max} was 55 Gy for mid bronchi and 65 Gy for mainstem bronchi. Our group of patients in this study is fragile, and their clinical toxicity depends on much more factors than only radiation-induced side effects of the bronchi. To assure the relation between clinical toxicity and side effects to the bronchi, further investigation is needed.

5

CHAPTER 5

Normal Tissue Complication Probability modeling of pulmonary toxicity after stereotactic and hypofractionated radiation therapy for central lung tumors

H. Tekatli* [1,] M. Duijm* [2], E. Oomen-de Hoop [2], W. Verbakel [1], W. Schillemans [2], B.J. Slotman [1], J.J. Nuyttens [2], S. Senan [1]

**Joint first authors*

[1] Department of Radiation Oncology, Cancer Center Amsterdam, VU University Medical Center, Amsterdam, The Netherlands

[2] Department of Radiation Oncology, Erasmus MC Cancer Institute, Rotterdam, The Netherlands

International Journal of Radiation Oncology • Biology • Physics, Vol. 100, No. 3, pp. 738 – 747, 2018

Abstract

Purpose

To evaluate clinical pulmonary and radiographic bronchial toxicity after stereotactic ablative radiation therapy and hypofractionated radiation therapy for central lung tumors, and perform normal tissue complication probability modeling and multivariable analyses to identify predictors for toxicity.

Methods and materials

A pooled analysis was performed of patients with a central lung tumor treated using ≤ 12 fractions at 2 centers between 2006 and 2015. Airways were manually contoured on planning planning computed tomography scans and doses were recalculated to an equivalent dose of 2 Gy per fraction with an α/β ratio of 3. Grade ≥ 3 (≥ G3) clinical pulmonary toxicity was evaluated by 2 or more physicians. Radiographic toxicity was defined as a stenosis or an occlusion with or without atelectasis using follow-up computer tomography scans. Logistic regression analyses were used for statistical analyses.

Results

A total of 585 bronchial structures were studied in 195 patients who were mainly treated using 5 or 8 fractions (60%). Median patient survival was 27.9 months (95% confidence interval 22.3 – 33.6). Clinical ≥ G3 toxicity was observed in 24 patients (12%) and radiographic bronchial toxicity in 55 patients (28%), both mainly manifesting ≤ 12 months after treatment. All analyzed dosimetric parameters correlated with clinical and lobar bronchial radiographic toxicity, with $V_{130Gy,EQD}$ having the highest odds ratio. Normal tissue complication probability modelling showed a volume dependency for the development of both clinical and radiographic toxicity. On multivariate analyses, significant predictors for ≥ G3 toxicity were a planning target volume overlapping the trachea or main stem bronchus (p = 0.005), chronic obstructive pulmonary disease (p = 0.034), and the total $V_{130Gy,EQD}$ (p = 0.012). Radiographic bronchial toxicity did not significantly correlate with clinical toxicity (p = 0.663).

Conclusions

We identified patient and dosimetric factors associated with clinical and radiographic toxicity after high-dose radiotherapy for central lung tumors. Additional data from prospective studies are needed to validate these findings.

5.1 Introduction

In contrast to the established role of stereotactic ablative radiotherapy (SABR) for peripheral non-small cell lung cancer (NSCLC), its role in centrally located tumors is less well defined (74). Data from prospective trials revealed severe toxicity to be uncommon for moderately central tumors when treated with 5-fraction SABR, and that high-grade toxicity was more frequently observed in tumors close to the main bronchi, than those close to the lobar bronchi (17, 75, 76). These findings are consistent with data from retrospective studies in patients with so-called "ultracentral" tumors, defined as target volumes overlapping the main stem bronchi or trachea (77, 78).

Stereotactic ablative radiotherapy is increasingly used for moderately central tumors, and recent guidelines recommend the use of risk-adapted SABR regimens delivering 4 or 5 fractions for central located lung tumors and more hypofractionated regimens in 6 – 15 fractions for ultracentral tumors (10, 79). Compliance with normal organs constraints used in prospective trials (NCT01795521, NCT00750269) has been recommended, even though such constraints had not been validated in large populations.

Patients with centrally located tumors have been treated since 2006 at VUmc and EMC, using both SABR and hypofractionated radiotherapy in ≤ 12 fractions. To identify patient and dosimetric predictors of clinical pulmonary and radiographic bronchial toxicity, we performed a pooled retrospective analysis using clinical records and follow-up computed tomography (CT) scans.

5.2 Methods and Materials

Patient selection and definitions

This retrospective study was approved by the institutional medical ethics committees of VUmc and EMC. Institutional databases were queried to identify patients treated with ≤ 12 fractions for primary NSCLC at VUmc and EMC and for lung metastasis at EMC. Patients were treated since 2006 (EMC) and 2008 (VUmc). Selected patients had a planning target volume (PTV) located ≤ 2 cm from the trachea, main stem-, intermediate-, upper-, middle- or lower lobe bronchus and at least 1 bronchial structure receiving ≥ 20.0 Gy (physical dose). Patients with thoracic irradiation before or after the index treatment were excluded.

Risk-adapted fractionation based on tumor location and volume was used at both institutions (48, 80). At VUmc, patients with a PTV overlapping main bronchi or trachea were treated with 12 fractions of 5 Gy; other central tumors were treated using 8 fractions of 7.5 Gy (Appendix 5A) (77, 81). At EMC, different fraction doses have been used and changed during the years with increasing experience and after introducing a Monte-Carlo based dose calculation algorithm. Briefly, 6 or 7 fractions were used for tumors close to the esophagus, and 5 fractions for other centrally located tumors (Appendix 5A). One patient was treated with 3 fractions.

Treatment planning and delivery

Treatment planning and delivery were as previously described (67, 82, 83). At VUmc, a free-breathing, 10-phase 4-dimensional CT scan was used to delineate the internal target volume, which was expanded with 5 mm to generate a PTV. Dose calculations were performed on the average intensity projection of the 4-dimensional CT scan, and treatment was delivered using volumetric modulated arc therapy (RapidArc, Varian Medical Systems, Palo Alto, CA) and online cone-beam CT. At least 95% and 99% of the PTV had to receive 100% and 90% of prescribed dose, respectively. An inhomogeneous dose distribution was planned, with a maximum of 110% to 140% of the prescribed dose. Planning target volume underdosage was permitted only to avoid exceeding dose limits to the esophagus, spinal canal, and brachial plexus (Appendix 5B). No institutional dose limits were applied for the heart, trachea and main stem or lobar bronchi. However, individual physicians sometimes requested maximum point doses in these organs. Since 2009, contralateral lung doses were limited (84, 85).

At EMC, gross tumor volumes (GTV) were delineated on a spiral CT scan, and PTV was generated by adding a 5 mm margin. Dose calculations were performed using MultiPlan (Accuray, Sunnyvale, CA). Patients were treated on a CyberKnife robotic radiosurgery system (Accuray) (67). Planning target volume dose was prescribed to the 70% to 90% isodose lines, which covered ≥ 95% of PTV. Gross tumor volume and PTV underdosage was allowed to meet dose limits of organs at risk summarized in Appendix 5B.

Delineation

For the purposes of this analysis, the following bronchial structures were manually delineated on planning CT scans: trachea, main stem and intermediate bronchi (MI), and upper-, middle -, and lower lobe bronchi (lobar bronchi). Both institutes randomly evaluated each other's delineations.

Dosimetric analysis

All doses were converted into a biologically equivalent dose (BED) and an equivalent dose of 2 Gy per fraction (EQD_2) and calculated using the following formulas: : $BED = D * (1 + (d/(\alpha/\beta))$ and $EQD_2 = D * (d + \alpha/\beta)/(2.0 + \alpha/\beta)$, where D = total dose and d = dose per fraction. An α/β ratio of 10 was used for the tumor and a ratio of 3 for the bronchi (86). All EMC treatment plans which were originally calculated with Ray-Tracing were first recalculated using Monte Carlo algorithm (Appendix 5A). Ipsilateral bronchial structures receiving ≥ 20.0 Gy at both institutes were further analyzed.

We report on maximum point doses ($D_{max,EQD}$), and volumes receiving an EQD_2 of 65 Gy ($V_{65Gy,EQD}$), 80 Gy ($V_{80Gy,EQD}$), 90 Gy ($V_{90Gy,EQD}$), 100 Gy ($V_{100Gy,EQD}$), and 130 Gy ($V_{130Gy,EQD}$). For

analyses regarding clinical toxicity, the maximum point dose in all analyzed bronchial structures ("total $D_{max,EQD}$") and a total volume of all bronchial structures receiving the specified doses ("total $V_{65Gy,EQD}$", "total $V_{80Gy,EQD}$" etc) were calculated for each patient. Radiographic toxicity was analyzed per bronchial structure, and dosimetric parameters of separate bronchial structures were therefore used.

Evaluation of disease control and toxicity

Clinical follow-up was generally performed at 3, 6, 12, 18, and 24 months after treatment and yearly thereafter. All available patient records, including information from general practitioners, were reviewed to determine disease control and high-grade pulmonary toxicity. All cases with potential grade 3 or higher toxicity (≥ G3) according to the Common Terminology Criteria for Adverse Events (version 4.03) were evaluated by at least 2 physicians and were consensus based. Potential treatment-related deaths were sub-classified into "possible'' (when no other likely cause was identified and treatment contribution could not be excluded) or "likely" (when the cause was considered to be radiation-related) treatment-related.

All available follow-up CT scans were used to evaluate radiographic bronchial toxicity. Posttreatment scans were compared with the planning CT, and the following features were reported if they were new or deteriorating with respect to the planning CT scan: stenosis, occlusion without atelectasis, or occlusion with atelectasis in the trachea, main stem, intermediate, or lobar bronchi. If there was also a local recurrence at the location of a stenosis/occlusion, this was not scored as toxicity, and that specific bronchial structure was excluded from analyses. High-grade toxicity was defined as an occlusion with or without atelectasis. All CT scans were evaluated by 2 physicians, and scans with relevant radiological changes were additionally evaluated by 2 senior radiation oncologists.

Statistical analysis

IBM SPSS (version 21.0; IBM, Armonk NY) and GraphPad Prism (version 7.0, Graphpad Software, Palo Alto, CA) were used for statistics. Kaplan-Meier estimates were generated for all clinical outcomes. Overall survival and disease-free survival were calculated using the first date of treatment and the date of death or disease recurrence, respectively. For patients without an event, the last date of follow-up visit or last date of contact with the patient, was used. Hence, in patients without disease recurrence, no competing event by means of death was present. Median follow-up times and 95% confidence intervals (95% CIs) were calculated using the reverse Kaplan-Meier method, and Kaplan-Meier curves were compared using the log-rank test (87). Normal tissue complication probability (NTCP) analysis was calculated to obtain probabilities for toxicity and was based on a logistic regression analysis. Dosimetric parameters with a p-value of < 0.05 were fitted into an NTCP

model. The odds were obtained and introduced in the equation ln(odds) for calculation of log odds: $\ln\left(\frac{p}{1-p}\right) \sum e^{\beta 0 + \beta * Vx}$. The following equation was used to generate an NTCP: $NTCP = \frac{1}{1+e^{-(\_0+\_*Vx)}}$ (88, 89).

A multivariable logistic regression analysis was performed to identify both clinical and dosimetric predictors for toxicity. Variables were first analyzed in univariable analyses and entered into a multivariable analysis if the p-value was ≤ 0.20. When more than 1 dosimetric parameter had a *p*-value of ≤ 0.20 in univariable analysis, the parameter with the highest odds ratio (OR) was included in multivariable analysis. A *p*-value < 0.05 was considered statistically significant. Two patients without data on clinical toxicity were excluded from all analyses regarding this endpoint.

5.3 Results

Patient and tumor characteristics

A total of 195 patients with follow-up CT scans and treated between July 2006 and January 2015 were eligible (*Table 1*). Ninety-one patients were treated at VUmc and 104 at EMC. Twelve patients from VUmc were treated for a primary NSCLC tumor accompanied by 1 or 2 hilar or mediastinal lymph nodes. Three EMC patients were treated for 2 adjacent metastatic tumors (n = 2) and two mediastinal lymph nodes (n = 1). Treatment was performed for a primary or recurrent NSCLC in 154 patients (79%), most consisting of stage I disease (34%). Staging fluorodeoxyglucose positron emission tomography scans were performed in the majority of patients (92%), and pathological diagnosis was available in 49% of patients. Thirty-one patients (16%) had an endobronchial tumor location. Median PTV was 80.4 cm^3 (range 5.2 – 522.6 cm^3), and PTV overlap with trachea or main bronchi (ultracentral location) was present in 66 patients (33%). The majority of patients were treated with either 5 or 8 fractions (60%).

Table 1 - Baseline patient and treatment characteristics

Characteristics	Total	VUmc	EMC
No. of patients	195	91	104
Male	123 (63%)	64 (70%)	59 (57%)
Age (y)	74 (65 – 81)	76 (69 – 83)	73 (62 – 80)
COPD in history	122 (63%)	58 (64%)	64 (62%)
Gold I/II	18 (9%) / 54 (28%)	10 (11%) / 27 (30%)	8 (8%) / 27 (26%)
Gold III/IV	36 (19%) / 9 (5%)	14 (15%) / 7 (8%)	22 (21%) / 2 (2%)
Gold status unknown	5 (3%)	-	5 (5%)
^{18}F-FDG PET/CT staging	180 (92%)	90 (99%)	90 (87%)
Pathological diagnosis	95 (49%)	55 (28%)	40 (38%)
Endobronchial tumor location	31 (16%)	24 (26%)	7 (7%)

Table 1 - Baseline patient and treatment characteristics (continued)

Characteristics	Total	VUmc	EMC
Charlson comorbidity index	2 (1 – 4)	3 (2 – 4)	2 (1 – 3)
0 – 2	101 (52%)	31 (34%)	70 (67%)
3 – 5	78 (40%)	53 (58%)	25 (24%)
6 – 9	16 (8%)	7 (7%)	9 (9%)
Metastasis	41 (21%)	-	41 (39%)
Primary NSCLC	154 (79%)	91 (100%)	63 (61%)
Tumor histology available*	85 (55%)	55 (60%)	30 (48%)
Adenocarcinoma	43 (28%)	13 (14%)	30 (48%)
Squamous cell carcinoma	29 (19%)	29 (32%)	-
NSCLC NOS	8 (5%)	8 (9%)	-
Large cell carcinoma	1 (1%)	1 (1%)	-
Undifferentiated carcinoma	1 (1%)	1 (1%)	-
Squamous dysplasia / CIS / adenosquamous carcinoma	3 (2%)	3 (3%)	-
Disease stage TNM 7th *			
IA/IB	25 (16%) / 41 (27%)	19 (21%) / 22 (24%)	6 (7%) / 19 (21%)
IIA/IIB	34 (22%) / 27 (18%)	11 (12%) / 15 (16%)	23 (25%) / 12 (13%)
IIIA	18 (12%)	16 (18%)	2 (2%)
IV	1 (1%)	1 (1%)	-
Recurrent NSCLC	7 (5%)	7 (8%)	-

Treatment characteristics #	Total	VUmc	EMC
Planning target volume (cm^3)	80.4 (43.7 – 149.4)	88.7 (51.3 – 153.1)	67.6 (36.9 – 134.3)
Ultracentral location	66 (33%)	43 (47%)	23 (22%)
Prescribed treatment schedules			
3 fractions	1 (1%)	-	1 (1%)
5 fractions	65 (33%)	-	65 (63%)
6 fractions	22 (11%)	-	22 (21%)
7 fractions	16 (8%)	-	16 (15%)
8 fractions	52 (27%)	52 (57%)	-
12 fractions	39 (20%)	39 (43%)	-
Prescribed dose (BED_{10} in Gy)	100.8 (90 – 105)	105 (90 – 105)	100 (86.4 – 115.5)
83.3 – 90.0	75 (38%)	39 (43%)	36 (35%)
91.0 – 100.0	26 (13%)	-	26 (25%)
101.0 – 130.0	70 (36%)	52 (57%)	18 (17%)
131.0 – 150.0	23 (12%)	-	23 (22%)
>150.0	1 (0.5%)	-	1 (1%)
PTV D_{max} (BED_{10} in Gy)	150.7 (129.1 – 170.1)	160.0 (142.4 – 168.4)	134.8 (119.4 – 173.4)

Abbreviations: BED_{10} = biologically equivalent dose with an α/β ratio of 10; CIS = carcinoma in situ; COPD = chronic obstructive pulmonary disease; CT = computed tomography; EMC = Erasmus Medical Center; FDG = fluorodeoxyglucose; IQR = interquartile range; NOS = not otherwise specified; NSCLC = non-small cell lung cancer; PET = positron emission tomography; PTV = planning target volume; VUmc = VU University Medical Center.

Values are number (percentage) or median (interquartile range).

**All percentages are calculated for the subgroup of patients with primary NSCLC. #All percentages are calculated for the total of analyzed PTVs (n = 195).*

Dosimetric analysis

Dosimetric details of 89 trachea, 121 main bronchi, 67 intermediate bronchi, and 308 lobar bronchi were analyzed (Figure 1). Median $D_{max,EQD}$ delivered to the trachea was 63 Gy (range 21 – 146 Gy, interquartile range (IQR) 38 – 102 Gy), 103 Gy (range 23 – 334 Gy, IQR 56 – 131 Gy) for the MI, and 119 Gy (range 23 – 416 Gy, IQR 69 – 142 Gy) for the lobar bronchi.

Figure 1 – Volume parameters in equivalent dose of 2 Gy per fractions (EQD_2) values (Gy) for the central airways. Circles and stars refer to outliers and extreme values, respectively

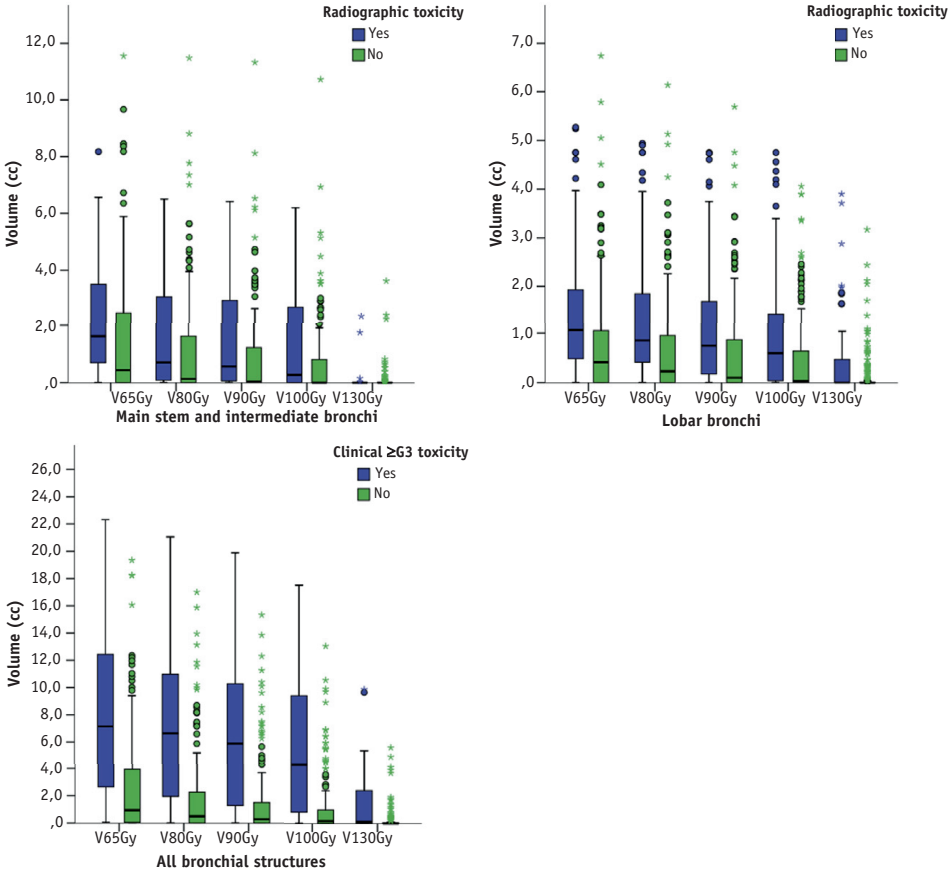

Overall survival and disease control

Median overall survival for all patients was 27.9 months (95% CI 22.3 – 33.6 months), and median follow-up of the surviving patients was 61.6 months (95% CI 50.9 – 72.4 months). Overall survival rates were 77.4% (95% CI 72.2 – 84.0%), 53.3% (95% CI 46.5 – 60.7%), and 41.2% (95% CI 34.1 – 48.5%) at 1, 2, and 3 years, respectively. Median survival rates were

similar between VUmc and EMC patients, with 29.8 months (95% CI 16.8 – 42.8 months) at VUmc and 24.7 months (95% CI 18.9 – 30.5 months) at EMC (p = 0.114). Median survival for patients with primary tumors was 26.6 months (95% CI 17.7 – 35.6 months) and 28.1 months (95% CI 21.3 – 34.9 months) for patients with metastatic lesions (p = 0.748). Survival rates at 1, 2, and 3 years were 74.6% (95% CI 68.5 – 82.3%), 51.4% (95% CI 43.7 – 59.7 %), and 42.3% (95% CI 34.4 – 50.5%) for primary NSCLC, respectively.

Median follow-up for disease control was 36.4 months (95% CI 30.7 – 42.1 months). Any disease failure was observed in 77 patients (39%), and median disease-free survival was 27.0 months (95% CI 15.5 – 38.5 months). Local, regional, and distant failure manifested in 13%, 10%, and 30% of patients, respectively. For patients with primary NSCLC, these rates were 10%, 8%, and 21%, respectively.

Clinical pulmonary toxicity

Details on clinical toxicity were available in 193 patients. Grade ≥ 3 pulmonary toxicity was observed in a total of 24 patients (12%) (Table 2), and the first toxicity event was observed within 12 months post-treatment in the majority of patients (67%). Radiation pneumonitis was the commonest G3 toxicity (n = 10), with 50% of the latter also having a radiographic bronchial toxicity, including 1 patient with an occlusion and 4 with an occlusion plus atelectasis. At the time of this analysis, 133 patients (68%) had died. No information was available on the cause of death in 22 patients (17%). A possible (n = 6) or likely (n = 9) treatment-related death was observed in 15 patients (8%). Fatal lung hemorrhage, the commonest treatment-related death, was considered either possible (n = 5) or likely (n = 6) treatment-related in 11 patients (6%). Two patients who died as a consequence of euthanasia were considered to have a likely treatment-related death, and the remaining two patients died due to a possible and likely treatment-related respiratory failure. (Table 2). Four patients scored as having a likely fatal toxicity had also developed a previous G3 toxicity.

Grade ≥ 3 clinical symptoms of a bronchus obstruction was observed in 2 patients (1%), both of them having an ultracentral PTV location (Table 2). One patient developed G3 symptoms from atelectasis of the left lung, after presenting with pretreatment occlusion of the main stem bronchus. The atelectasis was visible approximately 1 month before the clinical symptoms were recorded. Another patient with an endobronchial tumor developed G3 hemoptysis during treatment. Although the first follow-up scan at 4.7 months did not reveal any radiographic toxicities, clinical records stated that death at 11.3 months after treatment was a consequence of euthanasia, performed because of severe dyspnea arising from chronic obstructive pulmonary disease (COPD) and a bronchial obstruction. The bronchial occlusion was accompanied by atelectasis and edema of the main stem/lower lobe bronchus. However, only 1 follow-up CT scan was available for review.

Table 2 – High-grade clinical pulmonary and radiographic bronchial toxicity

	Toxicity	No. of patients (%)	Time after treatment (months)	Additional Remarks
High-grade (grade ≥ 3) clinical pulmonary toxicity (n = 193)				
Grade 3		12 (6%)	0.2 – 14.1	
	Radiation pneumonitis	10 (5%)	2.0 – 14.1	
	Atelectasis due to main stem bronchus occlusion	1 (1%)	13.7	
	Hemoptysis	1 (1%)	0.2	
Grade 4	Hemoptysis	1 (1%)	20.1	
Grade 5		15 (8%)	5.6 – 18.5	
Possible	Fatal lung hemorrhage	5 (3%)	6.5 – 18.5	
	Multifactorial respiratory failure	1 (1%)	5.6	
Likely	Fatal lung hemorrhage	6 (3%)	5.2 – 18.2	Two patients also developed G3 RP
	Respiratory failure due to radiation pneumonitis / pneumonia with septicaemia	1 (1%)	7.7	
	Euthanasia performed due to disease progression and dyspnea.	1 (1%)	13.1	Patient also developed G3 RP
	Euthanasia performed after severe dyspnea due to severe COPD, and atelectasis and edema, both arising from bronchial obstruction (main stem/lower lobe bronchus)	1 (1%)	11.3	Patient also developed G3 hemoptysis
Total		**24 (12%)**	**0.2 – 20.1**	
High grade (occlusion with or without atelectasis) radiographic bronchial toxicity (n = 195)				
	Main stem bronchus	1 (0.5%)	12.2	
	Intermediate bronchus	2 (1%)	6.6 – 6.9	
	Lobar bronchi	34 (17%)	2.3 – 38.4	
Total		**36 (18%)**	**2.3 – 38.4**	

Abbreviations: COPD = chronic obstructive pulmonary disease; G3 RP = grade 3 radiation pneumonitis.

Grade ≥ 3 lung hemorrhage was observed in a total of 13 patients (7%) (Table 2). The Charlson comorbidity index was ≥ 3 in 9 of them. An endobronchial tumor was present in 46% of this subgroup, and the PTV overlapped with the main bronchi or trachea in 70%. Of the 10 patients with a pathological diagnosis, 7 had squamous cell carcinoma / dysplasia. In 11 patients who developed a fatal lung hemorrhage, a radiographic bronchial toxicity was identified in 2. One patient had a stenosis of the lower lobe bronchus, and the other a stenosis of the right intermediate bronchus with occlusion and atelectasis of both the middle and lower lobe bronchus.

Radiographic bronchial toxicity

A total of 585 bronchial structures were evaluated for radiographic toxicity. The main bronchus, upper lobe bronchus, and lower lobe bronchus could not be evaluated owing to an in-field recurrence in 3 patients. Follow-up CT scans were available for ≤ 12 months after treatment in 86 patients (44%), for 12 to 24 months in 55 patients (28%), for 24 to 36

months in 21 patients (11%), for 36 to 48 months in 14 patients (7%), and for > 48 months in 19 patients (10%). Any grade of radiographic toxicity was observed in 9 main stem bronchi, 8 intermediate bronchi, and 64 lobar bronchi at follow-up scans of 55 patients (28%) (*Figure 2*, Appendix 5E). No patients developed radiographic toxicity of the trachea. A single bronchus was affected in 36 patients, 2 bronchi in 12 patients, and 3 bronchi in 7 patients. High-grade radiographic toxicity developed in 41 bronchial structures of 36 patients (18%), and mostly in the lobar bronchi (17%) (*Figure 2*, Table 2). The first radiographic toxicity event occurred within 12 months after SABR in 39 of the 55 patients (71%) with any grade of radiographic toxicity (range 1.7 – 48.2 months), and in 25 of the 36 patients (69%) with high-grade toxicity (range 2.3 – 38.4 months).

Figure 2 – Radiographic toxicity in the central airways: main stem bronchi (n = 9), intermediate bronchus (n = 8), upper lobe bronchi (n = 25), middle lobe bronchus (n = 6), and lower lobe bronchi (n = 33)

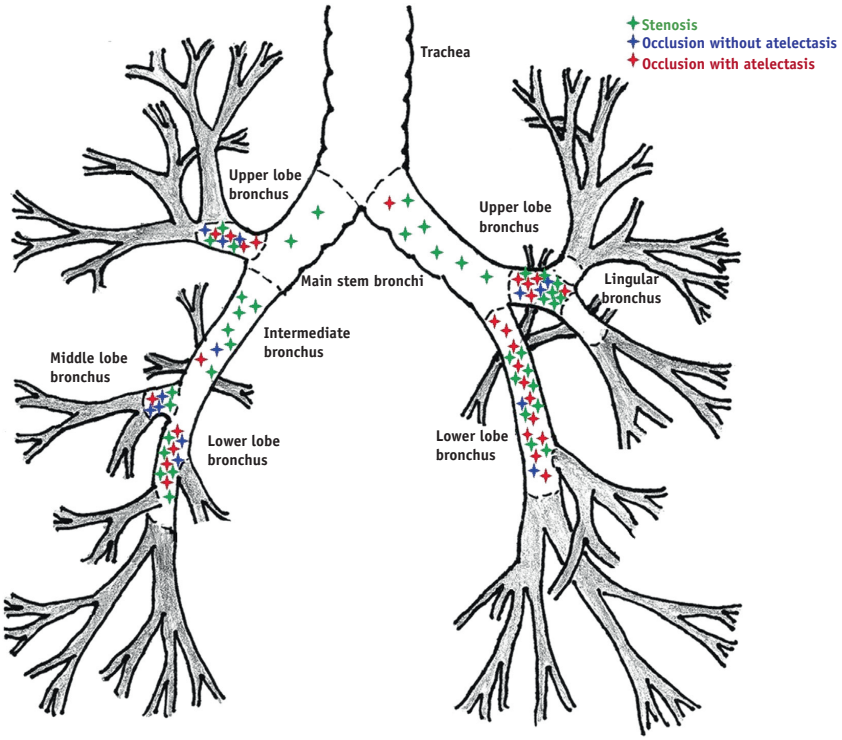

NTCP modelling for clinical and radiographic toxicity

Univariate logistic regression analysis was performed to identify significant dosimetric parameters for the purposes of an NTCP model. All analyzed dosimetric parameters were significantly associated with clinical toxicity, and the total $V_{130Gy,EQD}$ had the highest OR (OR

1.68; 95% CI 1.26 – 2.24; $p < 0.001$), which corresponds to ± 50 Gy in 5 fractions, ± 58 Gy in 7 fractions, ± 61 Gy in 8 fractions, and ± 72 Gy in 12 fractions *(Figure 3*, Appendix 5C and Appendix 5F-G). A 25% probability of ≥ G3 toxicity was observed at a total $V_{130Gy,EQD}$ of 2.35 cm^3 and at a $D_{max,EQD}$ of 190 Gy (*Figure 3*). Grade 5 toxicity was associated with all analyzed parameters except for the total $V_{130Gy,EQD}$, and a 5% probability was observed at a $D_{max,EQD}$ of 84 Gy (Figure 3). Additional subgroup analysis for a likely or possible treatment-related death revealed that the total $V_{65Gy,EQD}$, $V_{80Gy,EQD}$, $V_{90Gy,EQD}$, $V_{100Gy,EQD}$ were significantly associated with a likely treatment-related death, whereas none of the analyzed dosimetric parameters were correlated with possible fatal toxicity (Appendix 5C).

Any grade of radiographic bronchial toxicity in the main stem/intermediate bronchus was only significantly associated with maximum point doses delivered to the MI, with a 25% probability at a $D_{max,EQD}$ of 193 Gy (*Figure 3*, Appendix 5C). This corresponds to ± 63 Gy in 5, ± 72 Gy in 7, ± 77 Gy in 8, and ± 91 Gy in 12 fractions. An additional analysis for the development of a stenosis did not reveal any significantly associated parameters. All analyzed lobar bronchial dosimetric parameters were significantly associated with any grade and with high-grade toxicity in the lobar bronchi, and the lobar bronchial $V_{130Gy,EQD}$ had the highest OR for both (OR 2.47; 95% CI 1.52 – 4.00; $p < 0.001$, and, OR 2.29; CI 1.44 – 3.65; $p = 0.001$, respectively) (*Figure 3*, Appendix 5C, Appendix 5H-I). A 25% probability of any grade and high-grade lobar bronchial toxicity was observed at a $D_{max,EQD}$ of 133 Gy and 168 Gy, respectively.

Normal tissue complication probability models of the volume parameters for both clinical and radiographic toxicity were all comparable with each other and steeper than the models of the $D_{max,EQD}$.

Univariate and multivariate regression analyses

A univariate analysis was performed using clinical factors for the purposes of a multivariate analysis including both clinical and dosimetric predictors of toxicity (Appendix 5D). This revealed that radiographic bronchial toxicity was not significantly correlated with ≥ G3 clinical toxicity (OR 1.22; 95% CI 0.49 – 3.05; $p = 0.663$). Planning target volume overlap with the main stem bronchi/trachea (OR 4.16; 95% CI 1.54 – 11.23; $p = 0.005$), COPD (OR 4.09; 95% CI 1.11 – 15.05; $p = 0.034$), and the total $V_{130Gy,EQD}$ (OR 1.52; 95% CI 1.10 – 2.12; $p = 0.012$) were significantly correlated with the development of ≥ G3 clinical toxicity on multivariate analysis.

Figure 3 – Normal tissue complication probability models for clinical and radiographic toxicity

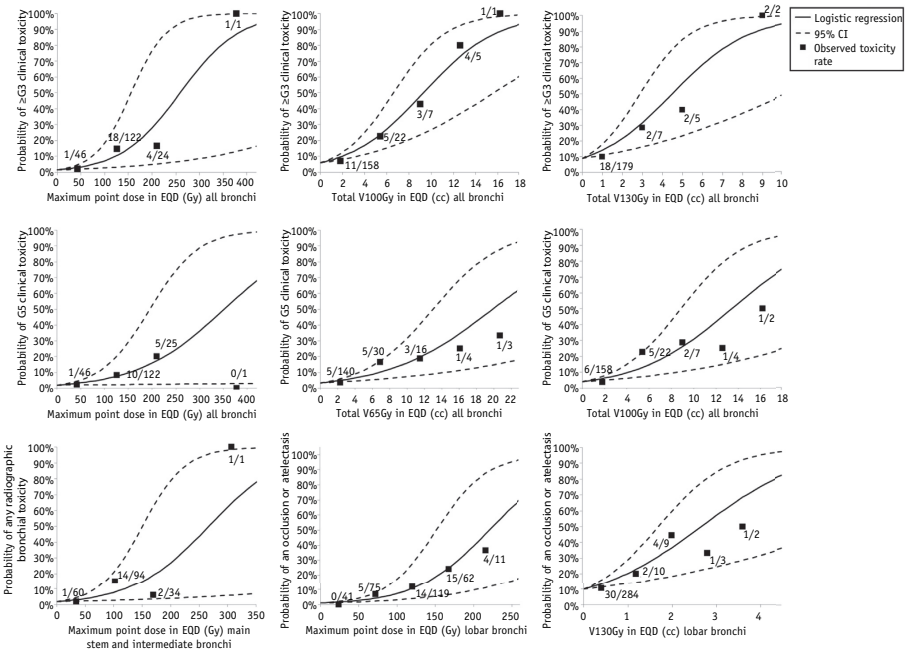

The x-axis shows the dose range and is divided into 5 equal parts ("bins"). Solid black squares represent the observed incidence of toxicity for each bin (%). Both the number of patients with toxicity and the numbers at risk in each bin are indicated. Bins not containing any patients had no square shown in the graph. For clinical normal tissue complication probability models, the maximum point dose in all analyzed structures, and a total volume of all structures receiving the specified doses, were calculated for each patient.

Abbreviations: CI = confidence interval; EQD = equivalent dose of 2 Gy per fraction; V_{xxGy} = volume receiving xx Gy in EQD values.

For high-grade radiographic toxicity, univariate analysis revealed that age and PTV overlapping main stem bronchi/trachea were significant clinical predictors (Appendix 5D). Entering these variables into a multivariate analysis with the total $V_{130Gy,EQD}$ showed that only PTV overlapping the main stem bronchi/trachea remained as a significant predictor for high-grade radiographic toxicity (OR 2.87; 95% CI 1.16 – 7.06; p = 0.022).

5.4 Discussion

To the best of our knowledge, this study represents the largest to date on the treatment of centrally located lung tumors with either SABR or hypo-fractionated radiotherapy delivered in ≤ 12 fractions. Grade ≥ 3 clinical pulmonary toxicity and radiographic toxicity were observed in 12% and 28% of patients, respectively. The majority of both toxicities manifested within 12 months post-treatment. A fatal lung hemorrhage was the commonest

cause of treatment-related death (6%), and most high-grade radiographic toxicities occurred in the lobar bronchi (17%). All analyzed dosimetric parameters were significantly correlated with clinical and radiographic lobar bronchial toxicity on univariate analysis, with $V_{130Gy,EQD}$ having the highest OR. Multivariate analysis revealed that PTV overlap with the trachea or main stem bronchus and COPD strongly correlated with ≥ G3 clinical toxicity, as did the total $V_{130Gy, EQD}$.

Rates of clinical toxicities observed in this study are consistent with ongoing prospective trials on central lung SABR, and with data from retrospective studies that have reported a 15 to 24% incidence of pulmonary toxicity (17, 29, 75, 90, 91). Preliminary results of the Radiation Therapy Oncology Group protocol 0813 reported 15% high-grade toxicity, and all observed G5 toxicity was due to a fatal lung haemorrhage (4%) (75). This trial permitted a maximum point dose of 105% for the main bronchi, corresponding to a $D_{max,EQD}$ of ± 197 Gy for a regimen with 5 fractions of 12 Gy. In our NTCP model, a $D_{max,EQD}$ of 190 Gy resulted in a 25% probability for ≥ G3 clinical toxicity and in a probability of 15% for fatal toxicity. The prospective HILUS trial included 42 patients with tumors close to a main stem bronchus (group A) and 31 patients with tumors close to a lobar bronchus (group B) (17). All patients were treated with 8 fractions of 7 Gy. Dose limits were mandatory for trachea and contralateral main bronchus ($D_{max,EQD}$ = 89 Gy), and for the ipsilateral main stem bronchus only dose guidelines were recommended ($D_{max,EQD}$ = 112 Gy). Early toxicity analysis showed severe toxicity in 28% of patients, and G4/5 toxicity occurred more in group A (19%) than in group B (3%). Six of the 7 patients with a fatal toxicity died of a lung hemorrhage (14%). The current pooled analysis found PTV overlap with main stem bronchus or trachea to be significantly correlated with both ≥ G3 clinical toxicity and high-grade radiographic toxicity. A PTV overlap was present in 33% of all patients, and in 70% of patients who developed ≥ G3 lung bleeding.

There are limited data available on radiographic bronchial toxicity after SABR. The HILUS trial reported a rate of 28% for G1/2 atelectasis and an 8% rate for G1/2 bronchus obstruction/stricture, which is in line with our rates of radiographic toxicity (28%) (17). Although the specific pathophysiological mechanism of radiation-induced bronchial damage is unclear, a correlation with airway diameter has been postulated (29). We observed no toxicities in the trachea, and the highest rate of radiographic toxicity was observed in the lobar bronchi. A 25% probability of any grade of toxicity in the lobar bronchi was observed at a $D_{max,EQD}$ of 133 Gy, whereas a higher point dose of 193 Gy was associated with toxicity to main stem and intermediate bronchi. However, radiographic bronchial toxicities were not significantly associated with clinical pulmonary toxicities in our series (Appendix 5D). A potential explanation could be the hypothesis that radiation damage to the lobar bronchi more often causes subclinical toxicity, as clinical relevant toxicity manifested in only two patients with radiological toxicity in the main stem bronchus. In

addition, factors besides radiographic bronchial damage, such as lung function and comorbidities, could play an important role in the development of clinical toxicity. We observed a volume dependency for the development of toxicity, consistent with previous work (62). The highest odd ratios for both clinical and radiographic toxicity were observed for the volumes receiving the highest doses, and the lowest OR was observed for the maximum point doses (Appendix 5D). Although the V_{130Gy} had the highest OR for both ≥ G3 clinical and radiographic toxicity, this parameter was not significantly associated with G5 toxicity. When patients were stratified into groups based on a possible or likely treatment-related death, dosimetric variables were found to be predictive only in patients scored to have a likely treatment-related death. This finding may reflect the inherent uncertainty when scoring G5 toxicity as "possibly treatment-related" if no other potential cause could be identified, leading to an over-reporting of G5 toxicity. However, our findings should be interpreted with caution given the small numbers of patients included in this subgroup analysis.

A number of limitations of this study are acknowledged. Although all potential high-grade toxicity was evaluated by at least 2 experienced radiation oncologists, the retrospective character of this pooled analysis and the variations in follow-up duration may have led to an under-reporting or less inaccurate scoring of toxicity. The difficulty of distinguishing between a recurrence and a bronchial injury in some cases may also have contributed to the latter. Observed dose-response relationships may have been confounded by differences in treatment techniques between the centers and possible discrepancies between planned versus delivered doses.

In conclusion, the high-grade toxicity rates observed in this pooled analysis of central lung tumors treated with SABR or hypofractionated radiotherapy in ≤ 12 fractions seem to be consistent with emerging data from prospective trials of central lung SABR. No significant correlation was observed between radiographic bronchial damage and clinically relevant pulmonary toxicity, and NTCP modelling confirms the volume dependency of both clinical and radiographic toxicity. Because an ultracentral tumor location strongly correlates with both radiographic and clinical toxicity, SABR for such tumors should be pursued with caution until more data are forthcoming.

6

CHAPTER 6

Esophagus toxicity after stereotactic and hypofractionated radiotherapy for central lung tumors: Normal Tissue Complication Probability modeling

M. Duijm* [1], H. Tekatli* [2], E. Oomen-de Hoop [1], W. Verbakel [2], W. Schillemans [1], B.J. Slotman [2], S. Senan [2], J.J. Nuyttens [1]

**Joint first authors*

[1] Department of Radiation Oncology, Erasmus MC Cancer Institute, Rotterdam, The Netherlands

[2] Department of Radiation Oncology, Cancer Center Amsterdam, VU University Medical Center, Amsterdam, The Netherlands

Radiotherapy & Oncology, Vol. 127, No. 2, pp. 233 – 238, 2018

Abstract

Purpose

To correlate esophagus toxicity and dose-volume histogram (DVH) parameters in order to assess risks, and derive a Normal Tissue Complication Probability (NTCP) model.

Methods and Materials

Patients with a central lung tumor from 2 centers, who underwent stereotactic or hypofractionated radiotherapy (≤ 12 fractions), were analyzed. Doses were recalculated to an equivalent dose of 2 Gy with an α/β ratio of 10 (EQD_2^{10}). The esophagus was manually delineated and DVH-parameters ($D_{max,EQD2}$, $D_{1cc,EQD2}$, $D_{2cc,EQD2}$, $D_{5cc,EQD2}$) were analyzed and used for NTCP modelling based on logistic regression analysis.

Results

Two-hundred-and-thirty-one patients with 252 tumors were eligible. No acute or late grade 3 – 5 esophageal toxicity was reported. Acute grade 1 – 2 esophagus toxicity was recorded in 38 patients (17%). All DVH-parameters were significantly higher in patients with toxicity. NTCP models showed a 50% probability of acute grade 1 – 2 toxicity at a D_{max} of 67 Gy EQD_2^{10} and D_{1cc} of 42 Gy EQD_2^{10}. No difference in overall survival was observed between patients with and without toxicity (p = 0.428).

Conclusion

As no grade 3 – 5 esophageal toxicity was observed in our cohort, a D_{max} of 56 Gy EQD_2^{10} and D_{5cc} of 35.5 Gy EQD_2^{10} could be delivered without high risks of severe toxicity. The NTCP models of this study might be used as practical guidelines for the treatment of central lung tumors with stereotactic radiotherapy.

6.1 Introduction

Stereotactic Body Radiation Therapy (SBRT), also referred as stereotactic ablative radiotherapy (SABR), has become the standard of care for patients with early stage Non-Small Cell Lung Cancer (NSCLC) who are medically or surgically inoperable or refuse surgery (92). Patients with central lung tumors are at higher risk of toxicities when treated up to a dose of 60 – 66 Gy in 3 fractions (13). Although risk-adapted fractionation schedules with accompanying dose constraints are now implemented, both retrospective studies and prospective trials report radiation related complications following the treatment of central lung tumors (17, 21, 77, 78).

While toxicity of the lung parenchyma, presenting as radiation pneumonitis, is not associated with tumor location (28, 93), central tumor position is an important factor in the development of toxicity of the bronchi. Bronchial stenosis, occlusion and atelectasis, have been associated with both the D_{max} and the bronchial volume receiving more than 65 Gy EQD_2 (α/β ratio of 3) (29). High grade esophagus toxicity has also been associated with high SBRT doses (38, 46, 94). Painful dysphagia followed by death due to an esophageal ulcer 5 months after treatment has been associated with a D_{max} of 50.5 Gy (94 Gy EQD_2 using α/β ratio of 3) (46). Chang et al. suggested a limit of $V_{30Gy} \leq 1$ cm^3 (in 4 fractions) after reporting grade 2 esophagitis in only 4% of the patients (38).

Although many institutions have published their experiences with treating central lung tumors, there is currently no consensus on standard dose constraints for organs at risk (14). Commonly recommended constraints, derived from ongoing prospective trials, have not been validated in large populations (NCT01795521, NCT00750269).

The goal of this study was to determine the incidence of esophageal toxicity in central lung tumors treated with SBRT and to identify dosimetric and clinical predictors for esophageal toxicity. Furthermore, the odds of toxicity were calculated and a Normal Tissue Complication Probability (NTCP) model was derived to predict the development of esophageal toxicity.

6.2 Materials and methods

We retrospectively analyzed patients from 2 centers, Erasmus Medical Center (EMC) and VU University Medical Center (VUmc), who were treated between 2006 and 2015 with SBRT or hypofractionated radiotherapy (≤ 12 fractions) for primary or metastatic central lung tumors. Central tumors were defined as tumors located within 2 cm of the trachea, mainstem-, intermediate-, upper-, middle- or lower- lobe bronchus or the esophagus.

At both centers, patients were treated with risk-adaptive SBRT schedules based on tumor location and tumor volume (48, 80). At EMC, dose prescription varied over time due to changing dose constraints and the introduction of the Monte-Carlo based algorithm. Tumors close to the esophagus were treated with 6 – 7 fractions of 7 – 8 Gy, while other central tumors received 5 fractions of 9 – 12 Gy, except 2 tumors which received 3 fractions of 20 Gy. At VUmc, tumors with a planning target volume (PTV) overlapping the trachea or main stem bronchi were treated with 12 fractions of 5 Gy and all other central tumors received 8 fractions of 7.5 Gy (*Appendix 6A*).

Treatment planning and delivery have been previously described (67, 82, 83). Briefly, at EMC the PTV consisted of the gross tumor volume plus 5 mm. The PTV dose was prescribed to the 70 – 90% isodose line covering at least 95% of the PTV. Organ at risk (OAR) dose constraints were given priority over PTV coverage (Appendix 6B). Dose calculations were performed using Multiplan® and patients were treated with a Cyberknife® Robotic Radiosurgery System (both Accuray Inc, Sunnyvale, CA). At VUmc, the PTV was generated using a 5mm expansion of the internal target volume. Dose calculations were performed on the average intensity projection (Ave-IP) of the 4D-CT scan. At least 95% and 99% of the PTV had to receive 100% and 90% of the prescribed dose, respectively. An inhomogeneous dose distribution was planned with a PTV maximum of 110 – 140% of the prescribed dose. A higher priority to the OAR was only given to avoid exceeding dose limits of the esophagus, spinal canal and brachial plexus (*Appendix 6B*). Treatment was delivered in free breathing using coplanar Volumetric Modulated Arc Therapy (VMAT) RapidArc™ (Varian Medical Systems, Palo Alto, USA) and online cone-beam CT based setup on the tumor.

For all patients, the esophagus was manually delineated on the planning CT scan using mediastinal window levels. Due to variations in the fractionation schemes, all doses were converted into an equivalent dose of 2Gy per fraction (EQD_2) using the following formula: $EQD_2 = D * (d + \alpha/\beta)/(2.0 + \alpha/\beta)$; with D = total dose, d = dose per fraction and α/β ratio of 10 Gy for tumor and esophagus (the abbreviation used for an EQD_2 with α/β ratio of 10 Gy is EQD_2^{10}). Doses delivered to specific volumes of the esophagus ($D_{max,EQD2}$, $D_{1cc,EQD2}$, $D_{2cc,EQD2}$ and $D_{5cc,EQD2}$) were derived from the dose volume histogram (DVH) of each patient.

Follow-up was generally performed 3, 6, 12, 18 and 24 months following radiation and annually thereafter. All patient medical records from hospitals and general practitioners were screened for esophageal toxicity and disease control. Esophageal toxicity was retrospectively scored using the Common Terminology Criteria for Adverse Events v4.0. Toxicity was considered to be acute when it occurred within 3 months after the end of treatment and as late if it occurred thereafter.

Logistic regression analysis was performed to define clinical or dosimetric predictors of toxicity. Toxicity was dichotomized into the presence or absence of toxicity. Variables with a p-value of ≤ 0.20 in univariate analysis were entered into a multivariable analysis. When more than 1 dosimetric parameter had a p-value of < 0.05 in the univariate analyses, the parameter with the highest odds ratio was included in the multivariable analysis. The NTCP analysis was calculated based on a logistic model. The univariate logistic regression analysis was used for the correlation of toxicity with DVH parameters. Each significant dosimetric parameter (p < 0.05) was modelled into an individual NTCP curve. The odds were obtained and introduced in the equation ln(odds) for calculation of log odds: $\ln\left(\frac{p}{1-p}\right) \sum e^{\beta 0 + \beta * Vx}$. The following equation was used to build the NTCP models: $\mathrm{NTCP} = \frac{100\%}{1+e^{-(\beta 0+\beta * Vx)}}$ (88, 89).

Overall survival was defined as the first day of treatment until the date of death, and local control was defined as the first day of treatment until the date of local recurrence. If no event was observed, the patient was censored at the last date of contact that the patient was still alive. Survival and local control were calculated using Kaplan-Meier analysis and differences between groups were tested with log-rank tests. Non normally distributed variables were compared using the Mann-Whitney *U* Test. P-values of < 0.05 were considered statistically significant. All analyses were performed using IBM SPSS statistics version 21.0 (IBM, Armonk NY). This study was granted approval from the institutional medical ethics committees at both institutions.

6.3 Results

A total of 231 patients with 252 tumors were identified. There were 149 males (65%) included and the median age was 74 years. Twenty patients had multiple tumors treated in a single plan, according to the following scenarios: 2 adjacent metastatic tumors (n = 3), 2 mediastinal lymph nodes (n = 1), a primary NSCLC tumor accompanied by a lymph node (n = 15) or a primary NSCLC accompanied by 2 lymph nodes (n = 1). One-hundred-and-eighty-seven patients (81%) had primary lung cancer and 44 patients (19%) metastatic lung lesions. The median PTV volume was 80.1 cc with an inter quartile range (IQR) of 47.1 – 148.7 cc. The median follow up was 16.0 months (IQR 8.4 – 29.0). Additional patient characteristics are shown in *Table 1*.

Table 1 – Patient- and tumor characteristics

Patient characteristics		Total – n (%) or median (IQR)	
Age (years)		74	(67 – 80)
Sex			
Female		82	(35%)
Male		149	(65%)
Disease			
Primary NSCLC		187	(81%)
Lung metastasis		44	(19%)
Charlson Comborbidity Index			
0 – 2		119	(52%)
3 – 5		93	(40%)
6 – 9		19	(8%)
Prescribed dose*			
7 x 7 Gy	69.4 Gy EQD_2^{10}	10	(4%)
5 x 9 Gy	71.3 Gy EQD_2^{10}	5	(2%)
6 x 8 Gy	72.0 Gy EQD_2^{10}	27	(12%)
12 x 5 Gy	75.0 Gy EQD_2^{10}	45	(19%)
5 x 10 Gy	83.3 Gy EQD_2^{10}	19	(8%)
7 x 8 Gy	84.0 Gy EQD_2^{10}	9	(4%)
8 x 7.5 Gy	87.5 Gy EQD_2^{10}	65	(28%)
5 x 11 Gy	96.3 Gy EQD_2^{10}	23	(10%)
5 x 12 Gy	110 Gy EQD_2^{10}	26	(11%)
3 x 20 Gy	150 Gy EQD_2^{10}	2	(1%)
PTV size (cc)		80.1	(47.1 – 148.7)
Follow-up (months)		16.0	(8.4 – 29.0)

Abbreviations: EQD_2^{10} = equivalent dose of 2 Gy per fraction with α/β ratio of 10; IQR = inter quartile range; PTV = planning target volume; NSCLC = non-small cell lung cancer

** For detailed information about the institutional fractionation schedules, see Appendix 6A*

Acute or late grade 3 – 5 esophageal toxicity was not reported. Thirty-eight patients (16.5%) developed acute grade 1 or 2 esophageal toxicity. Grade 1 toxicity was seen in 31 patients (13.5%) and grade 2 toxicity in 7 patients (3.0%). The number of patients that have experienced grade 1 – 2 toxicity for each fractionation schedule were 0 out of 2 patients, 9/73 patients, 9/27 patients, 8/19 patients, 5/65 patients and 7/45 patients for 3, 5, 6, 7, 8 and 12 fractions, respectively.

For all patients, the median esophagus D_{max} was 29.8 Gy EQD_2^{10} (IQR 18.1 – 44.7). The median D_{1cc}, D_{2cc} and D_{5cc} were 20.4 Gy EQD_2^{10}, 17.7 Gy EQD_2^{10} and 13.2 Gy EQD_2^{10}, respectively. Patients who developed acute esophageal toxicity received a significantly higher D_{max} than those who did not develop toxicity (median 46.9 Gy EQD_2^{10} (IQR 39.7 – 55.3) versus 26.7 Gy EQD_2^{10} (IQR 16.5 – 40.9), respectively; $p < 0.001$). The remaining dosimetric values, $D_{1cc,EQD2}$, $D_{2cc,EQD2}$ and $D_{5cc,EQD2}$, were also significantly higher in patients who experienced toxicity (*Table 2*).

Table 2 – Dosimetric parameters in EQD_2^{10} for the esophagus

		D_{max} (EQD_2^{10})	D_{1cc} (EQD_2^{10})	D_{2cc} (EQD_2^{10})	D_{5cc} (EQD_2^{10})
All patients	median	29.8	20.4	17.7	13.2
(n = 231)	IQR	18.1 – 44.7	13.0 – 29.5	11.8 – 25.5	8.3 – 18.7
	range	1.8 – 82.2	0.9 – 55.7	0.8 – 53.5	0.4 – 49.2
Patients with toxicity	median	46.9	32.7	28.8	21.3
(n = 38)	IQR	39.7 – 55.3	23.5 – 43.3	20.3 – 39.4	14.5 – 31.5
	range	23.4 – 62.4	15.9 – 53.8	12.7 – 52.1	7.6 – 43.0
Patients without toxicity	median	26.7	18.3	16.1	11.8
(n = 193)	IQR	16.5 – 40.9	11.9 – 26.6	10.5 – 22.9	7.8 – 17.1
	range	1.8 – 82.2	0.9 – 55.7	0.8 – 53.5	0.4 – 49.2
p – value *		< 0.001	< 0.001	< 0.001	< 0.001

Abbreviations: IQR = inter quartile range; EQD_2^{10} = equivalent dose of 2 Gy per fraction with α/β ratio of 10
** The groups with and without toxicity are compared using the Mann-Whitney U Test*

The univariate logistic regression analysis showed significant correlations between grade 1 – 2 acute toxicity and all analyzed dosimetric parameters (*Table 3*). Therefore, each parameter was entered into a separate NTCP model, which resulted in four NTCP-curves (*Figures 1 and 2*). The NTCP model for the maximum point dose showed a 50% probability of acute grade 1 – 2 esophageal toxicity at a D_{max} of 67Gy EQD_2^{10} (equal to ± 43 Gy in 5 fractions, ± 48 Gy in 7 fractions, ± 51 Gy in 8 fractions and ± 55 Gy in 12 fractions). The same probability (50%) applied for a D_{1cc} of 42 Gy EQD_2^{10} (equal to ± 31 Gy, ± 34 Gy, ± 35 Gy and ± 38 Gy in 5, 7, 8 and 12 fractions, respectively).

Table 3 – Results of logistic regression; acute grade 1-2 toxicity for each DVH parameter

	D_{max} (EQD_2^{10})	D_{1cc} (EQD_2^{10})	D_{2cc} (EQD_2^{10})	D_{5cc} (EQD_2^{10})
Odds Ratio	1.058	1.107	1.119	1.135
95% CI	1.034 – 1.082	1.069 – 1.147	1.077 – 1.162	1.086 – 1.187
p – value	< 0.001	< 0.001	< 0.001	< 0.001

Abbreviations: DVH = dose-volume histogram; EQD_2^{10} = equivalent dose of 2 Gy per fraction with α/β ratio of 10; 95% CI = 95% confidence interval; OR = odds ratio

A univariate logistic regression was performed for the following clinical factors: age, gender, charlson comorbidity score, PTV (cc), number of given fractions and dose per fraction. None of these factors were significantly associated with toxicity, and only PTV (OR 1.00; 95% CI 1.00 – 1.01; $p = 0.051$) and female gender (OR 1.81; 95% CI 0.90 – 3.67; $p = 0.097$) had a p-value of < 0.20. A multivariable analysis including the latter two variables and the dosimetric parameter $D_{5cc,EQD2}$ showed that only the $D_{5cc,EQD2}$ (OR 1.16; 95% CI 1.10 – 1.22; $p < 0.001$) and female gender (OR 3.02; 95% CI 1.30 – 6.99; $p = 0.010$) were significantly correlated with low grade esophageal toxicity (*Appendix 6C*).

Figure 1 – Normal tissue complication probability (NTCP) models for grade 1 – 2 acute toxicity in the esophagus

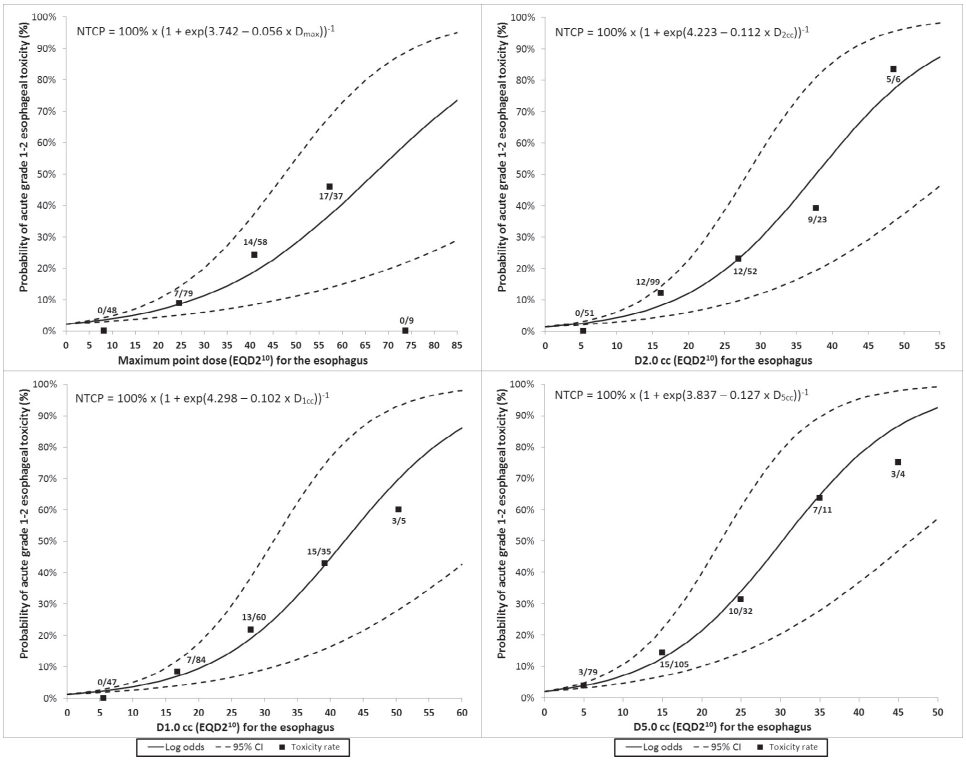

Abbreviations: EQD2[10] = equivalent dose of 2 Gy per fraction with α/β ratio of 10
The x-axis shows the dose range, and is divided into 5 equal parts ("bin"). For each bin, the square represents the mean incidence of toxicity (%). Both the number of patients with toxicity and the numbers at risk in each bin are indicated.

The overall survival rates were 73% (95% CI 67 – 78%), 50% (95% CI 43 – 56%) and 38% (95% CI 32 – 45%) at 1-, 2- and 3-years respectively, with a median overall survival of 24 months. No significant difference in survival was found between patients with and without toxicity, with 2-year survival rates of 44% (95% CI 28 – 59%) and 51% (95% CI 44 – 58%), respectively (p = 0.428). Local control rates were 84% (95% CI 77 – 90%) and 75% (95% CI 65 – 83%) at 2- and 3-years, respectively.

6.5 Discussion

In this study of centrally located lung tumors treated with stereotactic radiotherapy, high grade (≥ grade 3) acute or late esophageal toxicities were not observed. Acute grade 1 or 2 esophageal toxicity occurred in 17% of patients and correlated significantly with the

esophageal dosimetric parameters $D_{max,EQD2}$, $D_{1cc,EQD2}$, $D_{2cc,EQD2}$ and $D_{5cc,EQD2}$. For $D_{5cc,EQD2}$, each additional gray was associated with a 13.5% increased risk of toxicity. For $D_{max,EQD2}$, $D_{1cc,EQD2}$ and $D_{2cc,EQD2}$ each additional gray was associated with a 5.8%, 10.7% and 11.9% increased risk of acute grade 1 – 2 toxicity, respectively. Multivariable analysis including both dosimetric and clinical predictors showed that acute grade 1 – 2 esophageal toxicity was significantly associated with esophageal $D_{5cc,EQD2}$ and female gender.

At both institutes, a maximum point dose limit was mandatory for the esophagus, ranging from 50 to 56 Gy EQD_2^{10}, depending on the fractionation schedule. Our point dose limits were generally consistent with those used in the HILUS trial, which recommended an esophageal D_{max} of 52.7 Gy EQD_2^{10} (17). However, in the phase I/II RTOG 0813 dose-escalation trial, a substantially higher maximum point dose was allowed; a D_{max} of > 105% of the prescription dose was considered as a protocol violation. This equals to 89.7 Gy EQD_2^{10} for a schedule with 5 fractions of 10 Gy (21). In our cohort, the highest D_{max} was 82.2 Gy EQD_2^{10}, and 32% of the patients with a $D_{max} \geq 56$ Gy EQD_2^{10} (8 out of 25) developed grade 1 – 2 esophageal toxicity. The corresponding rate of esophageal toxicity in patients with a $D_{max} < 56$ Gy EQD_2^{10} was considerably lower at 15% (31 out of 207). Although the range of fractionation schedules makes it hard to directly compare studies, our failure to observe high grade toxicity suggests that higher point dose limits may be acceptable.

Both institutes in our series did not use a volumetric dose limit, however an esophageal D_{5cc} of ≤ 27.5 Gy in 5 fractions (35.5 Gy EQD_2^{10}) was recommended in RTOG 0813. A $D_{5cc} \geq 35.5$ Gy EQD_2^{10} was delivered to only 8 patients in our study, in whom a rate of 88% was reported for grade 1 – 2 toxicity, compared to only 14% for those with a $D_{5cc} < 35.5$ Gy EQD_2^{10}. This observation suggests that it could be worthwhile to use volumetric parameters as well during stereotactic treatment planning, as $D_{1cc,EQD2}$, $D_{2cc,EQD2}$,and $D_{5cc,EQD2}$ were all significant in the univariate analysis.

Our NTCP model predicts toxicity rates that are in line with previously published retrospective data, when factoring in that our model predicted grade 1 – 2 toxicity whereas most previous analyses have predicted higher grades of toxicity. In a study of 125 patients reported by Wu et al., 12% experienced grade ≥ 2 toxicity within 120 days post-treatment. Fitted logistic regression response curves showed predicted probabilities of complication less than 20% for $D_{max} \leq 44.2$ Gy EQD_2^{10} and $D_{5cc} \leq 21.9$ Gy EQD_2^{10} (95). In our model, a D_{max} of 44.2 Gy EQD_2^{10} corresponded to a 22% probability of toxicity, and a D_{5cc} of 21.9 Gy EQD_2^{10} to a 26% probability. Our slightly higher probability rates might be explained by the fact that our model predicted grade 1 and 2 toxicity, whereas Wu et al. reported grade 2 and 3 toxicity. Another study described late grade 3 esophageal toxicity in 2 patients at a $D_{0.01cc}$ of

51.5 Gy (65.0 Gy EQD_2^{10}) and 52 Gy (65.9 Gy EQD_2^{10}) and a D_{5cc} of 37.3 Gy (42.7 Gy EQD_2^{10}) and 21.5Gy (21.8 Gy EQD_2^{10}), respectively (96). However, patients were treated concurrently with VEGF modulating agents, which perhaps increased the sensitivity of the organs at risk to radiotherapy and consequently the risk on toxicity. In our cohort, 10 patients received a D_{max} of ≥ 65.0 Gy EQD_2^{10} without experiencing toxicity. Only two patients received a D_{5cc} higher than 42.7 Gy EQD_2^{10} with a toxicity rate of 50% and 42 patients received a D_{5cc} ≥ 21.8 Gy EQD_2^{10} with a toxicity rate of 42%. Nuyttens et al. (97) also reported esophageal SBRT dose limits. The doses corresponding to a 50% probability of grade 2 complications were 67.6 Gy EQD_2^{10} for D_{max}, 45.5 Gy EQD_2^{10} for D_{1cc} and 35.4 Gy EQD_2^{10} for D_{5cc}, which are higher than in the current study. This difference could be explained by the inclusion of both grade 1 and 2 in our study compared to only grade 2 in the study by Nuyttens, the higher complication rates in the current study (16.5% vs 8.6%) and the different methods used to model the NTCP. A comparison of dose-response models based on the previously mentioned studies (95, 96) between the 50% probability of grade 2 toxicity versus the 50% probability of grade 3 toxicity showed ± 20 Gy (absolute dose in 5 fractions) difference for the D_{max} and D_{1cc} (97).

High grade esophageal toxicity after SBRT is uncommon, but was described in a few other reports on both pulmonary and non-pulmonary tumors treated with SBRT (94, 98, 99). Following single-fraction paraspinal stereotactic radiosurgery of 16 to 24 Gy, grade ≥3 esophageal toxicity occurred in 6.8% of patients and a $D_{2.5cc}$ higher than 14.0 Gy (28.0 Gy EQD_2^{10}) was a significant predictor of grade ≥ 3 toxicity (98). High grade toxicity was also described in 2 patients treated with prior chemo- and/or radiotherapy before SBRT. One patient with early stage lung cancer, who received adjuvant chemotherapy (carboplatin, paclitaxel and gemcitabine) following 1 fraction of 25 Gy, developed a tracheoesophageal fistula 6 months after radiotherapy. A second patient with metastatic osteosarcoma in the 7^{th} thoracic vertebra, received conventionally fractionated radiation of 40 Gy in 20 fractions with concurrent chemotherapy (ifosfamide and etoposide) followed by 2 fractions of 12 Gy with SBRT and further adjuvant chemotherapy. Four months after SBRT, this patient developed an esophageal perforation and fatal mediastinitis. In both cases, the esophagus was within the high-dose radiation volume. High grade adverse events occurred at (single-fraction biologically effective dose using α/β ratio of 3, SFBED) a D_{max} of 21.0 Gy_3 and D_{5cc} of 16.5 Gy_3 for the first patient and D_{max} of 18.5 Gy_3 and D_{5cc} of 11.4 Gy_3 for the second patient (94). Severe esophageal toxicity has also been documented in a patient receiving adjuvant chemotherapy following a single fraction of 25 Gy; 6 months post-SBRT, tracheoesophageal and tracheavascular fistulas developed resulting in fatal hemoptysis (99). These studies highlight the potential role of prior radiotherapy or chemotherapy in severe esophageal

toxicity, especially following very high doses of SBRT. Antiangiogenic agents in combination with SBRT have previously been associated with gastro-intestinal toxicity (100).

Female gender was the only significant clinical predictor for low grade esophageal toxicity in our multivariable analysis including both clinical and dosimetric factors. This association was also observed in previous studies on chemoradiotherapy, however a clear explanation is nevertheless lacking (101-103).

Limitations of our study include the differences in treatment techniques between centers, as well as possible discrepancies between planned versus delivered doses, which may confound the observed dose-response relationships. Other limitations are those inherent to retrospective toxicity scoring, especially for lower toxicity grades. Given the difficulty in distinguishing between radiotherapy-related esophagitis and symptoms due to factors such as an acute airway infection, we did not collect rates of late grade 1 and 2 esophageal toxicity. Of note, we did not observe acute or late grade 3 – 5 toxicity, which could generally more easily be identified in retrospective data than lower grades of toxicity due to the severity of symptoms and the need for hospitalization. As low grade toxicity may be underestimated by retrospective scoring, the thresholds identified in our study have to be interpreted with caution.

In conclusion, there was a low incidence of acute esophageal toxicity and high grade acute or late esophageal toxicity was not observed in this study of centrally located lung tumors treated with stereotactic or hypofractionated radiotherapy (≤ 12 fractions). Doses to small volumes of the esophagus are associated with low grade esophageal toxicity. An esophageal D_{max} of 56.0 Gy EQD_2^{10} and a D_{5cc} of 35.5 Gy EQD_2^{10} could be delivered without high risks of severe toxicity. The NTCP-models described in this study might be used as guidelines for the stereotactic treatment of central lung tumors. Further studies are necessary to validate these parameters for acute esophagus toxicity.

7

CHAPTER 7

Predicting high-grade esophagus toxicity after treating central lung tumors with stereotactic radiotherapy using a Normal Tissue Complication Probability model

M. Duijm [1], N.C. van der Voort van Zyp [2], P. van de Vaart [2],
E. Oomen-de Hoop [1], M.E. Mast [2], M.S. Hoogeman [1], J.J. Nuyttens [1]

[1] *Department of Radiation Oncology, Erasmus MC Cancer Institute, Rotterdam, The Netherlands*
[2] *Department of Radiation Oncology, Haaglanden MC, The Hague, The Netherlands*

International Journal of Radiation Oncology • Biology • Physics, Vol. 106, No. 1, pp. 73 – 81, 2020

Abstract

Purpose

The treatment of central lung tumors with stereotactic body radiation therapy (SBRT) is challenged by the risk of excessive esophageal toxicity. To improve clinical decision making, we aimed to derive normal tissue complication probability (NTCP) models in a patient cohort with central lung tumors treated with SBRT and to evaluate the currently used esophagus dose constraints.

Methods and Materials

Patients with a central lung tumor who received SBRT (8 fractions of 7.5 Gy or 12 fractions of 5 Gy) were included. Doses were recalculated to an equivalent dose of 2 Gy with an α/β-ratio of 10 Gy for acute and 3 Gy for late toxicity (the cut-off was 3 months). The esophagus was manually delineated. NTCP modelling based on logistic regression was used to relate dose-volume histogram parameters (D_{max}, D_{1cc}, D_{2cc}, D_{5cc}) to acute and late toxicity. Parameters with a *p*-value < 0.05 were included in the model. Based on the NTCP models, we determined the probability of toxicity for the currently used dose constraints: $D_{1cc} \leq 40$ Gy for 8 fractions and $D_{1cc} \leq 48$ Gy for 12 fractions.

Results

For this study, 188 patients with 203 tumors were eligible. Esophagus toxicity occurred in 33 patients (18%). Late high-grade toxicity consisted of 2 possible treatment-related deaths (grade 5) and 2 patients with grade 3 toxicity. Acute toxicity only consisted of only grade 1 (n = 19) and grade 2 toxicity (n = 10). All investigated dose-volume histogram parameters were significantly correlated to acute and late toxicity. The probability of late high-grade toxicity is 1.1% for 8 fractions and 1.4% for 12 fractions, when applying the current dose constraints.

Conclusions

High-grade esophageal toxicity occurred in 2.1% of the patients including 2 possible treatment-related deaths. The currently used dose constraints correspond to a low risk of high-grade toxicity.

7.1 Introduction

Patients with early stage non-small cell lung cancer (NSCLC) or small lung metastases not suitable for surgery are often candidates for stereotactic body radiation therapy (SBRT) (5). The treatment of central lung tumors, however, may result in excessive toxicity (13). To reduce this risk, risk-adapted fractionated schedules have been used (10, 17). The prospective Radiation Therapy Oncology Group (RTOG) 0813 trial showed that these schedules resulted in outcomes comparable with those of peripheral located tumors, but cases of high-grade toxicity were observed. Plan details to link delivered dose to toxicity were not reported (16).

Tolerance data and predictive dosimetric parameters for the esophagus and central airways could help to select patients who can be safely treated with SBRT and to guide treatment planning (104). Previous studies reported on predictive parameters for esophageal toxicity after SBRT (97, 105, 106). None of them, however, described predictive parameters for high-grade esophageal toxicity.

Based on predictive parameters, a normal tissue complication probability (NTCP) model can be generated, which shows the relationship between predictive factors and toxicity probability. Hence, an NTCP model will help physicians in the trade-off between risk of toxicity and dose needed for adequate tumor control.

In this study, we analyzed dosimetric and toxicity data in a patient cohort with central lung tumors treated with SBRT to determine parameters that are related to high-grade esophageal toxicity. In addition, we derived NTCP models for late high-grade and acute low-grade esophageal toxicity and used them to estimate the risk of toxicity for the dose constraints within our institute and for the dose constraints of the RTOG 0813 trial (16).

7.2 Methods and materials

We analyzed treatment outcome in patients from Haaglanden Medical Center with central lung tumors treated with fractionated stereotactic radiotherapy between 2012 and 2016. This study was granted approval from the institutional medical ethics committee (METC Zuidwest Holland). Central lung tumors were defined as tumors located ≤ 2 cm from the esophagus, trachea, and mainstem, intermediate, upper, middle, or lower lobe bronchus (*Appendix 7A*). Patients were excluded if they received prior radiotherapy to any part of the current radiation field, were treated with chemotherapy during SBRT, or received a diagnosis of small cell lung cancer.

SBRT was initially delivered using a dedicated stereotactic linear accelerator (Novalis, Brainlab AG, Munich, Germany); from 2013, a linear accelerator with cone beam computed tomography (CT) guidance (Elekta AB, Stockholm, Sweden) was used. From the end of 2015 all patients were treated with the cone beam CT-equipped linear accelerator. Patients were treated with 60 Gy in 8 fractions 3 times a week or 60 Gy in 12 fractions 4 times a week. If

the planning target volume (PTV) overlapped or was too close to organs at risk (treating physician's discretion), 12 fractions were prescribed.

The gross tumor volume was contoured on a lung CT scan using lung and mediastinal setting. The esophagus was delineated on the average phase of the planning CT scan using mediastinal setting. Until 2014, the gross tumor volume was expanded to an internal target volume (ITV) based on 6 scans taken randomly during the breathing cycle. In 2014 this technique was replaced by a 4-dimensional CT scan, in which an ITV was obtained by contouring the tumor in 10 phases of the respiratory cycle. The ITV was expanded with 5 mm (6 mm in craniocaudal direction) to a PTV for the Novalis linear accelerator and 6 mm in all directions for the Elekta linear accelerator. Treatment planning was done using Monte Carlo and collapsed cone algorithm for patients treated on the Novalis linear accelerator and the Elekta linear accelerator, respectively. Dose prescription for patients treated with 12 fractions was based on ICRU-62 criteria such that the maximum dose of the PTV was ≤ 107%. In the case of 8 fractions, the dose was prescribed to the 100% isodose line, and the D_{max} was 110% to 140% of the prescribed dose. Regardless of the fractionation schedule, at least 95% of the PTV had to receive 100% of the prescribed dose and 99% of the PTV had to receive 90% of the prescribed dose.

Various parameters of the esophagus were derived: maximum point dose (D_{max}) and dose to specific volumes (D_{1cc}, D_{2cc}, D_{5cc}). For the current analysis, doses were recalculated to an equivalent dose of 2 Gy per fraction (EQD_{2Gy}) using the following formula: $EQD_{2Gy} = D * (d + \alpha/\beta)/(2.0 + \alpha/\beta)$, in which D = total dose, d = dose per fraction, and the α/β ratio was 10 Gy ($EQD_{2Gy,10Gy}$) for acute and 3 Gy ($EQD_{2Gy,3Gy}$) for late toxicity.

Toxicity rates and follow-up were retrospectively reviewed from medical hospital records. Follow-up for each patient was generally performed 3, 6, 9, 12, 18, and 24 months after radiation and annually thereafter. Esophageal toxicity was defined according to the Common Terminology Criteria for Adverse Events (version 4.03). Acute toxicity was defined as an event < 3 months after radiation and late toxicity as toxicity that occurred thereafter. In the case of multiple reports of toxicity in a single patient, the highest score was used for analysis.

Toxicity was dichotomized into the presence or absence of late high-grade (≥ 3) and acute low-grade (≤ 2) toxicity. Differences between dose in patients with and without toxicity were described with the Mann-Whitney *U* test. Logistic regression was used to define clinical or dosimetric predictors for toxicity. The following clinical factors were entered in univariate analyses: age, sex, tumor origin, World Health Organization performance status, classification of Chronic Obstructive Pulmonary Disease (COPD GOLD), Charlson Comorbidity Index, number of fractions and distance between tumor and esophagus (in case of multiple tumors in a single patient, the shortest distance was used). Potential relations between factors were tested with the Mann-Whitney *U* test or χ^2 test.

An NTCP model describes the relation between input variables and the observed toxicity probability. For this study we used the logistic regression model, which yields the sigmoidal relationship between the input variables and probability of toxicity. Each dosimetric parameter that was statistically significant (p-value ≤ 0.05) in the univariate logistic regression analysis was individually modelled with: $\mathrm{NTCP} = \frac{100\%}{1+ e^{-(\beta 0 + \beta 1 * \mathrm{Dx})}}$, in which D_x is the dose of the esophagus in the maximum point, 1 cc, 2 cc or 5 cc, and β_0 and β_1 are the constant term and the regression coefficient of D_x, respectively.

Probabilities of toxicity for the institutional and RTOG 0813 dose constraints were estimated using the derived NTCP model. Dose constraints at the institution are D_{1cc} ≤ 40 Gy in 8 fractions (64 Gy $EQD_{2Gy,3Gy}$ and 50 Gy $EQD_{2Gy,10Gy}$) and D_{1cc} ≤ 48 Gy in 12 fractions (67 Gy $EQD_{2Gy,3Gy}$ and 56 Gy $EQD_{2Gy,10Gy}$). Dose constraints of the RTOG trial are D_{max} ≤ 105% of the PTV prescription, which is 63 Gy in case of the maximum allowed dose of 12 Gy per fraction (197 Gy $EQD_{2Gy,3Gy}$ and 119 Gy $EQD_{2Gy,10Gy}$) and D_{5cc} < 27.5 Gy (47 Gy $EQD_{2Gy,3Gy}$ and 36 Gy $EQD_{2Gy,10Gy}$), where the volume maximum is a suggested limit. Based on mortality rates of surgical lung cancer treatment (lobectomy or pneumonectomy), doses coherent to the 5% probability rate were derived from NTCP curves (107).

Overall survival (OS) was defined as first day of treatment until date of death or last day of contact for patients who were still alive. Local control (LC) was defined as first day of treatment until date of local recurrence. When no event occurred, the patient was censored on the last day of follow-up. Survival and time to local recurrence were estimated using the Kaplan-Meier method, and the log-rank test was used to evaluate differences in OS and LC between patients who had NSCLC and patients who had a metastatic tumor. In all analyses, p-value of ≤ 0.05 was considered to be statistically significant. All analyses were performed using IBM SPSS statistics version 24.0.0.1 (SPSS Inc, Chicago, IL) and R version 3.4.1 (2017, R Foundation for Statistical Computing Platform).

7.3 Results

For this study, 191 patients with 206 central tumors were eligible. Three patients were excluded owing to absent follow-up data. Baseline patient and tumor characteristics of the remaining 188 patients are described in *Table 1*. Primary NSCLC was diagnosed in 82% (n = 154) of the patients and metastatic tumor in the lung in the remaining 18%. Most patients (n = 174, 93%) were treated for a single central tumor consisting of primary NSCLC or metastatic lesion, 10 patients were treated for a central primary together with a central lymph node, 2 patients for 2 central primary tumors, 1 patient for 2 central metastatic tumors and 1 patient for 3 central metastatic tumors. Seventy-five patients (40%) were treated with 12 fractions and 113 patients (60%) with 8 fractions. The median tumor diameter was 36 mm (interquartile range 27 – 47 mm).

Table 1 – Patient and tumor characteristics

Patient characteristics (n = 188)	*n (%) or median (IQR, range)*	
Age (y)	72	(66 – 79, 42 – 94)
Gender		
Female	79	(42%)
Male	109	(58%)
Tumor origin		
Non-small cell lung cancer	154	(82%)
Metastatic tumor in the lung	34	(18%)
Charlson Comorbidity Index		
0 – 2	117	(62%)
3 – 5	61	(33%)
6 – 9	10	(5%)
WHO performance Scale		
0	85	(45%)
1	93	(50%)
2	6	(3%)
3 – 4	4	(2%)
Radiation therapy indication		
Technically inoperable	31	(17%)
Comorbidities	153	(81%)
Refusing surgery	4	(2%)
Fractionation schedule		
8 fractions of 7.5 Gy	113	60%
12 fractions of 12 Gy	75	40%
Tumor characteristics (n = 203)	*n (%) or median (IQR, range)*	
Localization of the tumor		
Upper lobe	111	55%
Middle or lower lobe	57	28%
Mediastinum	35	17%
Tumor diameter (mm)	36	(27 – 47, 7 – 88)
Distance tumor to esophagus (mm)	21	(12 – 34, 0 – 75)

Abbreviations: IQR = interquartile range; WHO = world health organization.

Esophageal toxicity was seen in 33 patients (18%), of whom 6 reported late toxicity (3%). Late toxicity consisted of grade 5 (n = 2), grade 3 (n = 2), grade 2 (n = 1), and grade 1 (n = 1). Of the patients who died, 1 had a tracheoesophageal fistula 10 months after irradiation, for which a stent was placed. Two weeks after this procedure, the patient had hemoptoe and died within 2 days. Autopsy reported rupture of the vasa vasorum at a necrotic and fibrotic area close to the fistula, most likely caused by radiation. The other patient died 14 months after SBRT due to septic mediastinitis caused by a large esophagus perforation. This patient had increasing dysphagia 1 month after radiation therapy, resulting in grade 3 dysphagia 13 months after treatment. The CT scan showed progression of mediastinal lymph nodes for which 1 cycle of FOLFOX (leucovorin, 5-fluorouracil, oxaliplatin) was given. During this

treatment the patient developed sepsis and died. The perforation was most likely caused by radiation, but tumor growth of the lymph nodes through the esophagus could not be excluded. Both grade 5 events were treated with 12 fractions for a subcarinal lymph node metastasis from colorectal origin. Late grade 3 esophagus toxicity consisted of dysphagia in 1 patient resulting from circular ulceration of the esophagus 9.5 months after treatment, for which stent placement was scheduled. However, the patient died before this procedure from progressive metastatic disease complicated by severe pneumonia. The other grade 3 patient was hospitalized for dysphagia resulting from radiation esophagitis 4.5 months after treatment. In all high-grade toxicity cases, the tumor was adjacent to the esophagus. The tumor was located directly next to the esophagus in both grade 5 cases, resulting in a complete esophagus-PTV overlap in multiple axial slices of the planning CT scan. In the grade 3 cases, the tumor was located next to the esophagus resulting in almost complete overlap between esophagus and PTV in 1 patient and in 50% overlap of the esophagus and PTV in the other patient. Dosimetric and fractionation details are displayed in *Table 2*, showing that all 4 cases exceeded the dose constraints currently used in the institution. Compared with the RTOG 0813 constraints, none of the patients exceeded the D_{max} constraint, but all violated the suggested volume (D_{5cc}) limit.

Table 2 – Dosimetric details of patients with late high-grade (≥ 3) toxicity

	number of fractions	D_{max} ($EQD_{2Gy,3Gy}$)	D_{1cc} ($EQD_{2Gy,3Gy}$)	D_{2cc} ($EQD_{2Gy,3Gy}$)	D_{5cc} ($EQD_{2Gy,3Gy}$)
Patients within our cohort					
Grade 5	12	101 Gy	97 Gy	95 Gy	77 Gy
Grade 5	12	119 Gy	112 Gy	109 Gy	104 Gy
Grade 3	12	98 Gy	96 Gy	96 Gy	94 Gy
Grade 3	8	157 Gy	146 Gy	142 Gy	130 Gy
Patients within literature					
Onimaru et al.					
Grade 5	8	94 Gy	71 Gy	-	40 Gy
Modh et al.					
Grade 3	5	112 Gy	-	-	-
Stephans et al.					
Grade ≥ 3	10	84 Gy *	75 Gy	-	50 Gy
Grade ≥ 3	10	85 Gy *	80 Gy	-	22 Gy

* Dose to 0.01 cm^3

Logistic regression showed significant relationship between all dosimetric parameters and late high-grade esophageal toxicity (all *p*-values < 0.01, *Table 3*). Based on the NTCP models (*Figure 1*), a 5% probability of late high-grade toxicity corresponds to D_{max}, D_{1cc}, D_{2cc} or D_{5cc} of 113.2, 89.2, 80.4, or 68.9 Gy $EQD_{2Gy,3Gy}$, respectively (equal to D_{max} 46.2 Gy, D_{1cc} 40.3 Gy, D_{2cc} 38.0 Gy, D_{5cc} 34.7 Gy in a 5-fraction regimen). When the institution dose constraints are respected, the probability of late high-grade toxicity based on the NTCP model is 1.1% for

treatment with 8 fractions and 1.4% for 12 fractions. When applying the RTOG 0813 constraints, the probability is 45.5% based on the D_{max} constraint and 0.3% based on the D_{5cc} suggested volume limit.

Table 3 – Results of logistic regression used to determine the normal tissue complication probability model

Odds ratio of late high-grade toxicity for each DVH parameter				
	D_{max} ($EQD_{2Gy,3Gy}$)	**D_{1cc} ($EQD_{2Gy,3Gy}$)**	**D_{2cc} ($EQD_{2Gy,3Gy}$)**	**D_{5cc} ($EQD_{2Gy,3Gy}$)**
Odds ratio	1.03	1.06	1.08	1.14
95% CI	1.01 – 1.06	1.02 – 1.10	1.03 – 1.14	1.02 – 1.28
p-value	0.011	0.002	0.003	0.023

Odds ratio of acute low-grade toxicity for each DVH parameter				
	D_{max} ($EQD_{2Gy,3Gy}$)	**D_{1cc} ($EQD_{2Gy,3Gy}$)**	**D_{2cc} ($EQD_{2Gy,3Gy}$)**	**D_{5cc} ($EQD_{2Gy,3Gy}$)**
Odds ratio	1.04	1.05	1.06	1.07
95% CI	1.02 – 1.05	1.03 – 1.07	1.04 – 1.08	1.04 – 1.09
p-value	< 0.001	< 0.001	< 0.001	< 0.001

Abbreviation: 95% CI = 95% confidence interval

Figure 1 – Normal tissue complication probability models for late high-grade toxicity

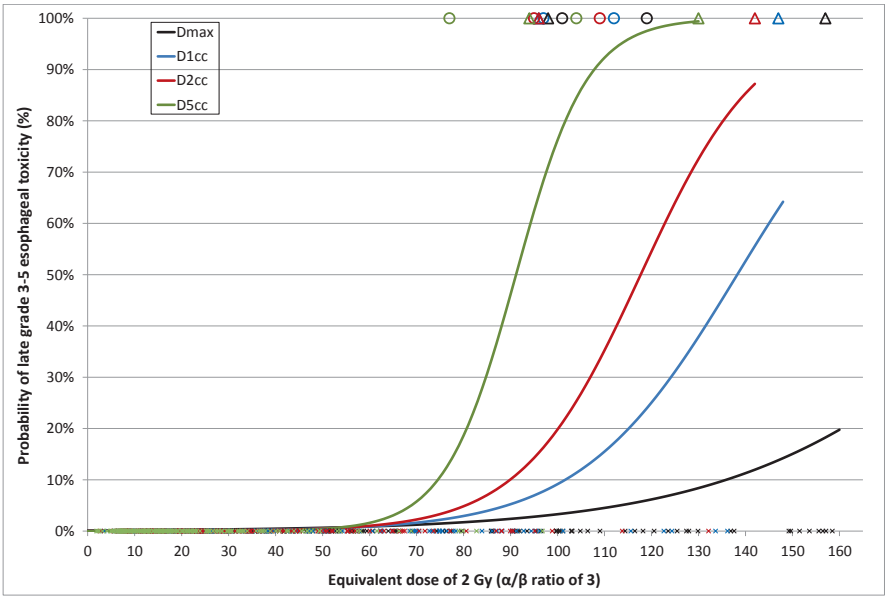

The crosses represent the dose of the 4 dose-volume histogram parameters in patients without late high-grade toxicity, the triangles the dose in patients with grade 3 toxicity, and the circles the dose in patients with grade 5 toxicity.

In 40 patients (21%) the tumor was located within 10 mm of the esophagus; 18 of these patients reported any kind of esophageal toxicity. Of the 9 patients with abutting tumors (distance from tumor to the esophagus is 0 mm or tumor and esophagus overlap), 7 reported esophageal toxicity: 4 cases of late high-grade toxicity, 1 case of acute grade 2 toxicity, and 2 cases of acute grade 1 toxicity. Regarding clinical factors related to acute toxicity, each extra millimeter distance between tumor and esophagus decreased the odds of acute toxicity with 9% (odds ratio 0.91; 95% confidence interval (CI) 0.88 – 0.95; *p*-value < 0.001) (*Table 4*). Additionally, receiving 12 fractions was correlated with increased acute toxicity (odds ratio 1.34 95% CI 1.09 – 1.64; *p*-value = 0.006). The distance between tumor and esophagus was significantly correlated with the number of fractions used (*p*-value = 0.004), and therefore no multivariate analysis was done.

Table 4 – Univariate logistic regression results for factors predicting acute grade 1 to 2 esophageal toxicity

					Univariate analysis	
Characteristic	**Toxicity**		**No toxicity**		**Odds Ratio (95% CI)**	***p*-value**
Age (y)						
median (IQR)	71	(65 – 79)	73	(66 – 80)	0.99 (0.95 – 1.03)	0.520
Distance tumor to esophagus*						
median (IQR)	7	(1 – 19)	24	(15 – 36)	0.91 (0.88 – 0.95)	< 0.001
Sex						
Male	n = 19	(17%)	n = 90	(83%)	1	
Female	n = 10	(13%)	n = 69	(87%)	0.69 (0.30 – 1.57)	0.373
Tumor origin						
Non-small cell lung cancer	n = 23	(15%)	n = 131	(85%)	1	
Metastatic tumor in lung	n = 6	(18%)	n = 28	(82%)	1.11 (0.68 – 1.81)	0.692
Charlson Comorbidity Index						
0-2	n = 18	(15%)	n = 99	(85%)	1	
≥ 3	n = 11	(15%)	n = 60	(85%)	1.01 (0.45 – 2.28)	0.984
WHO performance scale						
0	n = 13	(15%)	n = 72	(85%)	1	
≥ 1	n = 16	(16%)	n = 87	(84%)	1.01 (0.68 – 1.50)	0.964
COPD GOLD**						
0-1	n = 5	(12%)	n = 37	(88%)	1	
2-4	n = 19	(16%)	n = 97	(84%)	1.45 (0.50 – 4.17)	0.491
Amount of fractions						
8	n = 11	(9%)	n = 105	(91%)	1	
12	n = 18	(25%)	n = 54	(75%)	1.34 (1.09 – 1.64)	0.006

*Distance tumor-esophagus: in case of multiple tumors irradiated in a single patient, the smallest distance between tumor and esophagus is used; ** COPD status is missing in 30 patients

Abbreviations: COPD GOLD = classification of chronic obstructive pulmonary disease; IQR = interquartile range, WHO = world health organization; 95% CI = 95% confidence interval

Twenty-nine patients reported acute esophageal toxicity (15%) consisting only of grade 1 (n = 19) and grade 2 toxicity (n = 10). The median D_{max} was 35 Gy $EQD_{2Gy,10Gy}$ higher in patients with acute toxicity compared with patients without acute toxicity (68.7 Gy $EQD_{2Gy,10Gy}$ vs 31.4 Gy $EQD_{2Gy,10Gy}$). All dose-volume histogram parameters were significantly higher (*p*-

value < 0.001) in patients with acute toxicity (*Appendix 7B*). Furthermore, logistic regression showed increased odds of 4% to 7% on acute low-grade esophageal toxicity per extra gray given (*Table 3)*. The 4 individual NTCP curves were plotted and when applying the currently used dose constraints, the probability of acute low-grade toxicity is 24% for 8 fractions and 30% for 12 fractions (*Figure 2*). When applying the RTOG 0813 constraints this is 70% for the D_{max} and 26% for the D_{5cc}.

Figure 2 – Normal tissue complication probability models for acute grade 1-2 toxicity

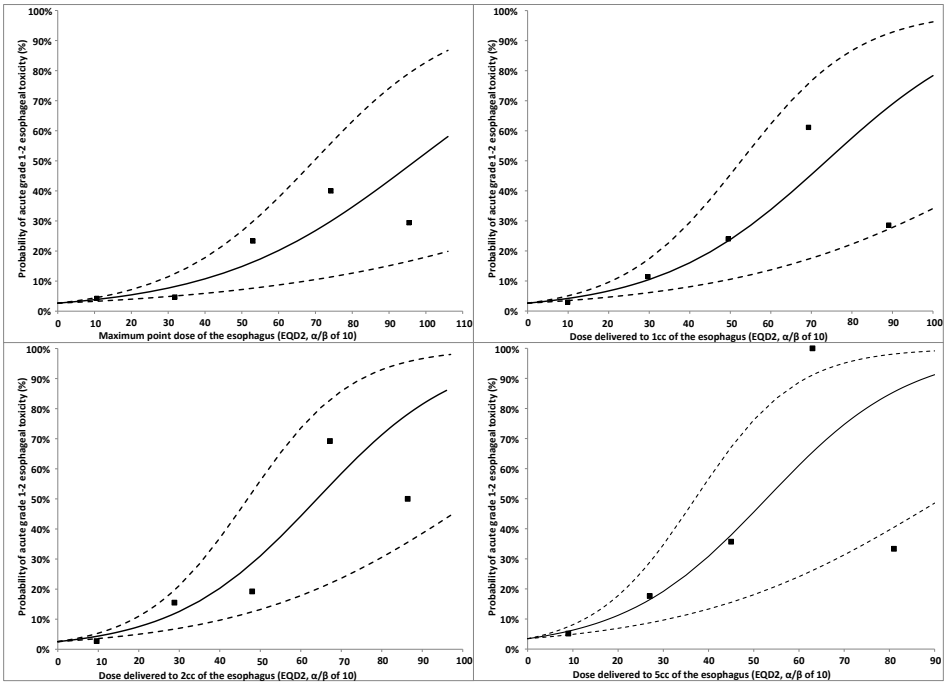

The black solid line shows the logistic regression. The dashed lines reflect the 95% confidence interval. The x-axis shows the dose range, and is divided into 5 equal parts (bins). For each bin, the square represents the mean incidence of toxicity (%).

Abbreviations: EQD_{2Gy} = equivalent dose in 2 Gy fractions (α/β-ratio 10)

Median OS for the whole group was 24.3 months (95% CI 17.3 – 31.2). The OS rates for 1, 2 and 3 years were 73%, 51%, and 42%, respectively. There was no difference in the OS rates between patients with NSCLC and patients with lung metastases: a median OS of 23.3 months (95% CI 14.9 – 31.7) versus 30.2 months (95% CI 6.6 – 53.7), respectively (*p*-value = 0.947). Local control for the whole group was 95% at 1 year and 88% at 2 years. The LC rate at 2 years was 88% within the NSCLC group (165 tumors) and 87% within the metastatic group (38 tumors, *p*-value = 0.387).

7.4 Discussion

Severe esophageal toxicity occurred in 2.1% of patients including 2 treatment-related deaths, and 15% of patients reported acute low-grade toxicity. In all high-grade late toxicity cases, the tumor abutted the esophagus, resulting in overlap of the PTV with the esophagus. Late high-grade esophageal toxicity in patients treated solely with SBRT (without any confounding therapies) is rarely reported. Because of the high variance between studies, we will discuss different clusters of literature.

Concerning late high-grade toxicity without any confounding therapies, Onimaru et al. reported, within a cohort of 46 patients, 1 case of grade 5 toxicity (2.2%). This patient died of a radiation-induced esophageal ulcer 5 months after receiving 48 Gy in 8 fractions to the PTV adjacent to the esophagus (46). In an analysis of 125 patients, Modh et al. reported grade 3 esophagitis 4 months after SBRT in 1 patient (0.8%) who had a tumor abutting the esophagus (53). Raman et al. reported 1 case of grade 3 esophagitis (cohort of 206 patients, 0.5%) 4.7 months after SBRT (48 Gy, 12 Gy/fr), but no dosimetric parameters were reported (59). If we apply our NTCP model to the data of Onimaru et al. (46), the probability of late high-grade toxicity would be 2.7%, 1.7% or 0.1% based on the D_{max}, D_{1cc} or D_{5cc}, respectively. The D_{max} of the patient described by Modh et al. (53) corresponds to a 4.8% probability of late high-grade toxicity. Dosimetric characteristics of the studies are shown in *Table 2*.

Four studies described late high-grade esophageal toxicity after SBRT in combination with possible confounding therapies, making it hard to directly compare these results with our analyses. The first study described a cohort of 32 patients with 1 fatal tracheoesophageal fistula (3.1%) after single-fraction radiotherapy (25 Gy) and chemotherapy (99). A second study described 2 patients (of a total 52 patients, 3.8%) with an esophageal fistula, both receiving adjuvant antiangiogenic agents within 2 months after SBRT (50 Gy, 5 Gy/fr) (96). In the study by Abelson et al., 2 of the 31 patients (6.5%) died within 6 months after radiation therapy and chemotherapy. One died of esophageal perforation causing mediastinitis, and the other patient had a tracheoesophageal fistula (94). The last study reported 8% (14 of 182 patients) high-grade esophageal toxicity after treatment with single-fraction SBRT (16 – 24 Gy) to metastases abutting the esophagus. In this study a $D_{2.5cc} < 14$ Gy (47.6 Gy $EQD_{2Gy,3Gy}$) was suggested to keep the high-grade toxicity at < 5%. However in 57% of these high-grade toxicity cases, patients received either doxorubicin or gemcitabine (98).

Several studies have published dosimetric predictors for late or combined (acute and late) grade 1 to 3 esophageal toxicity. First, based on data of 58 patients with 9% grade 2 toxicity, a D_{max} of 43.4 Gy (101.4 Gy $EQD_{2Gy,3Gy}$) and D_{1cc} of 32.9 Gy (63.0 Gy $EQD_{2Gy,3Gy}$) corresponded to 50% probability of late grade 2 esophageal toxicity after SBRT in 5 fractions (97). Chang et al. analyzed 100 patients with central NSCLC treated with 4 fractions of SBRT. Based on 3 patients with grade 2 esophagitis (moment of toxicity unknown), a $D_{max} \leq 35$ Gy

(82.2 Gy $EQD_{2Gy,3Gy}$) and $V_{30} \leq 1$ cc (V_{63Gy} $EQD_{2Gy,3Gy}$) were recommended (38). Yau et al. made an NTCP model for (acute and late) grade 1 to 3 esophagus toxicity. A 15% risk of toxicity corresponded to D_{max} of 142 Gy $EQD_{2Gy,3Gy}$, D_{1cc} of 124 Gy $EQD_{2Gy,3Gy}$ and D_{2cc} of 118 Gy $EQD_{2Gy,3Gy}$. The models of this study had low statistical power because of the small number of index events (106).

According to studies reporting acute esophagus toxicity, Wu et al. showed < 20% (sub)acute esophageal toxicity when $D_{max} \leq 44$ Gy $EQD_{2Gy,10Gy}$ and $D_{5cc} \leq 22$ Gy $EQD_{2Gy,10Gy}$ (95). The same doses predict a 12.3% to 12.5% risk of toxicity based on our NTCP models. A second study predicted an 11% risk of (sub)acute grade ≥ 2 esophageal toxicity when $D_{1.5cc} \geq 17.6$ Gy $EQD_{2Gy,10Gy}$ compared to 1% when $D_{1.5cc} < 17.6$ Gy $EQD_{2Gy,10Gy}$ (108). In the absence of a $D_{1.5cc}$ model, a D_{2cc} of 27.4 Gy $EQD_{2Gy,10Gy}$ corresponds to an 11% risk on acute toxicity in our NTCP model. Duijm et al. reported recently a 17% rate of acute low-grade esophageal toxicity within a cohort of 231 patients, which is comparable with our study. Note, that they did not report any grade 3 or higher toxicity, in contrast to our 4 cases of late high-grade toxicity. They showed that low-grade toxicity was correlated to the same dosimetric parameters found in our study (105). However, because the dose to the esophagus in our cohort was higher, the NTCP model derived by Duijm et al. calculates a lower probability of esophageal toxicity for a certain value of a dosimetric parameter than the model derived in this study. As also shown by other studies, there is a variety in probability rates and doses predictive of esophageal toxicity. Several explanations can be given for these differences. First, higher rates of toxicity are suggested in patients treated on consecutive days compared with patients treated on nonconsecutive days (109). Additionally, esophageal motion could result in a different delivered dose compared with the planned dose. This can lead to higher esophageal doses, which in turn may result in unexpected occurrence of toxicity (110). Moreover, there could be an additional influence of other dosimetric parameters aside from the D_{max} and dose to small volumes of the esophagus (D_{1cc}, D_{2cc} and D_{5cc}). Finally, retrospective scoring of low-grade toxicity can be challenging and could contribute to the differences in probability rates and predictive doses among various studies.

Recently, the RTOG 0813 trial published their outcomes. In 13 patients, the esophagus was the main organ at risk. One patient had a late grade 5 esophageal event may have been an esophageal ulcer, but no autopsy was performed. Additionally, 6 cases of grade 3 and 2 cases of grade 4 esophageal toxicity were reported (9% of high-grade toxicity) (16). Aside from the known dose constraints, no dosimetric information about these toxicity cases is available in the report, which limits comparison with our results. Therefore, we could only estimate the probability rates of toxicity for the D_{max} RTOG 0813 constraints using the derived NTCP models. The estimated rates were as high as 46% for the late high-grade toxicity and 70% for the acute low-grade toxicity. When there is no clarity on the dose

received by the esophagus in the trial, we recommend that physicians take care with such high D_{max} doses and use the suggested volume limit as a treatment planning goal as prescribed in the RTOG 0813 protocol. Some other prospective studies report either dosimetric or esophageal toxicity data, but not both, hindering direct comparisons with our results (71, 77).

The prevention of high-grade toxicity is crucial in defining safe dose constraints for the esophagus. Although the amount of high-grade toxicity events within our study is not enough to formally recommend new dose constraints, it is of interest to compare the NTCP calculated probability of toxicity after SBRT for central lung tumors with an alternative treatment: lobectomy or pneumonectomy. After these alternative treatments, rates of 1 to 5% are accepted (107, 111, 112). The reported esophageal doses coherent to the 5% probability of late high-grade toxicity could be seen as the limit within the stereotactic treatment of central lung tumors. Although we have reported 2 cases of grade 5 toxicity, the radiation-induced mortality rate within this study (1.06%, 2/188 patients) is at the lower bound of the lobectomy and pneumonectomy mortality range. Moreover, all patients with high-grade toxicity within our cohort were treated with a D_{1cc} higher than the currently used dose constraints.

Univariate analysis in our cohort showed 2 clinical predictors for acute esophagus toxicity: using 12 fractions as treatment and having a shorter distance between tumor and esophagus. A multivariate analysis including these 2 factors was not performed because a tumor close to the esophagus drives the physician's decision to use a schedule of 12 fractions. Hence, collinearity problems would arise when performing a multivariate analysis including these 2 factors. Likewise, the risk of acute esophagus toxicity decreases when the distance between tumor and esophagus increases. Harder et al. also mentioned the importance of the tumor-esophageal distance, showing significantly shorter distance for (sub)acute grade 2 to 3 esophageal toxicity compared with grade 0 to 1 (108).

Some limitations of our study have to be mentioned. In addition to the limitations inherent to a retrospective design, we based the NTCP models for late high-grade toxicity on a limited number of events. Therefore, we could not test the assumptions of logistic regression, and no subset analyses were possible. However, the 95% CIs were relatively narrow for the amount of events. The models shown are reflecting the limits within the treatment of central lung tumors.

7.5 Conclusion

Esophageal toxicity was reported in 18% of the patients treated with SBRT. Four patients had late high-grade toxicity including two treatment-related deaths (1.1%). No acute severe esophageal toxicity was reported. Late high-grade esophageal toxicity and acute low-grade esophageal toxicity were both significantly correlated with all dose-volume histogram parameters (D_{max}, D_{1cc}, D_{2cc}, D_{5cc}). The risk of late high-grade toxicity is low (< 1.5%) and the risk of acute toxicity is acceptable (< 30%) if the esophageal D_{1cc} is ≤ 40 Gy in 8 fractions and ≤ 48 Gy in 12 fractions.

8

CHAPTER 8

Discussion

8.1 Introduction

Since 2006, patients with centrally located lung tumors have been treated with risk-adapted fractionation schedules. However, these fractionation schedules have changed over time and there is still no clear consensus. National or even global guidelines could lead to more uniform treatment schedules. Prediction models showing results in terms of overall survival (OS), disease control and toxicity, can be used as a basis for these guidelines and also support decision making for individual patients. This thesis describes different models focusing on survival outcomes, tumor outcomes and organs at risk (OAR) outcomes after stereotactic body radiation therapy (SBRT) of centrally located lung tumors. The following sections discuss the interpretation and possible limitations of these models.

8.2 Outcome modelling; overall survival and local control

In the past years, 2 prospective studies exclusively focusing on centrally located lung tumors have published their survival and disease control outcomes. The RTOG 0813 trial (113) included 120 patients with a tumor ≤ 5 cm. Of the 77 patients treated with 5 fractions of 11.5 / 12 Gy, the 2 year OS was 68% to 73%. The 2 year LC (LC; defined as absence of infield, marginal or involved lobe failure) was 88% to 89% and the 2 year progression free survival (defined as local, regional or distant failure and development of a second primary or death as results of any cause) was 52% to 55%. The second prospective study enrolled 74 patients having non-small cell lung cancer (NSCLC) ≤ 7 cm in a phase I/II trial (39). The 2 year OS was 43% in the phase II group consisting of 51 patients. Four patients failed locally resulting in a 2 year LC rate of 85%. The 2 year disease free survival (DFS) was 28%. Other prospective studies like the HILUS and SUNSET have not published their (survival) outcomes yet (17).

The outcomes of these 2 prospective studies are conflicting, as they show different survival rates and did not use the same LC definition. Other available disease control rates are all based on retrospective studies. Some of them will be discussed and compared with our data in the following paragraphs.

Overall survival

Chapter 2 discussed the OS of patients diagnosed with centrally located stage I – IIIA NSCLC. The 2 year OS rate in our cohort was 55%, which corresponds to the survival rates published by Roach et al (39). Nevertheless, the 2 year OS rates reported in literature vary widely. The rates range from 46% to 81% (19, 27, 28, 38, 71, 114) for centrally located NSCLC and from 60% to 88% in studies reporting peripherally and centrally located NSCLC together (33, 36, 43, 57, 61, 115-118). This variation in outcome rates could be explained by the differences in patient selection. Some studies are only including potentially operable patients or are including tumors smaller than 5 cm, while other studies also include patients not suitable for surgery and/or all T-stages. Additionally, over the past 15 to 20 years there have been

significant developments in diagnostics, staging and treatment. For example, the PET-CT scan is nowadays a standard procedure within the diagnostic work-up, but in some literature the staging PET-CT scan was only used in 74% of the patients (28). All these factors together complicate the comparison of survival rates. The diversity within literature emphasizes the need of individualized survival predictions.

Therefore, in *Chapter 2,* we have focused on developing a nomogram to guide physicians in patient risk-stratification and treatment decision making. The nomogram creation allowed us to identify the characteristics that are predominantly responsible for the differences in survival rates. Our nomogram consisted of age, planning target volume (PTV), performance status, tumor lobe location and dose to the PTV. Previously, each of these variables have been linked to OS, but this was the first time they have been combined into one predictive model.

This first survival nomogram for centrally located NSCLC has been externally validated and showed acceptable predictive power. This nomogram is an important step towards personalized decision making, however there is certainly room for improvement. This can be realized by including the cause of death of each patient in the analysis. After all, OS not only reflects patient- or tumor-related factors, but also potential toxicity of the treatment. If, in future research, our nomogram is also able to predict for these non-treatment-related deaths, this could contribute to its predictive power.

Local control

Chapter 3 investigated the clinical consequence of prioritizing the dose constraints of the OAR over the PTV coverage within the treatment of centrally located lung tumors. Although there was no relation between any PTV related treatment factors and local failure, both tumor size and forced expiratory volume in 1 second (FEV_1) were found predictive for the development of a local recurrence.

The 2 year LC rate within our cohort was 88%, whereas in literature it ranged from 64% to 98% in centrally located NSCLC (27, 28, 38, 71), and 81% to 97% in the combined patient cohorts (19, 36, 37, 43, 56, 61, 115, 116). In addition to the previously mentioned differences in patient selection and treatment between institutes, the variation in the definition of a local recurrence creates additional uncertainty when comparing the LC rates of different studies. While some studies use the response evaluation criteria in solid tumors (RECIST) to define local progression, others define local progression as a recurrence within the same lobe or even the same lobe and ipsilateral hilum or mediastinum. This results in higher recurrence rates in studies using a broader definition.

Since LC rates after SBRT are promising, not many central lung studies were able to analyze possible predictors of local failure due to the low numbers of events. Predictive factors are mainly analyzed in combined groups in terms of centrally and peripherally

located early stage NSCLC. Next to tumor size, a frequently found predictive factor was the central location of the tumor (55, 56). An explanation for this can be that adapted fractionation schedules result in a lower biologically effective dose to the tumor. Moreover, central tumors tend to be bigger (27) which was a predictive factor for local recurrences in this thesis and multiple other studies (*Chapter 3*). The benefit of a prescribed dose > 100 Gy BED_{10} (biologically equivalent dose, using an α/β ratio of 10 Gy) was also observed in *Chapter 3* and confirmed in literature (19, 47).

We were not able to demonstrate a potential link between local recurrence and underdosage of the PTV (*Chapter 3*). This suggests that underdosage has less impact on the development of a local recurrence than previously expected. However, we cannot fully exclude that underdosage harms the outcome in SBRT of central lung tumors. To exclude the role of the absolute or relative volume receiving a dose lower than 100 Gy BED_{10}, a study with more statistical power is needed. Moreover, we have only investigated a threshold dose of 100 Gy BED_{10}, and therefore we cannot draw conclusions on threshold doses lower than 100 Gy BED_{10}.

Instead of accepting a local underdosage, conventional radiotherapy could be an alternative option. However, the superior effect of SBRT compared to protracted radiotherapy in peripherally located early stage NSCLC is known (12). Future research could focus on the extent to which underdosing is still acceptable and when conventionally fractionated treatment schedules become a better option for treating the patient.

The ICRU report 91 on prescribing, recording, and reporting of stereotactic treatments with small photon beams, recommends to report the median dose to the PTV and if the lesion is surrounded by lung parenchyma to also report the median dose to the clinical target volume (CTV) or gross tumor volume (GTV) (119). In addition, it recommends to report the near minimum dose and near maximum which is defined as $D_{98\%}$ and $D_{2\%}$ for target volumes larger than 2 cm^3. In *Chapter 3* we tested PTV median dose ($D_{50\%}$) and the $D_{98\%}$ and $D_{2\%}$. The CTV/GTV median dose was not tested, because the CTV/GTV was not separately contoured. However, centrally located tumor are less surrounded by lung parenchyma than peripherally located tumors. We found that these parameters did not predict LC and DFS. Nevertheless, we suggest that the dosimetric parameters recommended by ICRU will be included in future studies.

While defining cut-off values for dosimetric parameters would already be a major step forward, ideally treatment decision making is supported by an individualized tumor control probability (TCP) model. This sigmoid-shaped model could consist of patient, tumor and PTV parameters and predicts individual LC outcomes. To create a statistically sound model, a

patient group with multiple events is needed. Especially when the goal is to include 3 or more parameters. A rule of thumb within multivariate analysis states that one predictive variable can be studied for every 10 events. However, to create a model with better predictive accuracy 20 events per parameters have been suggested (120). Whereas only 27 local recurrences were found in our group of 220 patients, a group of at least 500 patients (approximately 60 events) having centrally located NSCLC treated with SBRT would be needed to create such a reliable model.

Disease free survival

In *Chapter 3,* disease progression has been defined as a tumor recurrence in any part of the body, resulting in a 2 year DFS rate of 66%. Literature reported rates of 63% to 81% for centrally and/or peripherally located tumors (37, 38, 56, 71). In addition to the predictive factors found for local recurrence, a patient having a tumor located in the lower lobe had a significantly higher risk of disease recurrence in this thesis. This finding was explained by the more often unsuspected nodal involvement when a patient was diagnosed with a tumor in the lower lobe (34). During surgery, this unsuspected nodal involvement would result in adjuvant systemic treatment. However, as SBRT patients do not undergo pathologic staging, a small nodal involvement can easily be missed. Since the field of PET-CT scans evolves rapidly, and the scans become increasingly sensitive to small metastasis (121, 122), the chance of treating patients with unexpected nodal involvement with SBRT will become lower in the future.

8.3 Toxicity modelling

Toxicity is one of the major concerns when treating central lung tumors with SBRT. To prevent high-grade toxicity, nowadays each institute has strict dose constraints for the OAR which are prioritized over the PTV coverage. Hence, in case of PTV-OAR overlap, the PTV dose in the overlapping part is related to the constraint dose of the OAR. So, OAR dose constraints should not be taken too low on the one hand, but not too high on the other to keep toxicity rates at an acceptable level. Toxicity prediction models could be helpful to redefine the dose constraints. To this end, in this thesis, we analyzed the bronchial and esophageal toxicity, and modeled Normal Tissue Complication Probability (NTCP) curves for both OARs.

Bronchial toxicity

Stereotactic body radiation therapy to the lungs can result in radiological changes in the lung. Stenosis and occlusion with or without atelectasis are patterns of toxicity that can be found in the bronchial branches (*Chapter 4*). Most of these radiological changes occurred in the smaller branches such as the upper, middle and lower lobe and the segmental bronchi.

Only stenosis has been found in the trachea and main bronchi. The diameter of the trachea and main bronchi is larger compared to the smaller branches. Therefore, fibrosis of these bronchi will result in stenosis, but in the smaller branches fibrosis also results in occlusion with or without atelectasis (*Chapter 4*).

The radiological changes in the smaller branches were correlated to D_{max}, and the volume receiving a dose of 65, 80, 90, 100 and 130 Gy EQD_2 (V_{65}, V_{80}, V_{90}, V_{100} and V_{130}, respectively). Despite being significantly different, the dose differences in the segmental bronchi with and without side effects were small and no difference in OS was found between these groups. Therefore, we decided to only focus on the radiographic toxicity in the main and lobar bronchi in *Chapter 5*.

Stereotactic body radiation therapy can cause several types of radiological changes. In this thesis, we focused mainly on radiological changes of the bronchial branches and related that to dose. Additionally, changes in the lung parenchyma can be found in almost all patients after SBRT (123). This fibrotic process can be dynamic for many years, which creates additional difficulties in the diagnosis of a local recurrence (124). Clinicians should be aware of these radiological changes, which sometimes indicates a local recurrence.

In *Chapter 5,* the correlation found in *Chapter 4* between the bronchial dosimetric parameters and the radiographic bronchial toxicity was confirmed in a larger cohort. However, these radiological changes were not correlated with high-grade clinical bronchial toxicity. As mentioned before, the radiological changes mainly occurred in the smaller branches, which most likely causes only subclinical symptoms.

Grade 3 or higher bronchial toxicity has been observed in 12% of our cohort. This rate was within the 6% to 15% range reported in literature (16, 53, 78, 90). Lung hemorrhage was one of the most frequently mentioned bronchial toxicities. In these cases, an endobronchial tumor location was more common, resulting in a PTV overlapping the main bronchi or trachea (*Chapter 5*). In this chapter, in 11 of the 13 patients the lung hemorrhage was fatal. However, fatal hemorrhage is not always the result of radiation induced toxicity. In case of a recurrence, the tumor can invade the vessels due to growth which can cause a fatal hemorrhage as well. Recent radiological images can confirm a possible recurrence. If this is not available, an autopsy could be taken to exclude radiation-induced toxicity.

Clinical toxicity is not only caused by dose, certainly not in a patient group in which the comorbidity rates are relatively high. Next to the total bronchial volume receiving 130 Gy EQD_2, chronic obstructive pulmonary disease and overlap of the PTV with the trachea / main stem bronchus were independently associated with high-grade toxicity.

In this thesis, only dosimetric parameters were modeled in 4 NTCP curves. To create more individualized predictions, dosimetric and clinical factors can be combined into one

NTCP model. Before combining these factors, a study is recommended that confirms the significance of parameters. Within such a study, the same parameters, including the dosimetric parameters, should be available for each of the patients. Moreover, the contours of the bronchial structures should be created following the same guidelines, as bronchial toxicity is related to volume dependent parameters.

Esophageal toxicity

Severe late esophageal toxicity can manifest as dysphagia, stricture, or the development of a fistula. The esophagus is a "serial organ", which means that its function is lost when a short segment or a part of this organ is destroyed. In this type of organ, a high dose to a small volume, such as the dose to 1 cc or 2 cc of the esophagus, can have serious life-threatening consequences (108, 125).

From the beginning of the SBRT era, the esophagus has been an organ of great concern. In multiple institutes the dose constraints of the esophagus have always had priority over PTV coverage, resulting mainly in low-grade esophageal toxicity. Acute low-grade esophageal toxicity, meaning swallowing problems where sometimes pain medication is needed, was reported in 17% of our population (*Chapter 6*). Although not causing hospitalization or worse, the toxicity was correlated with the dosimetric parameters D_{max} and the dose in 1 cc, 2 cc and 5 cc (D_{1cc}, D_{2cc}, D_{5cc}) of the esophagus. Additionally, the hazard ratios confirmed that the dose to small volumes were of more importance than the D_{max}. This could reflect the increased uncertainty in determining D_{max} or could reflect a small volume effect that plays a role in the occurrence of the toxicity.

The NTCP models that were created describe the relation between acute low-grade esophageal toxicity and dose. Unfortunately, the dose that would result in high-grade toxicity was missing in this analysis. Therefore, dose constraints derived from these models, will not automatically protect future patients from high-grade toxicity.

In *Chapter 7*, we used data from a patient cohort in which 4 cases of high-grade esophageal toxicity were identified. This gave us the opportunity to explore dose limits for high-grade toxicity. In all cases with high-grade toxicity, the PTV overlapped the esophagus and PTV coverage was likely prioritized over the dose constraints. We found that high-grade toxicity could be predicted with the same dosimetric parameters as were found for low-grade toxicity. Similarly as in *Chapter 6*, we modelled the NTCP of high-grade toxicity for each of the 4 dosimetric parameters, separately. The hazard ratios also emphasized the greater influence of D_{1cc} on esophageal toxicity compared to D_{max}. Based on our data we suggest to use the D_{1cc} parameter as a dose constraint instead of D_{max}.

Late high-grade esophageal toxicity has been rarely reported in literature. Three studies reported a single case of toxicity without confounding therapies, but not all of them

reported the corresponding dosimetric details (46, 53, 59). To validate our NTCP models, more cases of esophageal toxicity are needed. However, this will be a challenge due to the small number of cases available in literature. The RTOG 0813 reported 4 cases of high-grade esophageal toxicity. Hopefully, dosimetric data of these cases will become available to confirm our conclusions.

The rate of acute low-grade toxicity in *Chapter 7* (15%) was comparable to the other cohort in *Chapter 6*. However, the dose corresponding to the same toxicity rate was much higher. This could be explained by differences in scoring low-grade toxicity. Some patients do not report these complaints to their radiation-oncologist or they receive medication from their general practitioner or pulmonologist without informing the radiation-oncologist. This uncertainty in toxicity scoring could also be the reason for the different predictive patient and tumor characteristics that were found for acute low-grade toxicity within these 2 cohorts.

Cardiac toxicity

The bronchial structures and the esophagus have been considered the most important OARs in centrally located lung tumors in recent years. Recently, however, there has been increasing attention for the heart dose. Researchers are exploring the relation between (cardiac) death and heart dose received by SBRT. Because SBRT causes high doses in small volumes of the heart, the dose in these cardiac (sub)structures may cause non-cancer-related death. The results, however, derived from analyzing different dosimetric parameters for different cardiac (sub)structures are conflicting (117, 126, 127). In one study, a significant correlation was found between non-cancer-related death and the maximum dose to the left atrium and the dose to 90% of the superior vena cava (117). Another study found more cardiac events in patients with a history of heart problems, but could not find a relation with the radiation dose to cardiac substructures (127). In another study, cardiac dose was not found as a predictor for OS and a high dose to small volumes of the whole heart (substructures were not included in the analysis) appeared to be safe (126).

Analyzing non-cancer-related death is challenging because of the high rates of cardiac and pulmonary comorbidities within the SBRT patient group. This makes it hard to distinguish between death due to comorbidities and treatment-related death. By all means, the baseline heart condition should be taken into account when analyzing this group. More research is needed to confirm or exclude the impact of heart dose on non-cancer-related death.

8.4 Future perspectives

Each central lung patient is exposed to different risks of toxicity based on the location of the tumor and the patient's pre-treatment condition. Therefore, individualized outcome modeling has a strong rational. The NTCP models and predictors of disease control created and found in this thesis could be used for decision making in central lung patients considered for SBRT.

Based on expected survival probabilities, the radiation-oncologist can decide whether a patient qualifies for SBRT. The NCTP models make it possible to determine the expected toxicity on an individual basis. Thereafter, the radiation-oncologist and the patient can weigh the expected toxicity with the calculated disease control probability. In other words, the models can be used to aid shared decision making. Patients have indicated that maintaining independence and quality of life are more valued than survival or cancer recurrence (128). When the tumor is too close to the OAR, resulting in a high toxicity risk and/or a lower chance on LC, alternative treatment options should be discussed.

Stereotactic body radiation therapy is a safe treatment option for patients with centrally located NSCLC (*This thesis*). Some subgroups, however, such as patients with interstitial lung disease (ILD), have been identified to have a higher risk of treatment-related toxicity and mortality. Chen et al. found a relationship between these higher risks and the dose received by the lung parenchyma (129). This highlights the need to even more lower the dose received by the tumor surrounding OAR.

Recently introduced techniques, such as the MRI-linac and proton therapy, could provide more accurate radiotherapy and lead to lower high-grade toxicity risks. The MRI-linac includes real-time magnetic resonance (MR) image-guidance during treatment. This can be used for motion management, for example gated delivery, or online plan adaption based to the daily anatomy. The first results of treating high-risk patients with MR-guided SBRT are encouraging. While no compromise had to be made with regard to tumor control by using a breath hold technique, only 8% of patients reported grade 3 toxicities (130). Proton therapy uses fine proton beams that deposit their dose locally. This may lead to a significant dose reduction to OARs compared to using X-rays that deposit their dose along the entire path of the beam. In the Netherlands, a model-based approach is used to select the patients who may benefit from proton therapy. In order to validate these models, the toxicity data of prospective stereotactic body proton therapy trials is needed (131).

In the past years, the term "ultracentral tumor" has been introduced because of the expected higher toxicity rates due to its location (61). Some institutes have even decided to refuse these patients for SBRT and propose treating them with hypofractionated schemes

using 2.5 Gy to 3 Gy per fraction (77, 132). In this thesis, we have found higher toxicity risks for PTVs overlapping the trachea and main bronchus and for tumors close to the esophagus (*Chapter 5 and 7*). On the other hand, the NTCP curves can calculate the toxicity probabilities based on the dosimetric parameters. Therefore, we believe there is no need to decline this subgroup in advance from SBRT treatment. In patients with an ultracentral tumor, the toxicity risks can be weighed against the expected disease outcomes and a personalized decision can be made in each individual case.

The standard treatment for operable early stage NSCLC is still surgery. Within the field of peripherally located tumors, SBRT showed very good results with low toxicity rates, the perfect alternative for surgery. Therefore, it is suggested that there is clinical equipoise between the 2 treatment modalities, which would result in the use of SBRT in operable patients (133). Although equipoise has not yet been demonstrated in randomized control trials for peripheral tumors, the question arises whether this is also an option in the treatment of centrally located lung tumors.

Although the outcomes of SBRT in central tumors are promising, the toxicity rates are much higher compared to peripheral tumors. However, this increased risk is also seen in the surgical treatment of central lung tumors. Due to its anatomical position, more invasive procedures are generally needed, resulting in less pulmonary capacity and higher morbidity and mortality rates (107). Whether surgery or SBRT can be used depends on the individual situation of the patient. If the identification of occult nodal disease is needed, surgery would be the preferred option. However, if lung preservation is more important, SBRT would be the preferred option.

8.5 Conclusion

Stereotactic body radiation therapy is a safe treatment option in medically inoperable patients diagnosed with a centrally located lung tumor. When the dose constraints are respected and prioritized over PTV coverage, survival and disease control rates will be satisfactory without high rates of high-grade toxicity. Toxicity in the surrounding OARs can be predicted for each individual patient using the NTCP models developed in this thesis. This will help to minimize the development of toxicity.

The models provided in this thesis are based on data of multiple institutes, which limits institutional bias and supports the clinical applicability. In addition to developments in treatment techniques, improved NTCP models with a multivariate design along with models that predict tumor control probability, have the potential to improve the individualized treatment approach.

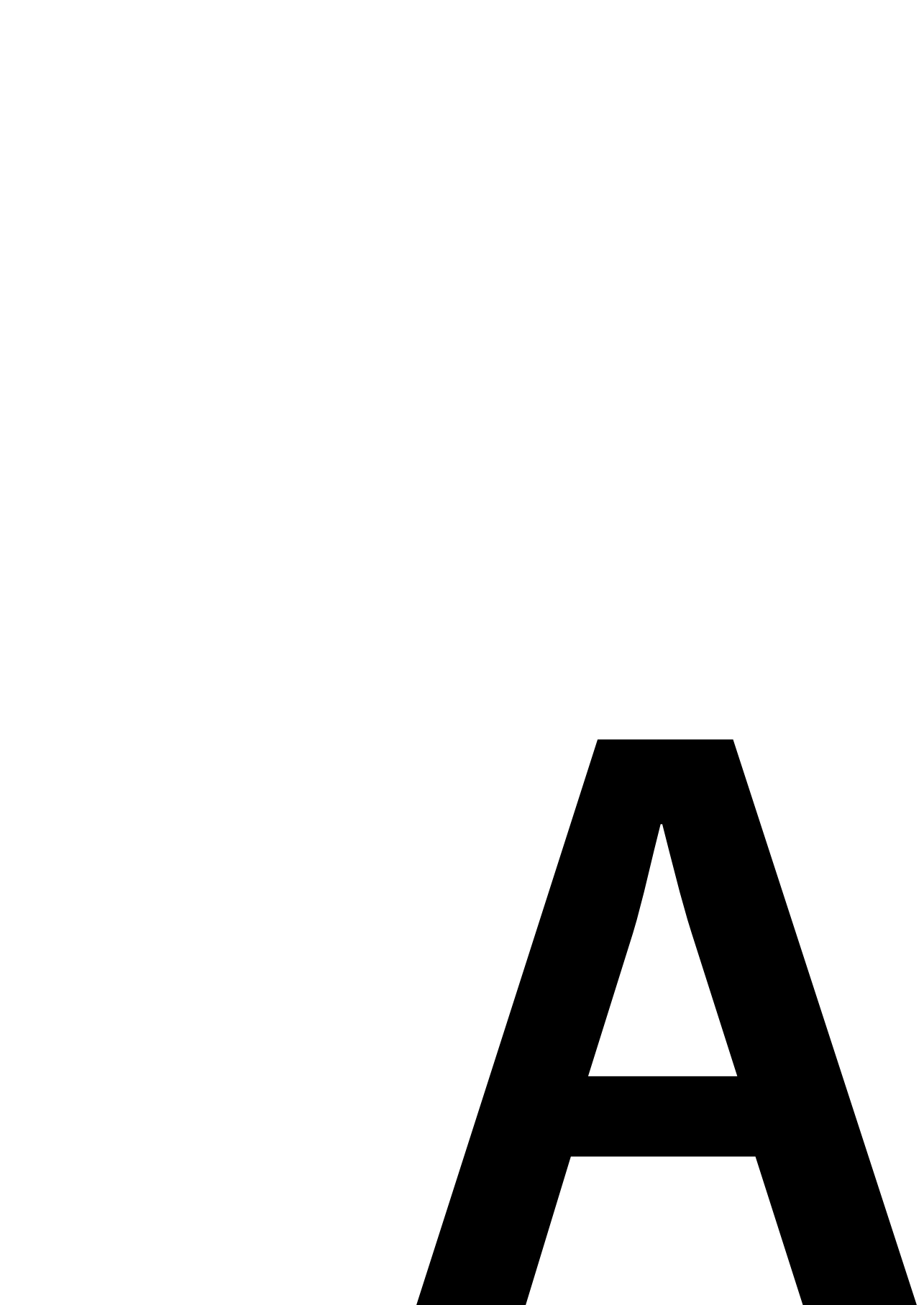

Appendices
References
Summary
Samenvatting
List of Publications
PhD Portofolio
Curriculum Vitae
Dankwoord

1A – T, N, and M descriptors for eighth edition of TNM classification for lung cancer

T: primary tumor		
Tx		Primary tumor cannot be assessed or tumor proven by presence of malignant cells in sputum or bronchial washings but not visualized by imaging or bronchoscopy
T0		No evidence of primary tumor
Tis		Carcinoma in situ
T1		Tumor ≤ 3 cm in greatest dimension surrounded by lung or visceral pleura without bronchoscopic evidence of invasion more proximal than the lobar bronchus (i.e., not in the main bronchus) [a]
	T1a(mi)	Minimally invasive adenocarcinoma [b]
	T1a	Tumor ≤ 1 cm in greatest dimension [a]
	T1b	Tumor > 1 cm but ≤ 2 cm in greatest dimension [a]
	T1c	Tumor > 2 cm but ≤ 3 cm in greatest dimension [a]
T2		Tumor > 3 cm but ≤ 5 cm or tumor with any of the following features [c]: - Involves main bronchus regardless of distance from the carina but without involvement of the carina - Invades visceral pleura - Associated with atelectasis or obstructive pneumonitis that extends to the hilar region, involving part or all of the lung
	T2a	Tumor > 3 cm but ≤ 4 cm in greatest dimension
	T2b	Tumor > 4 cm but ≤ 5 cm in greatest dimension
T3		Tumor > 5 cm but ≤ 7 cm in greatest dimension or associated with separate tumor nodule(s) in the same lobe as the primary tumor or directly invades any of the following structures: chest wall (including the parietal pleura and superior sulcus tumors), phrenic nerve, parietal pericardium
T4		Tumor > 7 cm in greatest dimension or associated with separate tumor nodule(s) in a different ipsilateral lobe than that of the primary tumor or invades any of the following structures: diaphragm, mediastinum, heart, great vessels, trachea, recurrent laryngeal nerve, esophagus, vertebral body, and carina
N: Regional lymph node involvement		
Nx		Regional lymph nodes cannot be assessed
N0		No regional lymph node metastasis
N1		Metastasis in ipsilateral peribronchial and/or ipsilateral hilar lymph nodes and intrapulmonary nodes, including involvement by direct extension
N2		Metastasis in ipsilateral mediastinal and/or subcarinal lymph node(s)
N3		Metastasis in contralateral mediastinal, contralateral hilar, ipsilateral or contralateral scalene, or supraclavicular lymph node(s)
M: Distant metastasis		
M0		No distant metastasis
M1		Distant metastasis present
	M1a	Separate tumor nodule(s) in a contralateral lobe; tumor with pleural or pericardial nodule(s) or malignant pleural or pericardial effusion [d]
	M1b	Single extrathoracic metastasis [e]
	M1c	Multiple extrathoracic metastases in one or more organs

a) The uncommon superficial spreading tumor of any size with its invasive component limited to the bronchial wall, which may extend proximal to the main bronchus, is also classified as T1a; b) Solitary adenocarcinoma, ≤ 3 cm with a predominately lepidic pattern and ≤ 5 mm invasion in any one focus; c) T2 tumors with these features are classified as T2a if ≤ 4 cm in greatest dimension or if size cannot be determined, and T2b if > 4 cm but ≤ 5 cm in greatest dimension; d) Most pleural (pericardial) effusions with lung cancer are due to tumor. In a few patients, however, multiple microscopic examinations of pleural (pericardial) fluid are negative for tumor and the fluid is non-bloody and not an exudate. When these elements and clinical judgment dictate that the effusion is not related to the tumor, the effusion should be excluded as a staging descriptor; e) This includes involvement of a single distant (nonregional) lymph node.

1B – Stage groupings of the eight TNM classification for lung cancer

Occult carcinoma	Tx	N0	M0
Stage 0	Tis	N0	M0
Stage IAI	T1a (mi)	N0	M0
	T1a	N0	M0
Stage IA2	T1b	N0	M0
Stage IA3	T1c	N0	M0
Stage IB	T2a	N0	M0
Stage IIA	T2b	N0	M0
Stage IIB	T1a-c	N1	M0
	T2a	N1	M0
	T2b	N1	M0
	T3	N0	M0
Stage IIIA	T1a-c	N2	M0
	T2a-b	N2	M0
	T3	N1	M0
	T4	N0-1	M0
Stage IIIB	T1a-c	N3	M0
	T2a-b	N3	M0
	T3	N2	M0
	T4	N1	M0
Stage IIIC	T3	N3	M0
	T4	N3	M0
Stage IVA	Any T	Any N	M1a
	Any T	Any N	M1b
Stage IVB	Any T	Any N	M1c

Abbreviations: TNM = tumor, node, metastasis; Tis = carcinoma in situ; T1a(mi) = minimally invasive

2A – Results of the univariate cox regression analyses focusing on patient- and dosimetric factors predicting overall survival for patients with early-stage NSCLC treated with SBRT

Characteristic		Alive		Death		Hazard Ratio	*p*-value
		median (IQR) / n (%)		median (IQR) / n (%)		(95%CI)	
Age		77	(67 – 80)	75	(68 – 82)	1.12 (1.02 – 1.24)[1]	0.021
FEV_1 *		67	(52 – 83)	60	(48 – 76)	0.99 (0.99 – 1.00)	0.230
Gender	Male	40	(31%)	91	(69%)	1	
	Female	35	(39%)	54	(61%)	0.81 (0.58 – 1.14)	0.233
Tumor lobe location	UMM	61	(39%)	95	(61%)	1	
	Lower	14	(22%)	50	(78%)	1.66 (1.17 – 2.34)	0.004
WHO performance status #	0	38	(51%)	36	(49%)	1	
	1 – 4	37	(27%)	100	(73%)	1.74 (1.19 – 2.56)	0.004
Pathology available	No	39	(43%)	52	(57%)	1	
	Yes	36	(28%)	93	(72%)	1.37 (0.98 – 1.93)	0.069
CCI	0 – 3	62	(36%)	110	(64%)	1	
	≥ 4	13	(27%)	35	(73%)	1.21 (0.83 – 1.77)	0.330
Previous malignancies	No	42	(32%)	91	(68%)	1	
	Yes	33	(38%)	54	(62%)	1.07 (0.76 – 1.50)	0.691
Previous lung cancer	No	65	(33%)	132	(67%)	1	
	Yes	10	(43%)	13	(57%)	0.74 (0.42 – 1.32)	0.309
Disease stage	I	40	(48%)	43	(52%)	1	
	II	32	(28%)	83	(72%)	1.74 (1.20 – 2.52)	0.003
	III	3	(14%)	19	(86%)	3.75 (2.15 – 6.51)	< 0.001
PTV		64	(34 – 118)	93	(49 – 155)	1.24 (1.10 – 1.38)[2]	< 0.001
PTV D_{max} BED_{10}		145	(134 – 173)	141	(121 – 175)	0.97 (0.92 – 1.02)[3]	0.261
PTV $D_{2\%}$ BED_{10}		140	(128 – 164)	137	(114 – 163)	0.96 (0.90 – 1.02)[3]	0.173
PTV D_{mean} BED_{10}		123	(107 – 137)	120	(97 – 135)	0.95 (0.88 – 1.03)[3]	0.208
PTV $D_{50\%}$ BED_{10}		124	(108 – 140)	120	(99 – 136)	0.95 (0.87 – 1.03)[3]	0.198
PTV $D_{98\%}$ BED_{10}		102	(87 – 105)	96	(82 – 105)	0.96 (0.87 – 1.06)[3]	0.379
PTV D_{min} BED_{10}		83	(68 – 91)	73	(62 – 88)	0.96 (0.88 – 1.05)[3]	0.361
PTV D_{mean} BED_{10}	< 100	8	(17%)	40	(83%)	1.52 (1.05 – 2.20)	0.026
	≥ 100	67	(39%)	105	(61%)	1	

*** 24 cases missing # 9 cases missing**

1) HR per 5 year, 2) HR per 100 cc, 3) HR per 10 Gy

Abbreviations: BED_{10} = biologically effective dose using α/β-ratio of 10 Gy; CCS = charlson comorbidity index; COPD = chronic obstructive pulmonary disease; D_{max} = maximum point dose; D_{mean} = mean dose; D_{min} = minimum point dose; D..% = dose to .. percent of the PTV; FEV_1 = forced expiratory volume in 1 second; HR = hazard ratio; NSCLC = non-small cell lung cancer; PTV = planning target volume; SBRT = stereotactic body radiation therapy; UMM = upper/middle lobe or mediastinum

2B – Results of internal validation of the model building procedure through 1000 bootstrap samples

	Original Sample	Training	Test	Optimism	Optimism – corrected
C-index	0.661	0.689	0.642	0.047	0.614
Slope	1.000	1.000	0.622	0.378	0.622

3A – Currently used dose contraints of the organs at risk per institution

Haaglanden MC		**8 fractions**	**12 fractions**
Esophagus	(D_{1cc})	40 Gy	48 Gy
Trachea and main stem bronchus	(D_{1cc})	44 Gy	54 Gy

Erasmus MC Cancer Institute		**5 fractions**	**7 fractions**
Esophagus	(D_{max})	40 Gy	45.5 Gy
Trachea	(D_{max})	45 Gy	51.8 Gy
Main stem bronchus	(D_{max})	50 Gy	52.5 Gy

5A – Institutional fractionation schedules for centrally located lung tumors

	Fractionation schedule	BED_{10} (Gy)
VU University Medical Center		
Central tumor adjacent to and/or minimal overlap with pericardium, hilus, plexus, stomach	8 fractions of 7.5 Gy	105.0
Central tumor with a substantial overlap with mediastinal structures and/or pathological ipsilateral mediastinal nodes	12 fractions of 5 Gy	90.0
Erasmus Medical Center*		
Central tumor close to the esophagus:		
Ray Tracing	6 or 7 fractions of 8 Gy	86.4 or 100.8
Monte Carlo	7 fractions of 7 Gy	83.3
Other central lung tumors:		
Ray Tracing	5 fractions of 9, 10 or 12 Gy	85.5, 100.0 or 132.0
Monte Carlo	5 fractions of 11 Gy	115.5

*Initially, tumors were planned and treated using a ray tracing algorithm. Over time the schedules used were changed as no severe toxicity was observed. After introduction of the Monte Carlo calculation algorithm, the prescriptions were again revised.

5B – Institutional point dose limits (D_{max}) for the organs at risk

VU University Medical Center		
	Fractionation schedule	
Organ(s)	**8 x 7.5 Gy (total EQD_2)**	**12 x 5 Gy (total EQD_2)**
Esophagus (α/β = 3)	40 Gy (64)	48 Gy (67)
Heart (α/β = 3)*	44 Gy (75)	54 Gy (81)
Trachea (α/β = 3)*	44 Gy (75)	54 Gy (81)
Main stem bronchus (α/β = 3)*	44 Gy (75)	54 Gy (81)
Great vessels (α/β = 3)*	-	-
Spinal canal (α/β = 2)	28 Gy (39)	32 Gy (37)
Brachial plexus (α/β = 3)	36 Gy (54)	42 (55)
Erasmus Medical Center		
	Fractionation schedule	
Organ(s)	**5 x 11 Gy (total EQD_2)**	**7 x 7 Gy (total EQD_2)**
Esophagus (α/β = 3)	35 Gy (70)	42 Gy (76)
Trachea (α/β = 3)	45 Gy (108)	49 Gy (98)
Main stem bronchus (α/β = 3)	55 Gy (154)	49 Gy (98)
Spinal cord (α/β = 2)	27.5 Gy (52)	32.9 Gy (55)
Brachial plexus (α/β = 3)	30 Gy (54)	35 Gy (56)

* = no specific dose limit was applied when the planning target volume is adjacent or overlapping the organ in question, but in practice the point D_{max} was frequently constrained during planning.

5C – Univariate logistic regression analyses of dosimetric parameters for clinical pulmonary or radiographic bronchial toxicity

Clinical high grade pulmonary toxicity (total number of patients = 193)*						
≥ G3 toxicity (number of patients with toxicity = 24)						
	Total $D_{max,EQD}$	**Total $V_{65Gy,EQD}$**	**Total $V_{80Gy,EQD}$**	**Total $V_{90Gy,EQD}$**	**Total $V_{100Gy,EQD}$**	**Total $V_{130Gy,EQD}$**
OR	1.02	1.21	1.25	1.28	1.35	1.68
95% CI	1.01 – 1.03	1.11 – 1.31	1.14 – 1.40	1.16 – 1.42	1.20 – 1.53	1.26 – 2.24
***p*-value**	**0.002**	**< 0.001**	**< 0.001**	**< 0.001**	**< 0.001**	**< 0.001**
Grade 5 toxicity (number of patients with toxicity = 15)						
	Total $D_{max,EQD}$	**Total $V_{65Gy,EQD}$**	**Total $V_{80Gy,EQD}$**	**Total $V_{90Gy,EQD}$**	**Total $V_{100Gy,EQD}$**	**Total $V_{130Gy,EQD}$**
OR	1.01	1.18	1.21	1.23	1.27	1.26
95% CI	1.00 – 1.02	1.08 – 1.30	1.10 – 1.34	1.11 – 1.37	1.12 – 1.43	0.98 – 1.62
***p*-value**	**0.029**	**< 0.001**	**< 0.001**	**< 0.001**	**< 0.001**	0.066
Likely G5 toxicity (number of patients with toxicity = 9)						
	Total $D_{max,EQD}$	**Total $V_{65Gy,EQD}$**	**Total $V_{80Gy,EQD}$**	**Total $V_{90Gy,EQD}$**	**Total $V_{100Gy,EQD}$**	**Total $V_{130Gy,EQD}$**
OR	1.01	1.20	1.23	1.25	1.28	1.22
95% CI	1.00 – 1.02	1.08 – 1.34	1.10 – 1.38	1.10 – 1.42	1.11 – 1.47	0.90 – 1.65
***p*-value**	**0.184**	**0.001**	**< 0.001**	**< 0.001**	**0.001**	0.195
Possible G5 toxicity (number of patients with toxicity = 6)						
	Total $D_{max,EQD}$	**Total $V_{65Gy,EQD}$**	**Total $V_{80Gy,EQD}$**	**Total $V_{90Gy,EQD}$**	**Total $V_{100Gy,EQD}$**	**Total $V_{130Gy,EQD}$**
OR	1.01	1.11	1.13	1.14	1.16	1.25
95% CI	1.00 – 1.02	0.98 – 1.26	0.98 – 1.30	0.98 – 1.32	0.98 – 1.37	0.90 – 1.75
***p*-value**	0.053	0.114	0.091	0.09	0.084	0.183

Radiographic toxicity of the main stem and intermediate bronchi (number of structures = 189)						
Any grade of toxicity (number of structures with toxicity = 17)						
	$D_{max,EQD}$	**$V_{65Gy,EQD}$**	**$V_{80Gy,EQD}$**	**$V_{90Gy,EQD}$**	**$V_{100Gy,EQD}$**	**$V_{130Gy,EQD}$**
OR	1.02	1.16	1.16	1.19	1.20	1.75
95% CI	1.00 – 1.03	0.96 – 1.40	0.94 – 1.43	0.95 – 1.49	0.93 – 1.56	0.81 – 3.77
***p*-value**	**0.010**	0.122	0.163	0.136	0.166	0.157

*Total volume of all bronchial structures receiving a specific dose (65 Gy EQD_2, 80 Gy EQD_2, 90 Gy EQD_2, 100 Gy EQD_2, 130 Gy EQD_2) was calculated for each patient.

Abbreviations: OR = odds ratio; 95% CI = 95% confidence interval; NTCP = normal tissue complication probability.

5C (continued) - Univariate logistic regression analyses of dosimetric parameters for clinical pulmonary or radiographic bronchial toxicity

Radiographic toxicity of the lobar bronchi (number of structures = 311)						
Any grade of toxicity (number of structures with toxicity = 64)						
	$D_{max,EQD}$	**$V_{65Gy,EQD}$**	**$V_{80Gy,EQD}$**	**$V_{90Gy,EQD}$**	**$V_{100Gy,EQD}$**	**$V_{130Gy,EQD}$**
OR	1.02	1.56	1.61	1.62	1.75	2.47
95% CI	1.01 – 1.02	1.25 – 1.93	1.28 – 2.01	1.28 – 2.04	1.35 – 2.28	1.52 – 4.00
***p*-value**	**< 0.001**	**< 0.001**	**< 0.001**	**< 0.001**	**< 0.001**	**< 0.001**
High grade toxicity (number of structures with toxicity = 38)						
	$D_{max,EQD}$	**$V_{65Gy,EQD}$**	**$V_{80Gy,EQD}$**	**$V_{90Gy,EQD}$**	**$V_{100Gy,EQD}$**	**$V_{130Gy,EQD}$**
OR	1.02	1.60	1.69	1.76	1.96	2.29
95% CI	1.01 – 1.03	1.26 – 2.02	1.32 – 2.16	1.37 – 2.28	1.47 – 2.61	1.44 – 3.65
***p*-value**	**0.021**	**< 0.001**	**< 0.001**	**< 0.001**	**< 0.001**	**0.001**

Abbreviations: OR = odds ratio; 95% CI = 95% confidence interval; NTCP = normal tissue complication probability.

5D – Univariate and multivariate logistic regression analyses for factors predicting high grade clinical (n = 193)

Grade ≥ 3 clinical pulmonary toxicity						
			Univariate analysis		**Multivariate analysis**	
Characteristic	**≥ G3 toxicity**	**No toxicity**	**OR (95% CI)**	***p*-value**	**OR (95% CI)**	***p*-value**
Age			0.98 (0.95 – 1.02)	0.306	-	-
Gender						
Female	n = 8	n = 64	0.82 (0.33 – 2.03)	0.668	-	-
Male	n = 16	n = 105	1			
COPD						
Yes	n = 21	n = 96	**5.03 (1.44 – 17.54)**	**0.011**	**4.09 (1.11 – 15.05)**	**0.034**
No	n = 3	n = 69	**1**		**1**	
Unknown*	n = 0	n = 4				
Previous treatment						
Yes	n = 4	n = 26	1.10 (0.35 – 3.48)	0.871	-	-
No	n = 20	n = 143	1			
Histology						
Primary	n = 22	n = 130	**1**	**0.117**	0.38 (0.07 – 2.06)	0.263
Metastastic	n = 2	n = 39	**0.30 (0.07 – 1.35)**		1	
PTV overlap with main stem bronchi/trachea						
Yes	n = 16	n = 48	**5.04 (2.03 – 12.55)**	**0.001**	**4.16 (1.54 – 11.23)**	**0.005**
No	n = 8	n = 121	**1**		**1**	

5D (continued) – Univariate and multivariate logistic regression analyses for factors predicting high grade clinical (n = 193)

			Univariate analysis		Multivariate analysis	
Characteristic	**≥ G3 toxicity**	**No toxicity**	**OR (95% CI)**	***p*-value**	**OR (95% CI)**	***p*-value**
Any grade of radiographic bronchial toxicity						
Yes	n = 8	n = 49	1.22 (0.49 – 3.05)	0.663	-	-
No	n = 16	n = 120	1			
High grade radiographic bronchial toxicity						
Yes	n = 4	n = 23	1.27 (0.40 – 4.05)	0.687	-	-
No	n = 20	n = 146	1			
Total $V_{130Gy,EQD}$ (all bronchial structures)			**1.68 (1.26 – 2.24)**	**< 0.001**	**1.52 (1.10 – 2.12)**	**0.012**

High grade radiographic toxicity in any bronchial structure

			Univariate analysis		Multivariate analysis	
Characteristic	**Toxicity**	**No toxicity**	**OR (95% CI)**	***p*-value**	**OR (95% CI)**	***p*-value**
Age			**1.05 (1.00 – 1.10)**	**0.036**	1.04 (0.99 – 1.10)	0.100
Gender						
Female	n = 4	n = 67	**0.262 (0.09 – 0.79)**	**0.018**	0.373 (0.12 – 1.19)	0.097
Male	n = 23	n = 101	**1**		1	
COPD						
Yes	n = 18	n = 100	1.28 (0.54 – 3.02)	0.573	-	-
No	n = 9	n = 64	1			
Unknown*	n = 0	n = 4				
Previous treatment						
Yes	n = 6	n = 24	1.71 (0.63 – 4.68)	0.293	-	-
No	n = 21	n = 144	1			
Histology						
Primary	n = 23	n = 131	1	0.397	-	-
Metastatic	n = 4	n = 37	0.62 (0.20 – 1.89)			
PTV overlap with main stem bronchi/trachea						
Yes	n = 16	n = 50	**3.43 (1.49 – 7.92)**	**0.004**	**2.87 (1.16 – 7.06)**	**0.022**
No	n = 11	n = 118	**1**		**1**	
Total $V_{130Gy,EQD}$ (all bronchial structures)			**1.35 (1.07 – 1.71)**	**0.012**	1.237 (0.95 – 1.62)	0.120

Bold values resemble a p-value of ≤ 0.20 on univariate analysis or < 0.05 on multivariate analysis. Variables with a p-value of ≤ 0.20 were included in a multivariate logistic regression analysis.

*This subgroup was not used in the analysis.

Abbreviations: CI = confidence interval; COPD = chronic obstructive pulmonary disease; OR = odds ratio; PTV = planning target volume.

5E – Example of a patient with an ultracentral tumor who was treated with 12 fractions of 5 Gy.

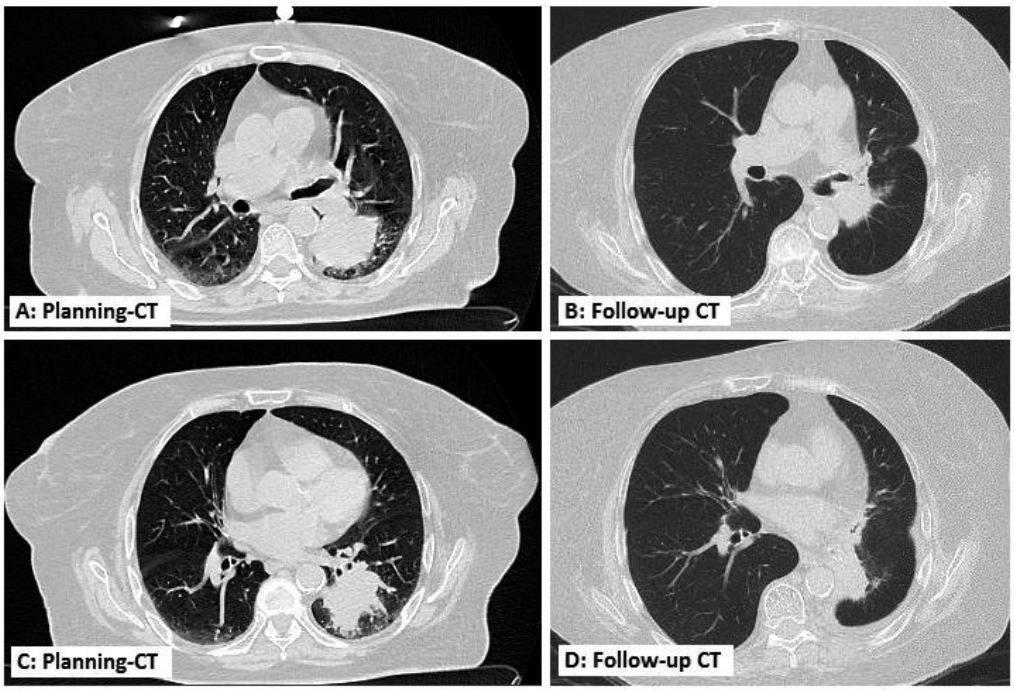

The left panel shows two axial slices of the planning CT-scan, and the right panel shows corresponding slices of the follow-up CT scan 12.7 months later. Patient developed a stenosis of the left upper lobe bronchus (images A and B), and also an occlusion with atelectasis of the left lower lobe bronchus (images C and D).

5F – I

In all figures: The x-axis shows the dose range and is divided into 5 equal parts ("bins"). Solid black squares represent the observed incidence of toxicity for each bin (%). Both the number of patients with toxicity and the numbers at risk in each bin are indicated. Bins not containing any patients had no square shown in the graph. For clinical normal tissue complication probability models, the maximum point dose in all analyzed structures, and a total volume of all structures receiving the specified doses, were calculated for each patient.

5F – NTCP models for grade 3 or higher clinical pulmonary toxicity

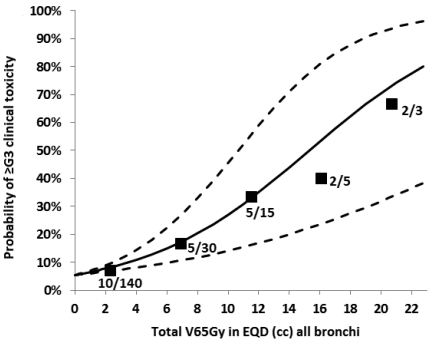

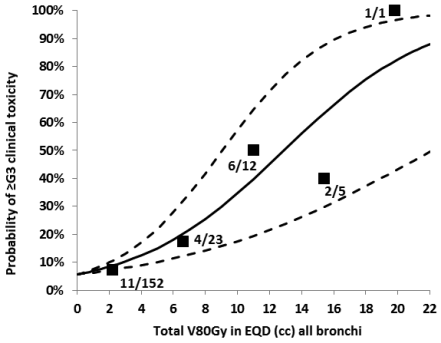

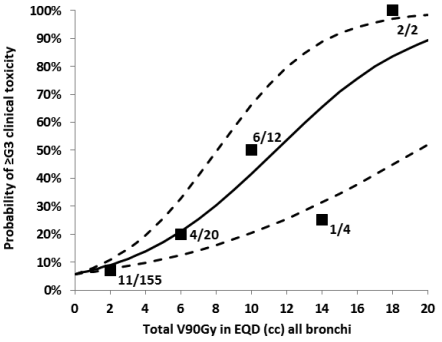

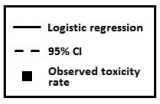

5G – NTCP models for possible or likely treatment-related death (G5 toxicity)

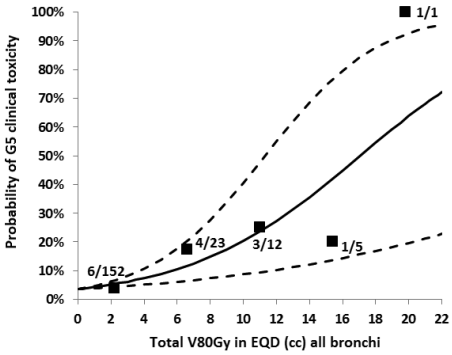

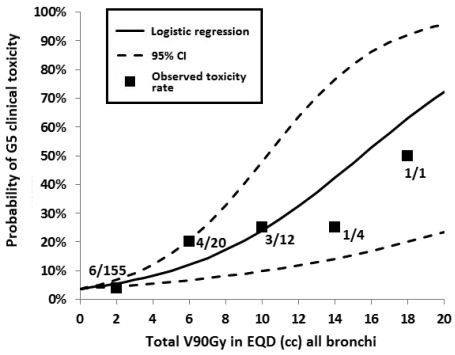

5H – NTCP models for any grade of radiographic toxicity (stenosis, occlusion without atelectasis, or occlusion with atelectasis) in the lobar bronchi

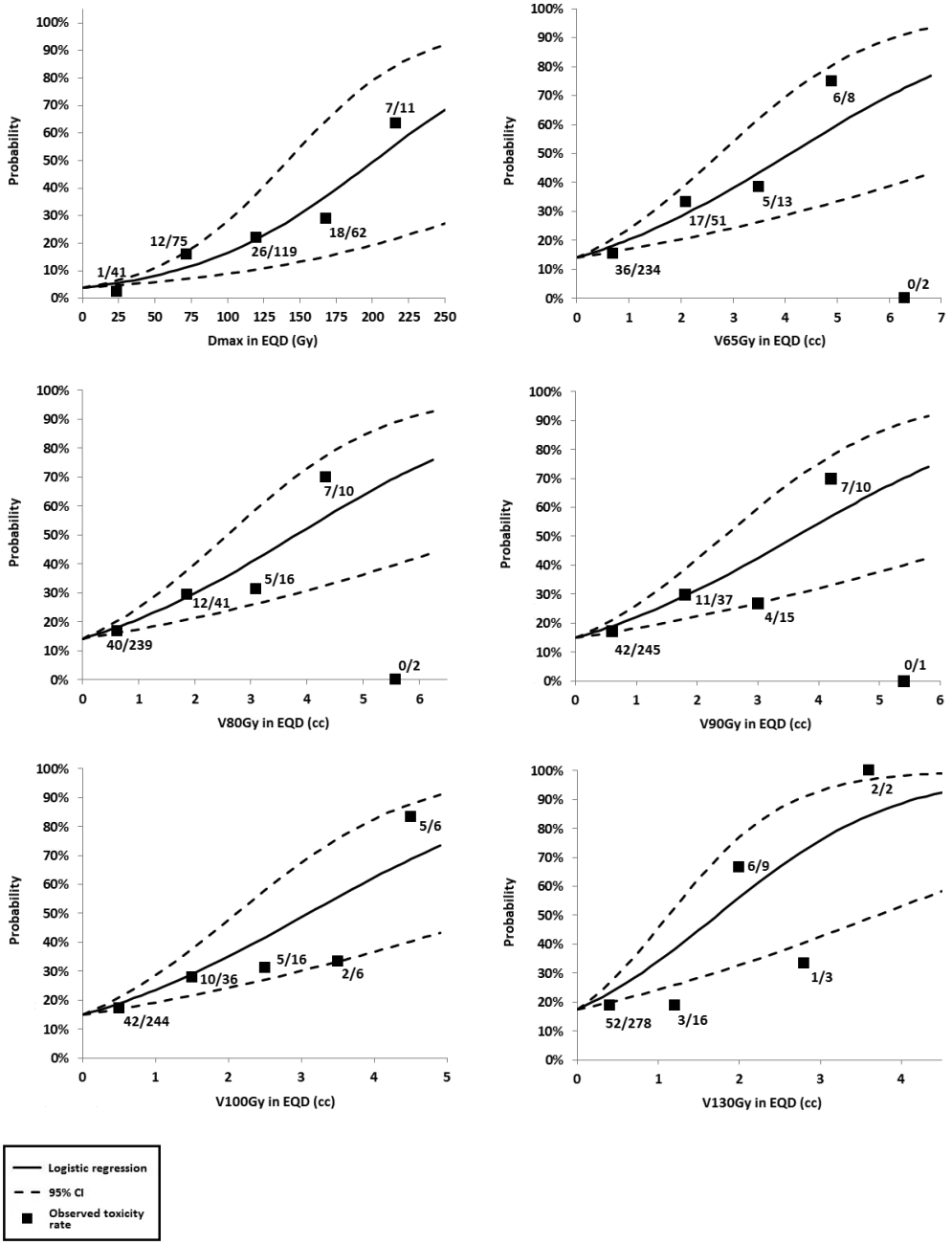

Figure 5I – NTCP models of an occlusion without or with atelectasis in the lobar bronchi

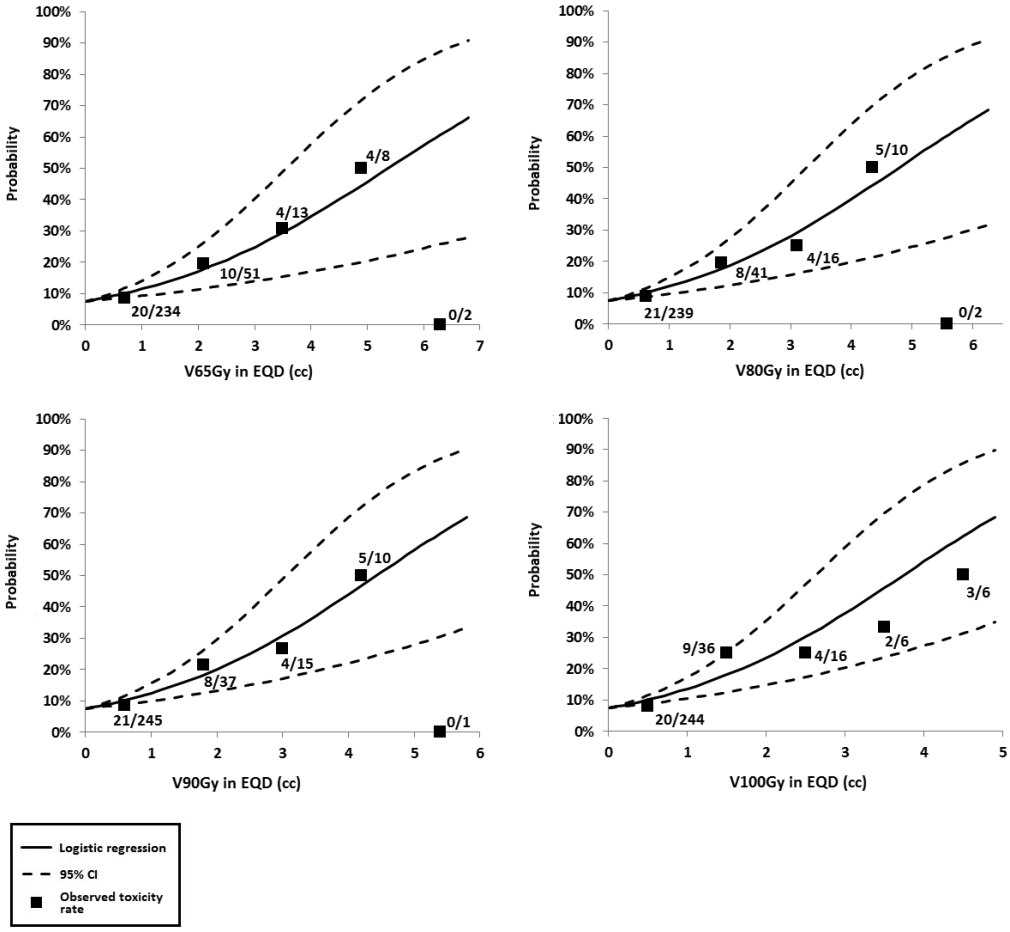

6A – Institutional fractionation schedules for central located lung tumors

	Fractionation schedule	BED_{10} (Gy)
VU University Medical Center (VUmc)		
Central tumor adjacent to and/or minimal overlap with pericardium, hilus, plexus, stomach	8 fractions of 7.5 Gy	105.0
Central tumor with a substantial overlap with mediastinal structures and/or pathological ipsilateral mediastinal nodes	12 fractions of 5 Gy	90.0
*Erasmus Medical Center (EMC)**		
Central tumor close to the esophagus:		
Ray Tracing algorithm	6 or 7 fractions of 8 Gy	86.4 or 100.8
Monte Carlo algorithm	7 fractions of 7 Gy	83.3
Other central lung tumors:		
Ray Tracing algorithm	5 fractions of 9, 10 or 12 Gy	85.5, 100.0 or 132.0
Monte Carlo algorithm	5 fractions of 11 Gy	115.5

*In the early period, tumors were planned using with Ray Tracing algorithm. Subsequently, treatment schedules were changed as no severe toxicity was observed. After introduction of the Monte Carlo calculation algorithm, the prescription changed.
Abbreviations: BED = biologically effective dose

6B – Institutional point dose limits (D_{max}) for the organs at risk

VU University Medical Center (VUmc)		
Organ(s)	**Fractionation schedule 8x 7.5 Gy**	**Fractionation schedule 12x 5 Gy**
Esophagus (α/β = 3)	40 Gy (64Gy EQD_2^3)	48 Gy (67Gy EQD_2^3)
Heart (α/β = 3)*	44 Gy (74.8Gy EQD_2^3)	54 Gy (81Gy EQD_2^3)
Trachea (α/β = 3)*	44 Gy (74.8Gy EQD_2^3)	54 Gy (81Gy EQD_2^3)
Main bronchus (α/β = 3)*	44 Gy (74.8Gy EQD_2^3)	54 Gy (81Gy EQD_2^3)
Great vessels (α/β = 3)*	-	-
Spinal Cord (α/β = 2)	28 Gy (39Gy EQD_2^2)	32 Gy (37Gy EQD_2^2)
Brachial plexus (α/β = 3)	36 Gy (54Gy EQD_2^3)	42 (55Gy EQD_2^3)
Erasmus Medical Center (EMC)		
Organ(s)	**Fractionation schedule 5x 11 Gy**	**Fractionation schedule 7x 7 Gy**
Spinal Cord (α/β = 2)	27.5 Gy (52Gy EQD_2^2)	32.9 Gy (55Gy EQD_2^2)
Esophagus (α/β = 3)	35 Gy (70Gy EQD_2^3)	42 Gy (75.6Gy EQD_2^3)
Trachea (α/β = 3)	45 Gy (108Gy EQD_2^3)	49 Gy (98Gy EQD_2^3)
Main Bronchus (α/β = 3)	55 Gy (154Gy EQD_2^3)	49 Gy (98Gy EQD_2^3)
Brachial plexus (α/β = 3)	30 Gy (54Gy EQD_2^3)	35 Gy (56Gy EQD_2^3)

* = no specific dose limit when the planning target volume is adjacent or overlapping, but in practice the point D_{max} is frequently constrained during planning.
Abbreviations: EQD_2^x = equivalent dose of 2 Gy per fraction with an α/β ratio of x

6C – Univariate and multivariate logistic regression analyses for factors predicting acute grade 1 – 2 esophageal toxicity

			Univariate analysis		Multivariate analysis	
Characteristic	**Toxicity**	**No toxicity**	**OR (95% CI)**	**p-value**	**OR (95% CI)**	***p*-value**
Age			0.982 (0.952 – 1.014)	0.270		
PTV (cc)			1.004 (1.000 – 1.007)	0.051	0.998 (0.993 – 1.003)	0.371
Gender						
Male	n = 20	n = 129	1		1	
Female	n = 18	n = 64	1.814 (0.897 – 3.667)	0.097	3.020 (1.304 – 6.994)	
Charlson						
0 – 2	n = 23	n = 96	1			
≥ 3	n = 15	n = 97	0.645 (0.318 – 1.312)	0.226		
Amount of fractions						
3 – 6	n = 18	n = 84	1			
7 – 12	n = 20	n = 109	0.856 (0.426 – 1.720)	0.663		
Dose per fraction						
5 – 7 Gy	n = 11	n = 44	1			
> 7 Gy	n = 27	n = 149	0.725 (0.333 – 1.577)	0.417		
D_{5cc} (EQD_2^{10})			1.135 (1.086 – 1.187)	< 0.001	1.158 (1.100 – 1.219)	< 0.001

Abbreviations: EQD_2^{10} = equivalent dose of 2 Gy per fraction with α/β ratio of 10; 95% CI = 95% confidence interval; PTV = planning target volume

7A – Bronchial structures

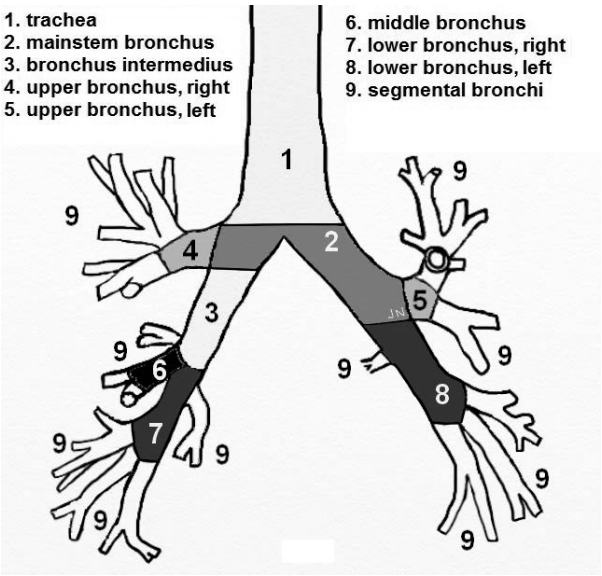

7B – Dosimetric parameters of all DVH-parameters, divided in group with and without acute toxicity

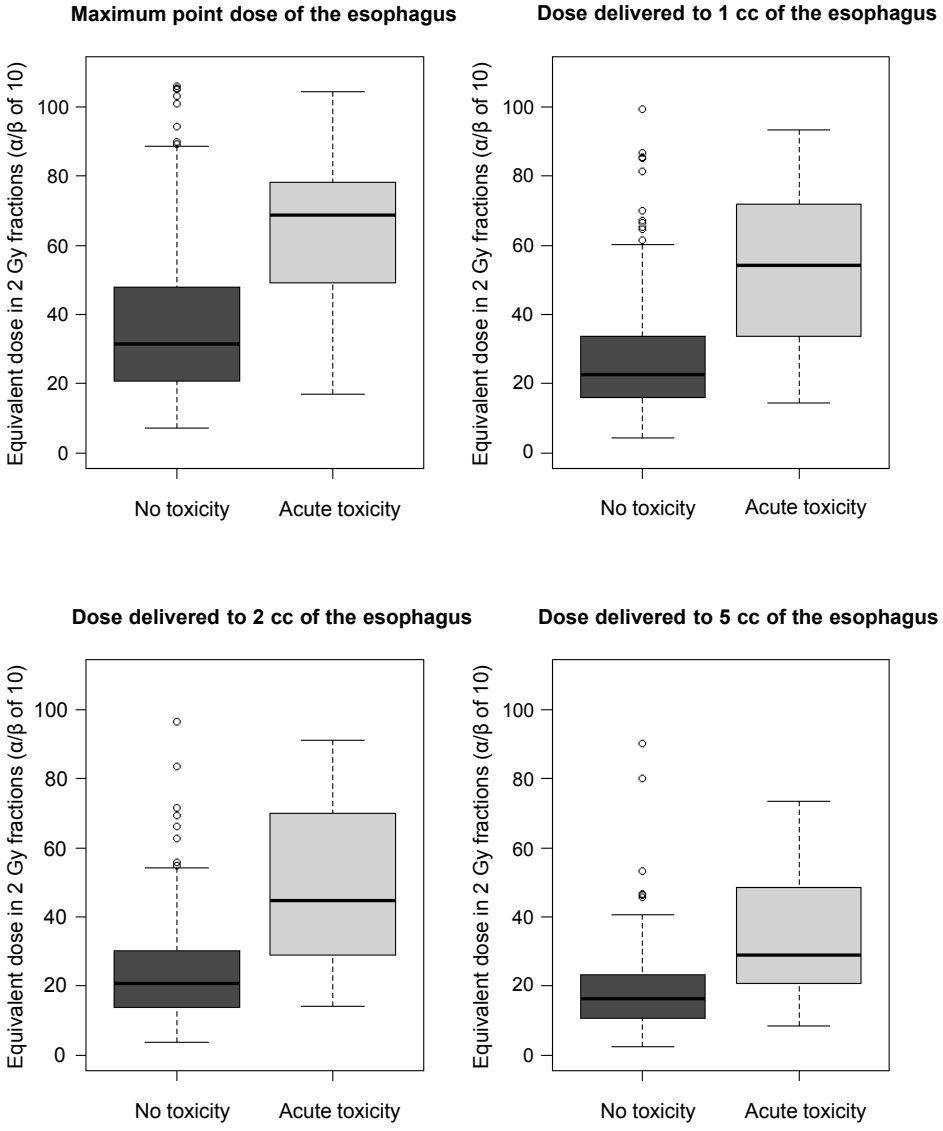

The band inside the box shows the median and the borders of the box the first and third quartile. The whiskers show 1.5 times the interquartile range and the circles the outliers.

References

1. Bray F, Ferlay J, Soerjomataram I, Siegel RL, Torre LA, Jemal A. Global cancer statistics 2018: GLOBOCAN estimates of incidence and mortality worldwide for 36 cancers in 185 countries. CA Cancer J Clin. 2018;68(6):394-424.
2. NKR-cijfers: Netherlands Cancer Registry; 2020 [Available from: www.cijfersoverkanker.nl.
3. Howlader N NA, Krapcho M, Miller D, Brest A, Yu M, Ruhl J, Tatalovich Z, Mariotto A, Lewis DR, Chen HS, Feuer EJ, Cronin KA (eds). SEER Cancer Statistics Review: National Cancer Institute. Bethesda, MD; 1975-2016 [Available from: https://seer.cancer.gov/csr/1975_2016/, based on November 2018 SEER data submission, posted to the SEER web site, April 2019.
4. Goldstraw P, Chansky K, Crowley J, Rami-Porta R, Asamura H, Eberhardt WE, et al. The IASLC Lung Cancer Staging Project: Proposals for Revision of the TNM Stage Groupings in the Forthcoming (Eighth) Edition of the TNM Classification for Lung Cancer. J Thorac Oncol. 2016;11(1):39-51.
5. Postmus PE, Kerr KM, Oudkerk M, Senan S, Waller DA, Vansteenkiste J, et al. Early and locally advanced non-small-cell lung cancer (NSCLC): ESMO Clinical Practice Guidelines for diagnosis, treatment and follow-up. Ann Oncol. 2017;28(suppl_4):iv1-iv21.
6. Landelijke Werkgroep Longtumoren. Landelijke Richtlijn Niet Kleincellig Longcarcinoom: Integraal Kankercentrum Nederland; 2015 [updated 18-12-2015. Available from: https://www.oncoline.nl/niet-kleincellig-longcarcinoom.
7. Onishi H, Araki T, Shirato H, Nagata Y, Hiraoka M, Gomi K, et al. Stereotactic hypofractionated high-dose irradiation for stage I nonsmall cell lung carcinoma: clinical outcomes in 245 subjects in a Japanese multiinstitutional study. Cancer. 2004;101(7): 1623-31.
8. Nagata Y, Takayama K, Matsuo Y, Norihisa Y, Mizowaki T, Sakamoto T, et al. Clinical outcomes of a phase I/II study of 48 Gy of stereotactic body radiotherapy in 4 fractions for primary lung cancer using a stereotactic body frame. Int J Radiat Oncol Biol Phys. 2005;63(5):1427-31.
9. Chi A, Liao Z, Nguyen NP, Xu J, Stea B, Komaki R. Systemic review of the patterns of failure following stereotactic body radiation therapy in early-stage non-small-cell lung cancer: clinical implications. Radiother Oncol. 2010;94(1):1-11.
10. Videtic GMM, Donington J, Giuliani M, Heinzerling J, Karas TZ, Kelsey CR, et al. Stereotactic body radiation therapy for early-stage non-small cell lung cancer: Executive Summary of an ASTRO Evidence-Based Guideline. Pract Radiat Oncol. 2017;7(5):295-301.
11. Guckenberger M, Andratschke N, Dieckmann K, Hoogeman MS, Hoyer M, Hurkmans C, et al. ESTRO ACROP consensus guideline on implementation and practice of stereotactic body radiotherapy for peripherally located early stage non-small cell lung cancer. Radiother Oncol. 2017;124(1):11-7.
12. Ball D, Mai GT, Vinod S, Babington S, Ruben J, Kron T, et al. Stereotactic ablative radiotherapy versus standard radiotherapy in stage 1 non-small-cell lung cancer (TROG 09.02 CHISEL): a phase 3, open-label, randomised controlled trial. Lancet Oncol. 2019;20(4):494-503.

13. Timmerman R, McGarry R, Yiannoutsos C, Papiez L, Tudor K, DeLuca J, et al. Excessive toxicity when treating central tumors in a phase II study of stereotactic body radiation therapy for medically inoperable early-stage lung cancer. J Clin Oncol. 2006;24(30):4833-9.

14. Senthi S, Haasbeek CJ, Slotman BJ, Senan S. Outcomes of stereotactic ablative radiotherapy for central lung tumours: a systematic review. Radiother Oncol. 2013;106(3):276-82.

15. Chang JY, Balter PA, Dong L, Yang Q, Liao Z, Jeter M, et al. Stereotactic body radiation therapy in centrally and superiorly located stage I or isolated recurrent non-small-cell lung cancer. Int J Radiat Oncol Biol Phys. 2008;72(4):967-71.

16. Bezjak A, Paulus R, Gaspar LE, Timmerman RD, Straube WL, Ryan WF, et al. Safety and Efficacy of a Five-Fraction Stereotactic Body Radiotherapy Schedule for Centrally Located Non-Small-Cell Lung Cancer: NRG Oncology/RTOG 0813 Trial. J Clin Oncol. 2019:JCO1800622.

17. Lindberg K, Bergström P, Brustugun OT, Engelholm S, Grozman V, Hoyer M, et al. OA24.05 The Nordic HILUS-Trial - First Report of a Phase II Trial of SBRT of Centrally Located Lung Tumors. Journal of Thoracic Oncology. 2017;12(1, Supplement):S340.

18. Palma D, Daly M, Urbanic J, Giuliani M. Stereotactic Radiation for Ultra-Central Lung Tumors: Good Idea, or Ultra-Risky? Int J Radiat Oncol Biol Phys. 2019;103(4):788-91.

19. Zhao L, Zhou S, Balter P, Shen C, Gomez DR, Welsh JD, et al. Planning Target Volume D95 and Mean Dose Should Be Considered for Optimal Local Control for Stereotactic Ablative Radiation Therapy. Int J Radiat Oncol Biol Phys. 2016;95(4):1226-35.

20. Loganadane G, Martinetti F, Mercier O, Krhili S, Riet FG, Mbagui R, et al. Stereotactic ablative radiotherapy for early stage non-small cell lung cancer: A critical literature review of predictive factors of relapse. Cancer Treat Rev. 2016;50:240-6.

21. Bezjak A, Paulus R, Gaspar LE, Timmerman RD, Straube WL, Ryan WF, et al. Efficacy and Toxicity Analysis of NRG Oncology/RTOG 0813 Trial of Stereotactic Body Radiation Therapy (SBRT) for Centrally Located Non-Small Cell Lung Cancer (NSCLC). International Journal of Radiation Oncology • Biology • Physics.96(2):S8.

22. Xie D, Allen MS, Marks R, Jiang G, Sun Z, Nichols F, et al. Nomogram prediction of overall survival for patients with non-small-cell lung cancer incorporating pretreatment peripheral blood markers. Eur J Cardiothorac Surg. 2018;53(6):1214-22.

23. Liang W, Zhang L, Jiang G, Wang Q, Liu L, Liu D, et al. Development and validation of a nomogram for predicting survival in patients with resected non-small-cell lung cancer. J Clin Oncol. 2015;33(8):861-9.

24. Louie AV, Haasbeek CJ, Mokhles S, Rodrigues GB, Stephans KL, Lagerwaard FJ, et al. Predicting Overall Survival After Stereotactic Ablative Radiation Therapy in Early-Stage Lung Cancer: Development and External Validation of the Amsterdam Prognostic Model. Int J Radiat Oncol Biol Phys. 2015;93(1):82-90.

25. Tanadini-Lang S, Rieber J, Filippi AR, Fode MM, Streblow J, Adebahr S, et al. Nomogram based overall survival prediction in stereotactic body radiotherapy for oligo-metastatic lung disease. Radiother Oncol. 2017;123(2):182-8.

26. Kang J, Ning MS, Feng H, Li H, Bahig H, Brooks ED, et al. Predicting 5-Year Progression and Survival Outcomes for Early Stage Non-small Cell Lung Cancer Treated with Stereotactic Ablative Radiation Therapy: Development and Validation of Robust Prognostic Nomograms. Int J Radiat Oncol Biol Phys. 2020;106(1):90-9.

27. Park HS, Harder EM, Mancini BR, Decker RH. Central versus Peripheral Tumor Location: Influence on Survival, Local Control, and Toxicity Following Stereotactic Body Radiotherapy for Primary Non-Small-Cell Lung Cancer. J Thorac Oncol. 2015;10(5):832-7.

28. Schanne DH, Nestle U, Allgauer M, Andratschke N, Appold S, Dieckmann U, et al. Stereotactic body radiotherapy for centrally located stage I NSCLC: a multicenter analysis. Strahlenther Onkol. 2015;191(2):125-32.

29. Duijm M, Schillemans W, Aerts JG, Heijmen B, Nuyttens JJ. Dose and Volume of the Irradiated Main Bronchi and Related Side Effects in the Treatment of Central Lung Tumors With Stereotactic Radiotherapy. Semin Radiat Oncol. 2016;26(2):140-8.

30. Duijm M, van der Voort van Zyp NC, van de Vaart P, Hoop EO, Mast ME, Hoogeman MS, et al. Predicting high-grade esophagus toxicity after treating central lung tumors with stereotactic radiotherapy using a Normal Tissue Complication Probability model. Int J Radiat Oncol Biol Phys. 2019.

31. Harrell FE J. Regression Modeling Strategies: With Applications to Linear Models, Logistic and Ordinal Regression, and Survival Analysis. Second ed. Switzerland2015.

32. Lee HW, Lee CH, Park YS. Location of stage I-III non-small cell lung cancer and survival rate: Systematic review and meta-analysis. Thorac Cancer. 2018;9(12):1614-22.

33. Shaverdian N, Veruttipong D, Wang J, Kupelian P, Steinberg M, Lee P. Location Matters: Stage I Non-Small-cell Carcinomas of the Lower Lobes Treated With Stereotactic Body Radiation Therapy Are Associated With Poor Outcomes. Clin Lung Cancer. 2017;18(2):e137-e42.

34. Rocha AT, McCormack M, Montana G, Schreiber G. Association between lower lobe location and upstaging for early-stage non-small cell lung cancer. Chest. 2004;125(4): 1424-30.

35. Olsen JR, Robinson CG, El Naqa I, Creach KM, Drzymala RE, Bloch C, et al. Dose-response for stereotactic body radiotherapy in early-stage non-small-cell lung cancer. Int J Radiat Oncol Biol Phys. 2011;81(4):e299-303.

36. Taremi M, Hope A, Dahele M, Pearson S, Fung S, Purdie T, et al. Stereotactic body radiotherapy for medically inoperable lung cancer: prospective, single-center study of 108 consecutive patients. Int J Radiat Oncol Biol Phys. 2012;82(2):967-73.

37. Stephans KL, Woody NM, Reddy CA, Varley M, Magnelli A, Zhuang T, et al. Tumor Control and Toxicity for Common Stereotactic Body Radiation Therapy Dose-Fractionation Regimens in Stage I Non-Small Cell Lung Cancer. Int J Radiat Oncol Biol Phys. 2018;100(2):462-9.

38. Chang JY, Li QQ, Xu QY, Allen PK, Rebueno N, Gomez DR, et al. Stereotactic ablative radiation therapy for centrally located early stage or isolated parenchymal recurrences of non-small cell lung cancer: how to fly in a "no fly zone". Int J Radiat Oncol Biol Phys. 2014;88(5):1120-8.

39. Roach MC, Robinson CG, DeWees TA, Ganachaud J, Przybysz D, Drzymala R, et al. Stereotactic Body Radiation Therapy for Central Early-Stage NSCLC: Results of a Prospective Phase I/II Trial. J Thorac Oncol. 2018;13(11):1727-32.

40. Dreyer J, Bremer M, Henkenberens C. Comorbidity indexing for prediction of the clinical outcome after stereotactic body radiation therapy in non-small cell lung cancer. Radiat Oncol. 2018;13(1):213.

41. Lee DS, Kim YS, Yoo Ie R, Kang YN, Kim SJ, Oh JK, et al. Long-term clinical experience of high-dose ablative lung radiotherapy: high pre-treatment [18F]fluorodeoxyglucose-positron emission tomography maximal standardized uptake value of the primary tumor adversely affects treatment outcome. Lung Cancer. 2013;80(2):172-8.

42. Stephans KL, Djemil T, Reddy CA, Gajdos SM, Kolar M, Mason D, et al. A comparison of two stereotactic body radiation fractionation schedules for medically inoperable stage I non-small cell lung cancer: the Cleveland Clinic experience. J Thorac Oncol. 2009;4(8):976-82.

43. Horner-Rieber J, Bernhardt D, Dern J, Konig L, Adeberg S, Paul A, et al. Histology of non-small cell lung cancer predicts the response to stereotactic body radiotherapy. Radiother Oncol. 2017;125(2):317-24.

44. Balachandran VP, Gonen M, Smith JJ, DeMatteo RP. Nomograms in oncology: more than meets the eye. Lancet Oncol. 2015;16(4):e173-80.

45. Song SY, Choi W, Shin SS, Lee SW, Ahn SD, Kim JH, et al. Fractionated stereotactic body radiation therapy for medically inoperable stage I lung cancer adjacent to central large bronchus. Lung Cancer. 2009;66(1):89-93.

46. Onimaru R, Shirato H, Shimizu S, Kitamura K, Xu B, Fukumoto S, et al. Tolerance of organs at risk in small-volume, hypofractionated, image-guided radiotherapy for primary and metastatic lung cancers. Int J Radiat Oncol Biol Phys. 2003;56(1):126-35.

47. Rowe BP, Boffa DJ, Wilson LD, Kim AW, Detterbeck FC, Decker RH. Stereotactic body radiotherapy for central lung tumors. J Thorac Oncol. 2012;7(9):1394-9.

48. Nuyttens JJ, van der Voort van Zyp NC, Praag J, Aluwini S, van Klaveren RJ, Verhoef C, et al. Outcome of four-dimensional stereotactic radiotherapy for centrally located lung tumors. Radiother Oncol. 2012;102(3):383-7.

49. Onishi H, Shirato H, Nagata Y, Hiraoka M, Fujino M, Gomi K, et al. Hypofractionated stereotactic radiotherapy (HypoFXSRT) for stage I non-small cell lung cancer: updated results of 257 patients in a Japanese multi-institutional study. J Thorac Oncol. 2007;2(7 Suppl 3):S94-100.

50. Chang JY, Bezjak A, Mornex F, Committee IART. Stereotactic ablative radiotherapy for centrally located early stage non-small-cell lung cancer: what we have learned. J Thorac Oncol. 2015;10(4):577-85.

51. Seuntjens J LE, Cora S et al. Prescribing, recording, and reporting of stereotactic treatments with small photon beams. J ICRU. 2014;14(2):1-160.

52. Duijm M, van der Voort van Zyp NC, van de Vaart P, Oomen-de Hoop E, Mast ME, Hoogeman MS, et al. Predicting high-grade esophagus toxicity after treating central lung tumors with stereotactic radiotherapy using a Normal Tissue Complication Probability modeL. International Journal of Radiation Oncology • Biology • Physics. 2019.

53. Modh A, Rimner A, Williams E, Foster A, Shah M, Shi W, et al. Local control and toxicity in a large cohort of central lung tumors treated with stereotactic body radiation therapy. Int J Radiat Oncol Biol Phys. 2014;90(5):1168-76.

54. Bral S, Gevaert T, Linthout N, Versmessen H, Collen C, Engels B, et al. Prospective, risk-adapted strategy of stereotactic body radiotherapy for early-stage non-small-cell lung cancer: results of a Phase II trial. Int J Radiat Oncol Biol Phys. 2011;80(5):1343-9.

55. Samson P, Rehman S, Juloori A, DeWees T, Roach M, Bradley J, et al. Local control for clinical stage I non-small cell lung cancer treated with 5-fraction stereotactic body radiation therapy is not associated with treatment schedule. Pract Radiat Oncol. 2018;8(6):404-13.

56. Ye L, Shi S, Zeng Z, Huang Y, Hu Y, He J. Nomograms for predicting disease progression in patients of Stage I non-small cell lung cancer treated with stereotactic body radiotherapy. Jpn J Clin Oncol. 2018;48(2):160-6.

57. Sun B, Brooks ED, Komaki RU, Liao Z, Jeter MD, McAleer MF, et al. 7-year follow-up after stereotactic ablative radiotherapy for patients with stage I non-small cell lung cancer: Results of a phase 2 clinical trial. Cancer. 2017;123(16):3031-9.

58. Kawaguchi T, Takada M, Kubo A, Matsumura A, Fukai S, Tamura A, et al. Performance status and smoking status are independent favorable prognostic factors for survival in non-small cell lung cancer: a comprehensive analysis of 26,957 patients with NSCLC. J Thorac Oncol. 2010;5(5):620-30.

59. Raman S, Yau V, Pineda S, Le LW, Lau A, Bezjak A, et al. Ultracentral Tumors Treated With Stereotactic Body Radiotherapy: Single-Institution Experience. Clin Lung Cancer. 2018;19(5):e803-e10.

60. Chang JH, Poon I, Erler D, Zhang L, Cheung P. The safety and effectiveness of stereotactic body radiotherapy for central versus ultracentral lung tumors. Radiother Oncol. 2018;129(2):277-83.

61. Chaudhuri AA, Tang C, Binkley MS, Jin M, Wynne JF, von Eyben R, et al. Stereotactic ablative radiotherapy (SABR) for treatment of central and ultra-central lung tumors. Lung Cancer. 2015;89(1):50-6.

62. Unger K, Ju A, Oermann E, Suy S, Yu X, Vahdat S, et al. CyberKnife for hilar lung tumors: report of clinical response and toxicity. J Hematol Oncol. 2010;3:39.

63. Gollins SW, Ryder WD, Burt PA, Barber PV, Stout R. Massive haemoptysis death and other morbidity associated with high dose rate intraluminal radiotherapy for carcinoma of the bronchus. Radiother Oncol. 1996;39(2):105-16.

64. Speiser BL, Spratling L. Radiation bronchitis and stenosis secondary to high dose rate endobronchial irradiation. Int J Radiat Oncol Biol Phys. 1993;25(4):589-97.

65. Miller KL, Shafman TD, Anscher MS, Zhou SM, Clough RW, Garst JL, et al. Bronchial stenosis: an underreported complication of high-dose external beam radiotherapy for lung cancer? Int J Radiat Oncol Biol Phys. 2005;61(1):64-9.

66. Kelsey CR, Kahn D, Hollis DR, Miller KL, Zhou SM, Clough RW, et al. Radiation-induced narrowing of the tracheobronchial tree: an in-depth analysis. Lung Cancer. 2006;52(1): 111-6.

67. Nuyttens JJ, van de Pol M. The CyberKnife radiosurgery system for lung cancer. Expert Rev Med Devices. 2012;9(5):465-75.

68. Baumann P, Nyman J, Lax I, Friesland S, Hoyer M, Rehn Ericsson S, et al. Factors important for efficacy of stereotactic body radiotherapy of medically inoperable stage I lung cancer. A retrospective analysis of patients treated in the Nordic countries. Acta Oncol. 2006;45(7):787-95.

69. Joyner M, Salter BJ, Papanikolaou N, Fuss M. Stereotactic body radiation therapy for centrally located lung lesions. Acta Oncol. 2006;45(7):802-7.

70. Oshiro Y, Aruga T, Tsuboi K, Marino K, Hara R, Sanayama Y, et al. Stereotactic body radiotherapy for lung tumors at the pulmonary hilum. Strahlenther Onkol. 2010;186(5):274-9.

71. Haasbeek CJ, Lagerwaard FJ, Slotman BJ, Senan S. Outcomes of stereotactic ablative radiotherapy for centrally located early-stage lung cancer. J Thorac Oncol. 2011;6(12):2036-43.

72. Ung YC, Yu E, Falkson C, Haynes AE, Stys-Norman D, Evans WK, et al. The role of high-dose-rate brachytherapy in the palliation of symptoms in patients with non-small-cell lung cancer: a systematic review. Brachytherapy. 2006;5(3):189-202.

73. Ozkok S, Karakoyun-Celik O, Goksel T, Mogulkoc N, Yalman D, Gok G, et al. High dose rate endobronchial brachytherapy in the management of lung cancer: response and toxicity evaluation in 158 patients. Lung Cancer. 2008;62(3):326-33.

74. Vansteenkiste J, De Ruysscher D, Eberhardt WE, Lim E, Senan S, Felip E, et al. Early and locally advanced non-small-cell lung cancer (NSCLC): ESMO Clinical Practice Guidelines for diagnosis, treatment and follow-up. Ann Oncol. 2013;24 Suppl 6:vi89-98.

75. Bezjak A, Paulus R, Gaspar LE, Timmerman RD, Straube WL, Ryan WF, et al. Primary Study Endpoint Analysis for NRG Oncology/RTOG 0813 Trial of Stereotactic Body Radiation Therapy (SBRT) for Centrally Located Non-Small Cell Lung Cancer (NSCLC). International Journal of Radiation Oncology • Biology • Physics.94(1):5-6.

76. Roesch J, Panje C, Sterzing F, Mantel F, Nestle U, Andratschke N, et al. SBRT for centrally localized NSCLC - What is too central? Radiat Oncol. 2016;11(1):157.

77. Tekatli H, Haasbeek N, Dahele M, De Haan P, Verbakel W, Bongers E, et al. Outcomes of Hypofractionated High-Dose Radiotherapy in Poor-Risk Patients with "Ultracentral" Non-Small Cell Lung Cancer. J Thorac Oncol. 2016;11(7):1081-9.

78. Haseltine JM, Rimner A, Gelblum DY, Modh A, Rosenzweig KE, Jackson A, et al. Fatal complications after stereotactic body radiation therapy for central lung tumors abutting the proximal bronchial tree. Pract Radiat Oncol. 2016;6(2):e27-33.

79. Ettinger DS, Wood DE, Aisner DL, Akerley W, Bauman J, Chirieac LR, et al. Non-Small Cell Lung Cancer, Version 5.2017, NCCN Clinical Practice Guidelines in Oncology. J Natl Compr Canc Netw. 2017;15(4):504-35.

80. Lagerwaard FJ, Haasbeek CJ, Smit EF, Slotman BJ, Senan S. Outcomes of risk-adapted fractionated stereotactic radiotherapy for stage I non-small-cell lung cancer. Int J Radiat Oncol Biol Phys. 2008;70(3):685-92.

81. Tekatli H, Senan S, Dahele M, Slotman BJ, Verbakel WF. Stereotactic ablative radiotherapy (SABR) for central lung tumors: Plan quality and long-term clinical outcomes. Radiother Oncol. 2015;117(1):64-70.

82. Verbakel WF, Senan S, Cuijpers JP, Slotman BJ, Lagerwaard FJ. Rapid delivery of stereotactic radiotherapy for peripheral lung tumors using volumetric intensity-modulated arcs. Radiother Oncol. 2009;93(1):122-4.

83. Underberg RW, Lagerwaard FJ, Slotman BJ, Cuijpers JP, Senan S. Use of maximum intensity projections (MIP) for target volume generation in 4DCT scans for lung cancer. Int J Radiat Oncol Biol Phys. 2005;63(1):253-60.

84. Ong CL, Palma D, Verbakel WF, Slotman BJ, Senan S. Treatment of large stage I-II lung tumors using stereotactic body radiotherapy (SBRT): planning considerations and early toxicity. Radiother Oncol. 2010;97(3):431-6.

85. Bongers EM, Botticella A, Palma DA, Haasbeek CJ, Warner A, Verbakel WF, et al. Predictive parameters of symptomatic radiation pneumonitis following stereotactic or hypofractionated radiotherapy delivered using volumetric modulated arcs. Radiother Oncol. 2013;109(1):95-9.

86. Joiner MC, van der Kogel A. Basic Clinical Radiobiology. London: Hodder Arnold Publication; 2009.

87. Schemper M, Smith TL. A note on quantifying follow-up in studies of failure time. Control Clin Trials. 1996;17(4):343-6.

88. Robertson JM, Sohn M, Yan D. Predicting grade 3 acute diarrhea during radiation therapy for rectal cancer using a cutoff-dose logistic regression normal tissue complication probability model. Int J Radiat Oncol Biol Phys. 2010;77(1):66-72.

89. Agresti A FB. Statistical Methods for Social Sciences. 4th ed2009.

90. Lischalk JW, Malik RM, Collins SP, Collins BT, Matus IA, Anderson ED. Stereotactic body radiotherapy (SBRT) for high-risk central pulmonary metastases. Radiat Oncol. 2016;11:28.

91. Karlsson K, Nyman J, Baumann P, Wersall P, Drugge N, Gagliardi G, et al. Retrospective cohort study of bronchial doses and radiation-induced atelectasis after stereotactic body radiation therapy of lung tumors located close to the bronchial tree. Int J Radiat Oncol Biol Phys. 2013;87(3):590-5.

92. Klapper JA, Hittinger SA, Denlinger CE. Alternatives to Lobectomy for High-Risk Patients With Early-Stage Non-Small Cell Lung Cancer. Ann Thorac Surg. 2017;103(4):1330-9.

93. Guckenberger M, Heilman K, Wulf J, Mueller G, Beckmann G, Flentje M. Pulmonary injury and tumor response after stereotactic body radiotherapy (SBRT): results of a serial follow-up CT study. Radiother Oncol. 2007;85(3):435-42.

94. Abelson JA, Murphy JD, Loo BW, Jr., Chang DT, Daly ME, Wiegner EA, et al. Esophageal tolerance to high-dose stereotactic ablative radiotherapy. Dis Esophagus. 2012;25(7): 623-9.

95. Wu AJ, Williams E, Modh A, Foster A, Yorke E, Rimner A, et al. Dosimetric predictors of esophageal toxicity after stereotactic body radiotherapy for central lung tumors. Radiother Oncol. 2014;112(2):267-71.

96. Stephans KL, Djemil T, Diaconu C, Reddy CA, Xia P, Woody NM, et al. Esophageal dose tolerance to hypofractionated stereotactic body radiation therapy: risk factors for late toxicity. Int J Radiat Oncol Biol Phys. 2014;90(1):197-202.

97. Nuyttens JJ, Moiseenko V, McLaughlin M, Jain S, Herbert S, Grimm J. Esophageal Dose Tolerance in Patients Treated With Stereotactic Body Radiation Therapy. Semin Radiat Oncol. 2016;26(2):120-8.

98. Cox BW, Jackson A, Hunt M, Bilsky M, Yamada Y. Esophageal toxicity from high-dose, single-fraction paraspinal stereotactic radiosurgery. Int J Radiat Oncol Biol Phys. 2012;83(5):e661-7.

99. Le QT, Loo BW, Ho A, Cotrutz C, Koong AC, Wakelee H, et al. Results of a phase I dose-escalation study using single-fraction stereotactic radiotherapy for lung tumors. J Thorac Oncol. 2006;1(8):802-9.

100. Pollom EL, Deng L, Pai RK, Brown JM, Giaccia A, Loo BW, Jr., et al. Gastrointestinal Toxicities With Combined Antiangiogenic and Stereotactic Body Radiation Therapy. Int J Radiat Oncol Biol Phys. 2015;92(3):568-76.

101. Werner-Wasik M, Pequignot E, Leeper D, Hauck W, Curran W. Predictors of severe esophagitis include use of concurrent chemotherapy, but not the length of irradiated esophagus: a multivariate analysis of patients with lung cancer treated with nonoperative therapy. Int J Radiat Oncol Biol Phys. 2000;48(3):689-96.

102. Dehing-Oberije C, De Ruysscher D, Petit S, Van Meerbeeck J, Vandecasteele K, De Neve W, et al. Development, external validation and clinical usefulness of a practical prediction model for radiation-induced dysphagia in lung cancer patients. Radiother Oncol. 2010;97(3):455-61.

103. Wijsman R, Dankers F, Troost EG, Hoffmann AL, van der Heijden EH, de Geus-Oei LF, et al. Multivariable normal-tissue complication modeling of acute esophageal toxicity in advanced stage non-small cell lung cancer patients treated with intensity-modulated (chemo-)radiotherapy. Radiother Oncol. 2015;117(1):49-54.

104. Lindberg K, Karlsson K, Grozman V, Andersson A, Lax I, Wersäll P, et al. HILUS-Retrospective - A Retrospective Toxicity Analysis of Patients Treated with SBRT for Centrally Located Lung Lesions. International Journal of Radiation Oncology • Biology • Physics. 2017;99(2):E474.

105. Duijm M, Tekatli H, Oomen-de Hoop E, Verbakel W, Schillemans W, Slotman BJ, et al. Esophagus toxicity after stereotactic and hypofractionated radiotherapy for central lung tumors: Normal tissue complication probability modeling. Radiother Oncol. 2018;127(2):233-8.

106. Yau V, Lindsay P, Le L, Lau A, Wong O, Glick D, et al. Low Incidence of Esophageal Toxicity After Lung Stereotactic Body Radiation Therapy: Are Current Esophageal Dose Constraints Too Conservative? Int J Radiat Oncol Biol Phys. 2018;101(3):574-80.

107. Pezzi CM, Mallin K, Mendez AS, Greer Gay E, Putnam JB, Jr. Ninety-day mortality after resection for lung cancer is nearly double 30-day mortality. J Thorac Cardiovasc Surg. 2014;148(5):2269-77.

108. Harder EM, Chen ZJ, Park HS, Mancini BR, Decker RH. Dose-Volume Predictors of Esophagitis After Thoracic Stereotactic Body Radiation Therapy. Am J Clin Oncol. 2017;40(5):477-82.

109. Sebastian NT, Xu-Welliver M, Williams TM. Stereotactic body radiation therapy (SBRT) for early stage non-small cell lung cancer (NSCLC): contemporary insights and advances. J Thorac Dis. 2018;10(Suppl 21):S2451-S64.

110. Pham AH, Yorke E, Rimner A, Wu AJ. Potential for Interfraction Motion to Increase Esophageal Toxicity in Lung SBRT. Technol Cancer Res Treat. 2017:1533034617711353.

111. Mokhles S, Verstegen N, Maat AP, Birim O, Bogers AJ, Mokhles MM, et al. Comparison of clinical outcome of stage I non-small cell lung cancer treated surgically or with stereotactic radiotherapy: results from propensity score analysis. Lung Cancer. 2015;87(3):283-9.

112. Bryant AK, Mundt RC, Sandhu AP, Urbanic JJ, Sharabi AB, Gupta S, et al. Stereotactic Body Radiation Therapy Versus Surgery for Early Lung Cancer Among US Veterans. Ann Thorac Surg. 2018;105(2):425-31.

113. Bang A, Bezjak A. Stereotactic body radiotherapy for centrally located stage I non-small cell lung cancer. Transl Lung Cancer Res. 2019;8(1):58-69.

114. Stam B, Kwint M, Guckenberger M, Mantel F, Hope A, Giuliani M, et al. Subgroup Survival Analysis in Stage I-II NSCLC Patients With a Central Tumor Partly Treated With Risk-Adapted SBRT. Int J Radiat Oncol Biol Phys. 2019;103(1):132-41.

115. Andratschke N, Zimmermann F, Boehm E, Schill S, Schoenknecht C, Thamm R, et al. Stereotactic radiotherapy of histologically proven inoperable stage I non-small cell lung cancer: patterns of failure. Radiother Oncol. 2011;101(2):245-9.

116. Lagerwaard FJ, Verstegen NE, Haasbeek CJ, Slotman BJ, Paul MA, Smit EF, et al. Outcomes of stereotactic ablative radiotherapy in patients with potentially operable stage I non-small cell lung cancer. Int J Radiat Oncol Biol Phys. 2012;83(1):348-53.

117. Stam B, Peulen H, Guckenberger M, Mantel F, Hope A, Werner-Wasik M, et al. Dose to heart substructures is associated with non-cancer death after SBRT in stage I-II NSCLC patients. Radiother Oncol. 2017;123(3):370-5.

118. Miller CJ, Martin B, Stang K, Hutten R, Alite F, Small C, et al. Predictors of Distant Failure After Stereotactic Body Radiation Therapy for Stages I to IIA Non-Small-Cell Lung Cancer. Clin Lung Cancer. 2019;20(1):37-42.

119. Wilke L, Andratschke N, Blanck O, Brunner TB, Combs SE, Grosu AL, et al. ICRU report 91 on prescribing, recording, and reporting of stereotactic treatments with small photon beams : Statement from the DEGRO/DGMP working group stereotactic radiotherapy and radiosurgery ICRU-Bericht 91 uber die Verschreibung, Aufzeichnung und Dokumentation von stereotaktischen Behandlungen mit kleinen Photonenfeldern : Stellungnahme der DEGRO/DGMP-Arbeitsgruppe Stereotaktische Strahlentherapie und Radiochirurgie. Strahlenther Onkol. 2019;195(3):193-8.

120. Ogundimu EO, Altman DG, Collins GS. Adequate sample size for developing prediction models is not simply related to events per variable. J Clin Epidemiol. 2016;76:175-82.

121. Vandenberghe S, Mikhaylova E, D'Hoe E, Mollet P, Karp JS. Recent developments in time-of-flight PET. EJNMMI Phys. 2016;3(1):3.

122. Johnson GB, Peller PJ, Kemp BJ, Ryu JH. Future of thoracic PET scanning. Chest. 2015;147(1):25-30.

123. Dahele M, Palma D, Lagerwaard F, Slotman B, Senan S. Radiological changes after stereotactic radiotherapy for stage I lung cancer. J Thorac Oncol. 2011;6(7):1221-8.

124. Ronden MI, van Sornsen de Koste JR, Johnson C, Slotman BJ, Spoelstra FOB, Haasbeek CJA, et al. Incidence of High-Risk Radiologic Features in Patients Without Local Recurrence After Stereotactic Ablative Radiation Therapy for Early-Stage Non-Small Cell Lung Cancer. Int J Radiat Oncol Biol Phys. 2018;100(1):115-21.

125. Adebahr S, Collette S, Shash E, Lambrecht M, Le Pechoux C, Faivre-Finn C, et al. LungTech, an EORTC Phase II trial of stereotactic body radiotherapy for centrally located lung tumours: a clinical perspective. Br J Radiol. 2015;88(1051):20150036.

126. Tembhekar AR, Wright CL, Daly ME. Cardiac Dose and Survival After Stereotactic Body Radiotherapy for Early-stage Non-Small-cell Lung Cancer. Clin Lung Cancer. 2017;18(3):293-8.

127. Reshko LB, Kalman NS, Hugo GD, Weiss E. Cardiac radiation dose distribution, cardiac events and mortality in early-stage lung cancer treated with stereotactic body radiation therapy (SBRT). J Thorac Dis. 2018;10(4):2346-56.

128. Sullivan DR, Eden KB, Dieckmann NF, Golden SE, Vranas KC, Nugent SM, et al. Understanding patients' values and preferences regarding early stage lung cancer treatment decision making. Lung Cancer. 2019;131:47-57.

129. Chen H, Senan S, Nossent EJ, Boldt RG, Warner A, Palma DA, et al. Treatment-Related Toxicity in Patients With Early-Stage Non-Small Cell Lung Cancer and Coexisting Interstitial Lung Disease: A Systematic Review. Int J Radiat Oncol Biol Phys. 2017;98(3):622-31.

130. Finazzi T, Haasbeek CJA, Spoelstra FOB, Palacios MA, Admiraal MA, Bruynzeel AME, et al. Clinical outcomes of stereotactic MR-guided adaptive radiation therapy for high-risk lung tumors. Int J Radiat Oncol Biol Phys. 2020.

131. Chang JY, Jabbour SK, De Ruysscher D, Schild SE, Simone CB, 2nd, Rengan R, et al. Consensus Statement on Proton Therapy in Early-Stage and Locally Advanced Non-Small Cell Lung Cancer. Int J Radiat Oncol Biol Phys. 2016;95(1):505-16.

132. Wu AJ. Safety of stereotactic ablative body radiation for ultracentral stage I non-small cell lung cancer. Transl Lung Cancer Res. 2019;8(Suppl 2):S135-S8.

133. Chang JY, Senan S, Paul MA, Mehran RJ, Louie AV, Balter P, et al. Stereotactic ablative radiotherapy versus lobectomy for operable stage I non-small-cell lung cancer: a pooled analysis of two randomised trials. Lancet Oncol. 2015;16(6):630-7.

Summary

The aim of this thesis was to improve decision making in stereotactic body radiation therapy (SBRT) of centrally located lung tumors by modelling the outcome in terms of overall survival, local disease control and toxicity probabilities.

Chapter 1 contains a general introduction into the field of SBRT for centrally located lung tumors and ends with an outline of this thesis. The subgroup of central lung patients has been treated with risk adapted fractionation schedules and accompanying dose constraints for more than 10 years, however evidence-based guidelines are still missing. The models provided within this thesis could be used to support nationwide or even worldwide consensus.

Chapter 2 offers a nomogram to predict overall survival in patients having centrally located early stage NSCLC treated with SBRT. This nomogram includes the variables planning target volume (PTV), age, WHO performance status, tumor lobe location and mean dose to the PTV. The discriminatory ability was moderate and the calibration plots showed favorable predictive accuracy. The external validation in a cohort of 94 central lung patients showed acceptable validity. The 5 factors together predict overall survival at 6 months, 1, 2 and 3 years.

The impact of underdosage of the PTV on local control is discussed in **Chapter 3**. Twelve percent of the 220 patients developed a local recurrence resulting in local control rate of 88% at 2 years. There was no correlation between a local recurrence and the relative or absolute PTV receiving less than 100 Gy BED_{10}. Additionally, no correlation was found with any of the other analyzed PTV parameters. Bigger tumor size and lower forced expiratory volume in 1 second (FEV_1) were independently predictive for the development of a local recurrence. Disease progression was reported in 75 patients with a 2-year disease free survival rate of 66%. Disease recurrence was associated with larger tumor diameter, a tumor located in the lower lobe and decreased FEV_1.

Chapter 4 describes radiological changes of the bronchi after SBRT and its relation to the prescribed dose. The radiological changes were divided in stenosis and occlusion with or without atelectasis. No changes were found in the trachea and only stenosis was reported in the main bronchi and intermediate bronchus. Occlusion with and without atelectasis was seen in the smaller branches; the upper, middle, and lower lobe bronchi and the segmental bronchi. The dose was significantly higher in these branches with radiological changes. Normal tissue complication probability (NTCP) models were derived for the maximum point dose (D_{max}) and the bronchial volume receiving 65, 80 and 100 Gy EQD_2 ($V_{65\text{-}100Gy}$) in the

main bronchi and bronchus intermedius, in the upper, middle, and lower lobe bronchi and in the segmental bronchi.

In **Chapter 5** both clinical pulmonary (grade 3 or higher) and radiological bronchial toxicity were evaluated in a group of 195 patients. Several dosimetric parameters, D_{max} and V_{65Gy}, V_{80Gy}, V_{90Gy}, V_{100Gy}, V_{130Gy} (in EQD_2), were analyzed and all of them were correlated with clinical and lobar bronchial radiological toxicity. After identifying the predictors, NTCP models were derived showing volume dependency for the development of both toxicities.

High-grade clinical toxicity was independently correlated with a PTV overlapping the trachea or main stem bronchus, chronic obstructive pulmonary disease (COPD) and the total V_{130Gy}. Radiological toxicity did not correlate with clinical toxicity, which was explained by the subclinical symptoms caused by occlusion of the lobar bronchi.

Chapter 6 reports the incidence of low-grade radiation esophagitis after SBRT and its relation to the prescribed dose. Acute low-grade toxicity was reported in 17% of the 221 patients without the occurrence of high-grade toxicity. All analyzed DVH-parameters, the D_{max} and the dose in 1 cc, 2 cc and 5 cc of the esophagus ($D_{1cc-5cc}$, in EQD_2), were correlated with low-grade toxicity. NTCP-curves of each dosimetric parameter were modelled. A multivariable analysis showed significant correlation with the development of low-grade esophageal toxicity for D_{5cc} and female gender.

Chapter 7 discusses 4 cases of high-grade esophageal toxicity and their relation with SBRT in a cohort of 188 central lung patients. Two patients reported grade 3 toxicity and 2 patients died due to esophageal toxicity. Acute low-grade toxicity occurred in 15% of the patients. All investigated DVH-parameters (D_{max}, D_{1cc}, D_{2cc}, D_{5cc}, in EQD_2) were significantly correlated with acute and late toxicity. NTCP-curves for acute and late toxicity were derived for all DVH-parameters. Both a smaller distance between tumor and esophagus and the use of 12 fractions (versus 8 fractions) were correlated with increased acute low-grade toxicity in the univariate analysis. No multivariate analysis was possible due to the correlation between both parameters.

In **Chapter 8** the main findings and limitations of the studies in this thesis are described. Finally, the results of this thesis are put into perspective of current developments and future research.

Samenvatting

Het doel van dit proefschrift was het verbeteren van besluitvorming door het modelleren van algehele overleving, lokale ziekte controle en toxiciteitskansen bij patiënten met een centraal gelokaliseerde longtumor die behandeld worden met stereotactische radiotherapie.

Hoofdstuk 1 bevat een algemene inleiding over de stereotactische behandeling van centraal gelokaliseerde longtumoren en eindigt met een kort overzicht van dit proefschrift. De groep centrale longtumor patiënten wordt al meer dan 10 jaar behandeld met risico aangepaste fractioneringsschema's en de bijhorende dosis-constraints, maar desondanks ontbreken op wetenschap gebaseerde richtlijnen nog steeds. De modellen in dit proefschrift kunnen gebruikt worden om landelijke of zelfs wereldwijde consensus te ondersteunen.

Hoofdstuk 2 introduceert een nomogram om de algehele overleving te voorspellen bij patiënten met een centraal gelokaliseerd vroeg stadium niet-kleincellig longcarcinoom behandeld met stereotactische radiotherapie. Dit nomogram bevat de variabelen 'planning target volume' (PTV), leeftijd, WHO status, tumor kwab locatie en de gemiddelde dosis in het PTV. Het onderscheidend vermogen was acceptabel en de kalibratie grafieken toonden een gunstige voorspellende nauwkeurigheid. De externe validatie in een cohort van 94 centrale longtumor patiënten liet acceptabele validiteit zien. De 5 genoemde factoren voorspellen samen de algehele overleving op 6 maanden, 1 jaar, 2 jaar en 3 jaar.

De invloed van onderdosering van het PTV op de lokale controle wordt besproken in **Hoofdstuk 3**. Twaalf procent van de 220 patiënten ontwikkelde een lokaal recidief resulterend in een lokale controle van 88% op 2 jaar. Er was geen correlatie tussen de ontwikkeling van een lokaal recidief en de relatieve of absolute PTV die minder dan 100 Gy BED_{10} ontving. Bovendien werd er ook geen relatie gevonden met één van de andere PTV parameters. Een grotere tumorafmeting en een lager geforceerd expiratoir volume in 1 seconde (FEV_1) waren onafhankelijk voorspellend voor de ontwikkeling van een lokaal recidief. Ziekte progressie werd vermeld in 75 patiënten met een ziektevrije overlevingskans van 66% op 2 jaar. Recidief van ziekte werd geassocieerd met grotere tumorafmeting, een tumor in de onderste kwab en afgenomen FEV_1.

Hoofdstuk 4 beschrijft de radiologische veranderingen in de bronchiale structuren na stereotactische radiotherapie in relatie met de voorgeschreven dosis. De radiologische veranderingen werden opgedeeld in stenose en occlusie met of zonder atelectase. Er werden geen veranderingen gevonden in de trachea, en in de hoofdstambronchus en de bronchus intermedius was alleen stenose aanwezig. Occlusie met en zonder atelectase

werd gevonden in de kleinere aftakkingen; de bovenste, middelste en onderste kwab bronchus en de segmentale bronchiën. In deze aftakkingen met radiologische veranderingen was de dosis significant hoger. 'Normal tissue complication probability' (NTCP) modellen werden afgeleid van de maximale punt dosis (D_{max}) en het bronchiaal volume dat 65, 80 en 100 Gy EQD_2 ($V_{65\text{-}100Gy}$) ontving in de hoofdstam bronchus en de bronchus intermedius, in de bovenste, middelste en onderste kwab bronchus en in de segmentale bronchiën.

In **Hoofdstuk 5** werd binnen een groep van 195 patiënten zowel de klinische long (graad 3 of hoger) als de radiologische bronchiale toxiciteit geëvalueerd. Verschillende dosimetrische parameters, D_{max} en V_{65Gy}, V_{80Gy}, V_{90Gy}, V_{100Gy}, V_{130Gy} (in EQD_2), werden geanalyseerd en allemaal waren deze gecorreleerd met klinische toxiciteit en lobulaire bronchiale radiologische toxiciteit. Na het identificeren van de voorspellers, werden er NTCP-modellen afgeleid. Deze toonden volume afhankelijkheid voor de ontwikkeling van beide soorten toxiciteit.

Hooggradige klinische toxiciteit was onafhankelijk gecorreleerd met een PTV die de trachea of hoofdstambronchus overlapt, chronische obstructieve longziekten en de totale V_{130Gy}. Radiologische toxiciteit correleerde niet met de klinische toxiciteit. Dit werd verklaard door de subklinische symptomen die veroorzaakt worden bij de occlusie van lobulaire bronchi.

Hoofdstuk 6 behandelt de incidentie van laaggradige radiatie oesofagitis na stereotactische radiotherapie en de relatie van deze bijwerking met de voorgeschreven dosis. Acute laaggradige toxiciteit werd gemeld bij 17% van de 221 patiënten zonder het optreden van hooggradige toxiciteit. Alle geanalyseerde DVH-parameters, de D_{max} en de dosis in 1 cc, 2 cc en 5 cc van de slokdarm ($D_{1cc\text{-}5cc}$, in EQD_2), waren gecorreleerd met laaggradige toxiciteit. NTCP grafieken werden gemodelleerd voor elk van deze parameters. Een multivariate analyse toonde een significante correlatie met de ontwikkeling van laaggradige slokdarm toxiciteit voor de D_{5cc} en het vrouwelijk geslacht.

Hoofdstuk 7 bespreekt 4 casussen van hooggradige slokdarm toxiciteit en de relatie hiervan met stereotactische radiotherapie in een cohort van 188 centrale longtumor patiënten. Twee patiënten hadden klachten van graad 3 toxiciteit en 2 patiënten zijn overleden aan de slokdarm toxiciteit. Acute laaggradige toxiciteit trad op in 15% van de patiënten. Alle onderzochte DVH-parameters (D_{max}, D_{1cc}, D_{2cc}, D_{5cc}, in EQD_2) waren significant gecorreleerd met acute en late toxiciteit. Voor alle DVH-parameters werden NTCP grafieken voor acute en late toxiciteit afgeleid. In de univariate analyse werd toename van acute slokdarm toxiciteit gezien bij een kleinere afstand tussen de tumor en de slokdarm en bij het

voorschrijven van 12 fracties (versus 8 fracties). Door de correlatie tussen beide parameters was geen multivariate analyse mogelijk.

In **Hoofdstuk 8** worden de belangrijkste bevindingen en eventuele beperkingen van de studies in dit proefschrift beschreven. Tenslotte, worden de resultaten van dit proefschrift in perspectief tot huidig en toekomstig onderzoek besproken.

List of Publications

Age and the effect of physical activity on breast cancer survival: A systematic review.
Fontein BD*, de Glas NA*, **Duijm M**, Bastiaannet E, Portielje JE, van de Velde CJ, Liefers GJ.
Cancer Treat Rev. 2013 Dec;39(8): 958-65

Dose and volume of the irradiated main bronchi and related side effects in the treatment of central lung tumors with stereotactic radiotherapy.
Duijm M, Schillemans W, Aerts JG, Heijmen B, Nuyttens JJ.
Semin Radiat Oncol. 2016 Apri;26(2):140-8

Normal Tissue Complication Probability modeling of pulmonary toxicity after stereotactic and hypofractionated radiation therapy for central lung tumors.
Tekatli H*, **Duijm M***, Oomen-de Hoop E, Verbakel W, Schillemans W, Slotman BJ, Nuyttens JJ, Senan S.
Int J Radiat Oncol Biol Phys. 2018 Mar 1;100(3):738-747.
** Both authors contributed equally to this paper*

Esophagus toxicity after stereotactic and hypofractionated radiotherapy for central lung tumors: Normal Tissue Complication Probability modeling.
Duijm M*, Tekatli H*, Oomen-de Hoop E, Verbakel W, Schillemans W, Slotman BJ, Senan S, Nuyttens JJ.
Radiother Oncol. 2018 May;127(2):233-238.
** Both authors contributed equally to this paper*

Factors affecting local control of pulmonary oligometastases treated with stereotactic body radiotherapy.
Sharma A, **Duijm M**, Oomen-de Hoop E, Aerts JG, Verhoef C, Hoogeman M, Nuyttens JJ.
Acta Oncol. 2018 Aug;57(8):1031-1037.

Local reirradiation of recurrent non-small cell lung carcinoma resulting in long disease-free survival, although in the presence of osteonecrosis.
Duijm M, Schipaanboord B, Granton PV, Nuyttens J.
Cureus. 2018 Oct 22;10(10):e3471.

Stereotactic body radiotherapy for oligometastatic soft tissue sarcoma.
Loi M, **Duijm M**, Baker S, Rossi L, Grunhagen D, Verhoef C, Nuyttens J.
Radiol Med. 2018 Nov;123(11):871-878.

Survival and prognostic factors of pulmonary oligometastases treated with stereotactic body radiotherapy.
Sharma A, **Duijm M**, Oomen-de Hoop E, Aerts JG, Verhoef C, Hoogeman M, Nuyttens JJ.
Acta Oncol. 2019 Jan;58(1):74-80.

Predicting high-grade esophagus toxicity after treating central lung tumors with stereotactic radiotherapy using a Normal Tissue Complication Probability model.
Duijm M, van der Voort van Zyp NC, van de Vaart P, Oomen-de Hoop E, Mast ME, Hoogeman MS, Nuyttens JJ.
Int J Radiat Oncol Biol Phys. 2020 Jan 1;106(1):73-81.

Prognostic factors for local control and survival for inoperable pulmonary colorectal oligometastases treated with stereotactic body radiotherapy.
Sharma A, Baker S, **Duijm M,** Oomen-de Hoop E, Cornelissen R, Verhoef C, Hoogeman M, Nuyttens JJ.
Radiother Oncol. 2020 Mar;144:23-29.

Prediction of overall survival in patients with early-stage lung cancer following stereotactic body radiotherapy: development of a nomogram.
Baker S, Bakunina K, **Duijm M**, Milder M, Hoogeman MS, Aerts JG, Antonisse I, Praag J, Heemsbergen WD, Nuyttens JJ
Radiother Oncol. 2020 Apr 22; 15(1):89.

Prognostic factors of local control and disease free survival in centrally located non-small cell lung cancer treated with stereotactic body radiation therapy.
Duijm M, van der Voort van Zyp NC, Granton PV, van de Vaart P, Mast ME, Oomen-de Hoop E, Hoogeman MS, Nuyttens JJ.
Acta Oncol. 2020 Apr 14:1-9. (epub ahead of print)

PhD Portofolio

Name PhD student:	Marloes Duijm
Erasmus MC Department:	Radiation Oncology
Research School:	Molecular Medicine
PhD period:	2015 – 2019
Promotor:	prof. dr. M.S. Hoogeman
Copromotor:	dr. J.J. Nuyttens

	Year	Workload (ECTS)
General courses		
Biomedical English Writing and Communication	2017	2.0
Research Integrity	2018	0.3
Basic Introduction Course on SPSS	2017	1.0
Survival Analysis Course	2017	0.6
BROK ('Basiscursus Regelgeving Klinisch Onderzoek')	2017	1.5
Basistraining OpenClinica	2017	0.3
Specific courses		
Basic and Translational Oncology	2017	1.8
Cyberknife School	2017	1.0
Medical Physics Teaching by prof. Pignol	2017 – 2018	1.0
ESTRO course: Clinical Practice and Implementation of Image-Guided Stereotactic Body Radiotherapy	2018	1.8
Presentations at international conferences		
Oral presentation ASTRO *Dose to bronchial structures and the related side effects in the treatment of central lung tumors treated with stereotactic radiotherapy*	2016	2.0
Poster viewing ASTRO *The contribution of underdosage to the local control for central tumors in the lung treated with stereotactic radiotherapy*	2016	0.5
Poster presentation ESTRO *Esophagus toxicity after stereotactic radiotherapy of central lung tumor: NTCP modelling*	2018	1.7
Presentations at national conferences		
Oral presentation longsymposium IKNL Zuidwest-Nederland *Synchroon gemetastaseerde tumoren in de long*	2016	1.0

	Year	Workload (ECTS)
Oral presentation regiobijeenkomst IKNL Longtumoren *Stereotactische radiotherapie bij centrale longtumoren - dosis en gerelateerde bijwerkingen*	2017	1.0
In-house presentations		
Research day, department of Radiation Oncology *Stereotactic radiotherapy of central lung tumors dose and toxicity to the bronchial structures*	2015	1.0
Research day, department of Radiation Oncology *Esophagus toxicity after stereotactic radiotherapy for central lung tumors*	2018	1.0
Oral presentation HMC *Stereotactische bestraling van centrale longtumoren in HMC*	2018	1.0
Refereerlunches	2016 – 2020	2.0
Seminars and workshops		
PhD Day	2018 / 2019	0.6
Research Rounds, department of Radiation Oncology	2016 – 2019	1.0
Refereerlunch, department of Radiation Oncology	2016 – 2019	2.0
Journal Club, department of Radiation Oncology	2016 – 2019	1.0
Teaching activities		
Bijscholing laboranten – RETHO trial	2018 / 2019	1.0
Cyberknife School	2018 / 2019	1.5
Clinical Research Trials		
Reirradiation for recurrent lung cancer in the thorax: overall survival, local control and toxicity: a phase 2 trial	2017 – now	2.0

Curriculum Vitae

Marloes Duijm was born on the 5th of August 1991 in Leiden, the Netherlands. In 2009 she obtained her gymnasium degree at Visser 't Hooft Lyceum in Leiden. After graduation, she started the bachelor 'policy and management in health care' at the Erasmus University in Rotterdam. After obtaining her propaedeutic year, she switched to Medical School at the Erasmus University in 2010. During her master thesis, she was introduced to the field of Radiation Oncology, this work resulted in her first publication (*Chapter 4*). During her internships she continued further research on stereotactic radiotherapy and lung cancer. After receiving her medical degree in August 2016, she continued this research by starting her PhD under supervision of dr. Nuyttens and prof. dr. Hoogeman. Since August 2019, she is a resident in Radiation Oncology at the Erasmus MC Cancer Institute.

Dankwoord

Dit proefschrift zou er niet zijn zonder de hulp van vele mensen. Een aantal van deze mensen wil ik graag in het bijzonder bedanken.

Allereerst mijn copromotor, dr. J.J. Nuyttens. Joost, ik kan me nog als de dag van gisteren herinneren dat ik voor het eerst in de Daniel kwam om te praten over de mogelijkheden voor mijn master onderzoek. Vanaf dat moment heb jij mij begeleid en geïntroduceerd in de wereld van de radiotherapie. Zowel jouw enthousiasme voor het vak als voor onderzoek werkten aanstekelijk. Dit heeft ervoor gezorgd dat ik na mijn opleiding geneeskunde heb gekozen voor een promotie binnen de radiotherapie en dat ik een paar jaar later vol enthousiasme ben begonnen aan mijn opleiding tot radiotherapeut. Ik wil je bedanken voor al je tijd, de vele overleggen en je geduld om mij het vak radiotherapie stap voor stap beter te laten begrijpen. Gelukkig is mijn tijd bij het Erasmus MC nog niet voorbij en hoop ik in de toekomst nog vaak samen te kunnen werken.

Mijn promotor, prof. dr. M.S. Hoogeman. Beste Mischa, ondanks dat jij halverwege mijn promotietraject bent ingestapt, heb ik vanaf het begin het gevoel gehad dat je volledig op de hoogte was. Ik waardeer de rust die jij creëerde tijdens onze overleggen en je kritische blik die mij heeft geleerd om niet zomaar tevreden te zijn. Jouw begeleiding heeft mijn wetenschappelijke blik verbreed en verbeterd.

Dank aan alle leden van de leescommissie, prof. R.A. Nout, prof. dr. J.G.J.V. Aerts en prof. D.K.M. de Ruysscher, en de leden van de grote commissie voor jullie tijd en interesse in mijn proefschrift.

Noëlle, bedankt voor al je hulp en tijd tijdens het verzamelen en het verwerken van de HMC data. Jij hebt ervoor gezorgd dat meerdere van mijn manuscripten wetenschappelijk sterker en taalkundig beter zijn geworden. Daarnaast dank aan alle andere mensen in het HMC die mij geholpen hebben, ik kijk met een fijn gevoel terug op de tijd bij jullie.

Graag wil ik alle coauteurs bedanken voor hun inzet en tijd. Esther, bedankt voor je statische begeleiding, je uitleg en eindeloze geduld. Hilâl, ik heb onze samenwerking als erg fijn en leerzaam ervaren. Ik heb veel van je geleerd in de eerste maanden van mijn promotie traject. Wilco, bij de eerste stappen van mijn onderzoek heb jij mij wegwijs gemaakt in de wereld van scripts en dataverwerking en ook in de latere jaren heb je altijd klaar gestaan voor eventuele hulp, dank hiervoor. Patrick, ondanks dat uit onze samenwerking niet is voortgekomen wat we eigenlijk voor ogen hadden, zorgden onze gezamenlijke overleggen er altijd voor dat ik weer vol goede moed door ging met mijn onderzoek.

Lieve oud AIOS, bedankt voor de opvang tijdens mijn masteronderzoek. In het begin voelde het wat onwennig en hield ik me wellicht wat afzijdig, maar door de tijd heen voelde ik me volledig op mijn gemak. Mede door jullie heb ik besloten mijn weg in de radiotherapie te vervolgen.

Lieve huidige AIOS, vanaf het eerste moment voelde ik me welkom en onderdeel van de groep. Ik ben blij met jullie eerlijkheid en oprechtheid, en de hulp die ik vaak van jullie krijg. Mede dankzij jullie ga ik elke dag met plezier naar mijn werk.

Manouk en Marjan, dankjewel voor de mogelijkheid om tijdens mijn opleiding mijn promotie af te ronden. Dit heeft me veel rust gegeven.

Lieve mede-promovendi van de Radiotherapie, ondanks dat ik me soms een vreemde eend in de bijt voelde tijdens jullie gesprekken over programmeren en andere moeilijke fysica dingen, heb ik genoten van onze koffietjes, eetafspraken en drankjes. Dankzij jullie weet ik nu dat figuren die je niet in Paint maakt, er toch echt een stuk mooier uitzien.

Bas, begonnen als buren in de Daniel en geëindigd als kamergenoten in de EE-toren. Wellicht dat onze productiviteit niet altijd optimaal was op de momenten dat we tegelijk aanwezig waren, maar jij hebt mijn promotie traject wel een stuk leuker en gezelliger gemaakt! Daarom voelt het ook niet meer dan logisch om jou als paranimf naast mij te hebben staan tijdens mijn verdediging. Dank voor het nalezen van mijn stukken, de vele koffietjes en de steun door de jaren heen

Anne, beiden zijn we via een BMG-omweg uitgekomen bij onze grote droom: geneeskunde. Vanaf het begin van onze studietijd kan ik bij jou relativeren, klagen en frustraties uiten, en bovenal met jou successen vieren. Dank voor al je steun en aanwezigheid als paranimf tijdens mijn verdediging.

Lieve vrienden en (schoon)familie, ik wil jullie bedanken voor de steun, de interesse en de afleiding door de jaren heen.

Opa, jij hebt mij geleerd trots te zijn op mezelf en vertrouwen te hebben in mijn eigen kunnen. Ondanks dat jouw achtergrond in de psychologie lag, heb jij meerdere van mijn artikelen volledig uitgeplozen en begreep je deze, tot je eigen verbazing, ook nog. Dank voor je vertrouwen in mij en dat ik je mocht begeleiden in de laatste jaren van je leven. Beiden hadden we gehoopt dat je tijdens mijn verdediging vol trots in de zaal zou zitten, maar ik weet zeker dat je nu vol trots vanaf boven meekijkt. Oma, ik voel me bevoorrecht om zo'n goede band met jou te hebben, ik hoop daar nog jaren van te kunnen genieten.

Lieve papa, mama en Max, wat is het een luxe om thuis te kunnen komen in zo'n stabiel en liefdevol gezin. Dank voor het luisterend oor in de afgelopen jaren.

Jasper, vanaf dag één kan ik mezelf zijn bij jou, heb je mij gesteund in mijn ambities en me bijgestaan in mijn promotietraject. Ik kijk uit naar onze toekomst met ons gezin.